UC Santa Barbara

UC Santa Barbara Electronic Theses and Dissertations

Title

Stream Channel Erosion in a Rapidly Urbanizing Semi-Arid Region: Channel Dynamics of Los Laureles Canyon Watershed in Tijuana, Mexico

Permalink

https://escholarship.org/uc/item/9pr3d29p

Author

Taniguchi, Kristine Teru

Publication Date

2018

Peer reviewed|Thesis/dissertation

eScholarship.org Powered by the California Digital Library
University of California

SAN DIEGO STATE UNIVERSITY AND

UNIVERSITY OF CALIFORNIA

Santa Barbara

Stream Channel Erosion in a Rapidly Urbanizing Semi-Arid Region: Channel Dynamics of Los Laureles Canyon Watershed in Tijuana, Mexico

A Dissertation submitted in partial satisfaction of the

requirements for the degree Doctor of Philosophy

in Geography

by

Kristine Teru Taniguchi

Committee in charge:

Professor Trent Biggs, Chair

Professor Douglas Stow

Professor Thomas Dunne

Professor Oliver Chadwick

Professor Derek Booth

March 2019

The dissertation of Kristine Teru Taniguchi is approved.

_____

Trent Biggs, Chair

_____

Douglas Stow

_____

Thomas Dunne

_____

Oliver Chadwick

_____

Derek Booth

December 2018

Copyright © 2018
by
Kristine Teru Taniguchi
All Rights Reserved

DEDICATION

For my amazing grandparents, Midori Tayama, Lois Taniguchi, and Ned Taniguchi.

ABSTRACT OF THE DISSERTATION

Stream Channel Erosion in a Rapidly Urbanizing Semi-Arid Region: Channel Dynamics of Los Laureles Canyon Watershed in Tijuana, Mexico

by

Kristine Teru Taniguchi

Urbanization can lead to stream channel erosion and ecological degradation. The majority of studies have focused on the impacts of urban development on channel morphology in developed regions, such as the United States and Europe, where urbanization is typically characterized by watershed-scale land alterations, such as the conversion of undeveloped land to impervious urban areas. This dissertation focuses on a rapidly developing, semi-arid region, Los Laureles Canyon watershed (LLCW), located in Tijuana, Mexico, which is characterized by steep slopes and highly erodible material. Urban development in Tijuana has led to excessive hillslope and channel erosion, and subsequent infrastructure failure of homes, water main pipes, and unpaved roads and sedimentation of the downstream Tijuana Estuary in San Diego, CA. The main objectives of this dissertation are to investigate the impact of urbanization and in-channel alterations on stream channel evolution, highlight channel sources and sinks of sediment, and evaluate the overall importance of channel erosion on the sediment budget of LLCW for future sediment mitigation plans. First, traditional geomorphic survey methods and Structure-from-Motion (SfM) photogrammetry techniques were utilized to describe the spatial patterns in stream

channel geometry in LLCW and to provide a regional comparison of channel erosion in Tijuana, MX to reference and urbanized watersheds in southern California. Channels in Tijuana are statistically larger than urban and reference channels in southern California and major hotspots of erosion are located downstream of hardpoints, or non-erodible features. Second, to quantitatively evaluate channel evolution and to determine the driving mechanisms to channel instability downstream of hardpoints, field data were used to develop a computational model of channel evolution, CONCEPTS (CONservational Channel Evolution and Pollutant Transport System), for LLCW. A scenario analysis was conducted to quantitatively assess the impact of urban channel alterations, including hardpoint installation, slope alteration, bed composition change, and vegetation removal, on channel incision, widening, and sediment load. Hardpoints prevented incision in the upstream direction by serving as grade control, and only caused local channel instabilities downstream. Channel erosion is caused mainly by the destruction of the natural channel, including channel burial, straightening, steepening, and removal of riparian vegetation, often performed in the process of turning channels into roads. Reformation of an enlarged river reach that is disconnected from the floodplain, leads to higher flow depths constrained in the channel, larger shear stresses, and accelerated channel incision. Lastly, a watershed-scale model of hillslope processes, AnnAGNPS, integrated with CONCEPTS was developed for LLCW to determine the spatial pattern of channel sources and sinks of sediment in the watershed and evaluate the overall importance of channel processes on the sediment budget for future sediment mitigation plans. Channel erosion contributes approximately 60% of the total sediment budget and only a third of the entire stream channel network is generating 90% of the channel-derived sediment load. This indicates that channel erosion is a dominant source

of sediment in LLCW and targeted stream stabilization measures could potentially reduce a large proportion of sediment load to the Tijuana Estuary. However, coarsening of the bed alone may not decrease mean annual channel-derived sediment yield, as armoring of the bed can decrease channel incision but channel widening may be exacerbated. Overall, urbanization of the valley floor and alterations to the stream channel have led to constrained and enlarged stream channels. This dissertation provides an example of the use of a variety of geomorphic field methods, including traditional topographic survey methods and Structure-from-Motion (SfM) photogrammetry techniques, paired with a comprehensive modelling framework to provide an understanding of the driving mechanisms of channel instability and the overall importance of channel processes on the sediment budget to support local and federal sediment management plans in a rapidly developing, semi-arid region.

TABLE OF CONTENTS

PAGE

LIST OF TABLES

PAGE

CHAPTER 2:

CHAPTER 4:

LIST OF FIGURES

CHAPTER 1: PAGE

CHAPTER 2:

ACKNOWLEDGEMENTS

As an undergraduate, I would have never known that a fieldtrip to the Tijuana Estuary sediment basins would shape the way that I thought about water forever and pave the way to my future career as a fluvial geomorphologist. I would like to express my greatest gratitude to my advisor, mentor, and friend, Dr. Trent Biggs, for being my role model and endless support for the past several years of my undergraduate and graduate career. Trent has accompanied me on multiple field excursions across the border, always encouraged me to pursue my curiosity in geomorphology, and has opened up countless doors of opportunity for me professionally.

I would also like to thank my advisors, Dr. Tom Dunne, Dr. Doug Stow, Dr. Oliver Chadwick, and Dr. Derek Booth, for being members on my dissertation committee and for their critical feedback and mentorship throughout the course of my doctoral journey. Tom, thank you for being my UCSB advisor, the countless hours you spent with me discussing hydraulic and sediment transport theory, and for your insightful comments and support. Doug, thank you for the invaluable knowledge and inspiration you have given me on all things remote sensing and your never-ending encouragement throughout my years at SDSU. Oliver and Derek, thank you for your invaluable feedback and for challenging me to think outside of the box. A special thanks to my academic mentors and role models, Diana Richardson, Dr. Molly Costello, and Dr. Hilary McMillan for always keeping an open door, and offering me words of wisdom and encouragement. Thank you to Pete Coulter who spent the time to teach me how to create flight plans for our unmanned aerial vehicle (UAV) and accompanied me on one of my first UAV flights.

Additionally, I am immeasurably grateful for the funding and support from the US Environmental Protection Agency (USEPA) and all of our project team collaborators: Dr. Eddy Langendoen (USDA), Dr. Napoleon Gudino-Elizondo (CICESE), Dr. Carlos Castillo (University of Cordoba, Spain), Dr. Ronald Bingner (USDA), Dr. Yongping Yuan (USEPA, Doug Liden (USEPA), and Cindy Lin (formerly USEPA). Eddy, thank you for your mentorship and support with building and implementing the CONCEPTS model and for the multiple trips to San Diego, Ensenada, and Santa Barbara for CONCEPTS training and support. Napoleon, many thanks for being the greatest colleague, field partner, and friend

through the ups and downs of graduate school. Carlos, thank you for sharing your knowledge and passion for Structure-from-Motion photogrammetry techniques, from the field data collection to the post-processing. Ron, Yongping, Doug, and Cindy, it has been a pleasure working with such knowledgeable and passionate scientists who work so hard to support the betterment of the environment and society and help to bridge the gap between science and policy. Additionally, it has been a pleasure to work with the researchers at the Tijuana Estuary and the University of California, Irvine (UCI) FloodRISE/SedRISE team including Dr. Jeff Crooks, Kristen Goodrich, Dr. Brett Sanders, and Adam Luke, to list a few. A special thank you to Southern California Coastal Water Research Project (SCCWRP), in particular, Dr. Eric Stein, for taking a leap of faith in me and motivating me to wrap up my dissertation to start my career as a scientist at SCCWRP.

A special thank you to all of the amazing graduate students and colleagues in the Biggs Lab, Taya Lazootin, Whitney Seymore, Luis de la Torre, Alex Messina, Joel Kramer, Rodney Feddema, and Maegan Salinas (plus many more) and my SDSU/UCSB JDP cohort, Dara Seidl, Seda Selap, Barbara Quimby, Cindy Tsai, Steve Crook, and Chris Allen, for being my support system and always providing words of encouragement and a shoulder to lean on. A special thanks to the environmental science senior undergraduate students who helped me in the field and sieved multiple soil samples in the lab.

Last but not least, thank you to my parents, Jeanne and Gregg Taniguchi, for your constant love and support and instilling in me the importance of education. To my husband, An Quan, for encouraging me to pursue my career, for always taking care of me, and for supporting me through the long months in the dissertation cave. Thank you to my amazing sisters, Noelle and Linda Taniguchi, for their words of wisdom, thoughtful good luck trinkets, and constant support. Thank you to the Taniguchi, Kanemaki, Tayama, Quan, Tran, and Ho families for your unwavering support. To my amazing grandparents, Lois and Ned Taniguchi and Midori Tayama, you are my drive, you are my motivation, you are my everything.

CHAPTER 1

INTRODUCTION

Urbanization can lead to stream channel erosion through the increase in total and peak runoff and a decrease in hillslope sediment supply (Wolman, 1967; Hammer, 1972; Trimble, 1997; Hawley & Bledsoe, 2011). Wolman (1967) developed a conceptual model on urban processes, sediment production, and channel erosion for developed countries. The Wolman model includes an initial pre-disturbance phase with highly vegetated surfaces and low upstream sediment production, followed by a one to three-year construction phase characterized by high amounts of exposed soil, high sediment yield, and channel aggradation, and a final stage where the bare soil is replaced by impervious cover and landscaped vegetation with low sediment production, higher discharges, and stream channel erosion. With an increase in discharge and decrease in sediment supply, channels adjust to establish a dynamic equilibrium or a point in time where the sediment supply transported to the stream is approximately equal to the rate at which sediment is carried away by the stream (Lane, 1955).

Conceptual channel evolution models (CEMs) are used to describe the evolution of stream channel morphology over time in response to a disturbance in developed countries (Schumm et al., 1984; Thorne & Osman, 1988; Simon, 1989; Bledsoe et al., 2012; Booth & Fischenich, 2015). The traditional CEM for incised, single-thread streams include evolutionary stages of (I) a pre-disturbed stable channel followed by a disturbance that leads to (II) degradation via downcutting, (III) bank failure and widening, (IV) aggradation, and (V) an establishment of a quasi-equilibrium state (Schumm et al., 1984). Although CEMs can be used to predict the *likely* response of the channel to a disturbance, a single observation of channel condition can rarely predict the evolutionary trajectory of *every* stream channel due to differences in local geomorphic and/or hydrologic settings (Booth & Fischenich, 2015). Conceptual models developed by Wolman (1967) and Schumm et al. (1984) provide a

valuable foundation in understanding urban processes and channel evolution, however, these models may not apply to rapidly urbanizing, developing countries.

The process of urbanization can differ in developed and developing countries in ways that can impact stream channel morphology, including the patterns and rates of establishment of impervious surfaces (Biggs et al., 2010), the construction sequence of channelization, and complete removal of riparian buffers. Unauthorized developments account for a large fraction of the urban surface in many developing countries, including those within Latin America, Africa, and Asia (Davis, 2006). Unauthorized developments may have less access to resources for infrastructure development, and the lack of a city-wide planning authority which can lead to spatially discontinuous infrastructure (Balbo, 1993), and highly altered stream systems.

Despite decades of research on urbanization and stream channel erosion, primarily in humid environments (see reviews by Chin, 2006; Gregory, 2006) and more recently in arid environments (Chin & Gregory, 2001; Coleman et al., 2005; Hawley & Bledsoe, 2011; Hawley et al., 2012; Taniguchi & Biggs, 2015), very few studies have been conducted in semi-arid climates in developing countries that experience rapid urban growth, unregulated urban development on erodible soils, and variable enforcement of environmental regulations. Moreover, there are no conceptual or computational models of urban impacts on stream channel morphology in such contexts. The US-Mexico border presents a unique setting for investigating the impact of urban development on channel evolution, as such impacts can be quantified for cities in the United States (San Diego, CA) and Mexico (Tijuana, BC).

In Tijuana, Mexico, rapid urbanization has led to excessive erosion of the exposed soils and erodible stream channels during rainfall events (Figure 1), which contributes to sediment deposition that buries native vegetation, blocks tidal channels, and negatively alters the estuarine ecosystem in the Tijuana Estuary in San Diego, California (Zedler & Norby, 1986). Erosion also leads to a lower quality of life for people residing in Tijuana through the damage of homes built adjacent to alluvial stream channels, gully formation in dirt roads (Biggs et al., 2010), and deposition of solid waste (Grover, 2011). In the United States, large sedimentation basins were built at the outlet of Los Laureles Canyon watershed (LLCW), a small watershed (11.6 km^2) whose main channel flows from Tijuana, Mexico, under the U.S.-Mexico border through culverts, and empties into the southern arm of the Tijuana

Estuary, to try to capture the sediment and trash before it enters into the estuary, but millions of dollars are spent annually on basin excavation and the problem of erosion persists. Little is known about the dynamics of urbanization, hillslope and channel erosion processes, and sediment loadings to the Tijuana Estuary and in semi-arid developing countries in general. In response to this concern, the US Environmental Protection Agency (EPA), US Department of Agriculture (USDA) and various institutions are investigating the impact of land use changes in Tijuana, Mexico on the hydrology and sediment supply of LLCW to the Tijuana Estuary. Los Laureles Canyon watershed serves as a classic example of a hydrologically-flashy watershed in semi-arid southern California, but is located in a developing nation that has unregulated urban development adjacent to the stream channel and uncoordinated in-channel structure development, including concrete-lined reaches and culverts, mixed with highly erodible earthen channels.

A sediment budget for LLCW is vital for proper sediment mitigation plans, including a greater understanding of both hillslope and stream channel geomorphic processes. This dissertation focuses on the stream channel dynamics of Los Laureles Canyon, in collaboration with a Mexican doctoral candidate who is focusing his research on the hillslope processes (see Figure 2 for a conceptual sediment budget schematic). A sediment budget provides a valuable framework for managers to identify key erosional sources, whether from the hillslope or channel, and to make informed decisions about upstream sediment reduction practices (Owens, 2005; Walling & Collins, 2008). Understanding the role of channel processes in watershed sediment budgets is vital for proper sediment management and mitigation (Walling & Collins, 2008), especially in regions where the channel contribution is dominant (Trimble, 1997).

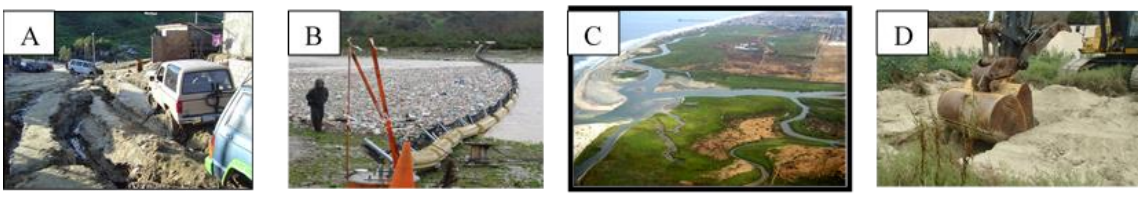

Figure 1. Field pictures depicting the sequence of events following rainfall in Tijuana, Mexico: A) Erosion from rainfall on unpaved roads; B) Flow carries sediment and trash across the U.S.-Mexico border; C) Sediment buries vegetation; D) Millions of dollars are spent on sediment removal in the Tijuana Estuary.

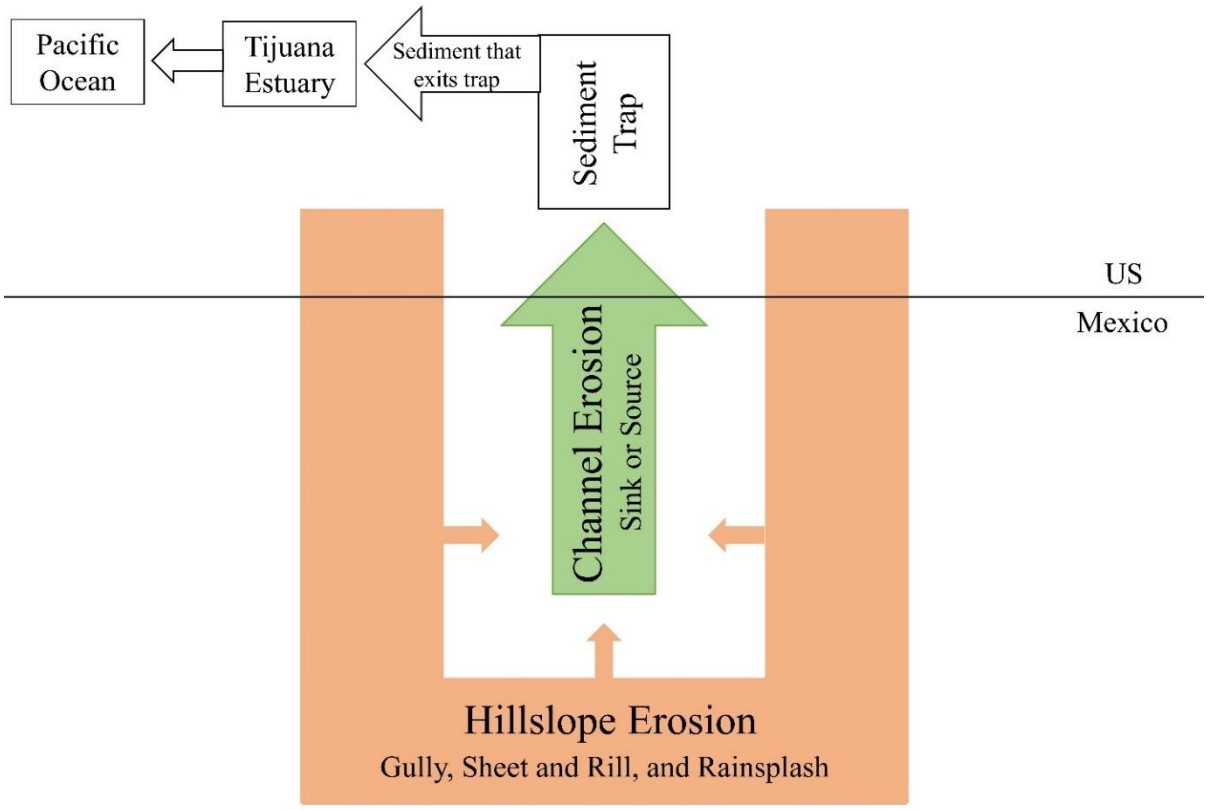

Figure 2. Conceptual sediment budget for Los Laureles Canyon in Tijuana, Mexico draining to the Tijuana Estuary in San Diego, California. This dissertation focuses on stream channel erosion.

Overview of Chapters

This dissertation is structured around three separate papers (Chapters 2-4) that investigates the impacts of urbanization and in-channel alterations on stream channel evolution in semi-arid Tijuana, Mexico.

Chapter 2, *Stream channel erosion in a rapidly urbanizing region of the US-Mexico Border: Documenting the importance of channel hardpoints with Structure-from-Motion photogrammetry*, describes the spatial patterns in stream channel geometry in a rapidly urbanizing watershed, Los Laureles Canyon (LLCW), in Tijuana, Mexico and provides a regional comparison of channel erosion in Tijuana to reference and urbanized watersheds in southern California. This paper highlights the prevalence of channel instability downstream of hardpoints, or in-channel structures such as culverts and concrete flumes, and provides a

foundation for examining the effect of urban development on channel erosion in semi-arid, developing countries. However, the mechanisms driving channel instability downstream of hardpoints are unknown. To quantitatively evaluate channel evolution and determine the driving mechanisms to channel instability, field data collected in Chapter 2, serves as input data to the numerical model utilized in Chapters 3 and 4.

Chapter 3, titled *Quantifying the Relative Effects of Compounded Channel Alterations on Stream Channel Evolution in a Rapidly Urbanizing, Semi-Arid Region*, uses field data collected in Chapter 2 and CONCEPTS (CONservational Channel Evolution and Pollutant Transport System), a computational model of channel evolution developed by the USDA, to provide a mechanistic explanation of channel evolution downstream of hardpoints in Tijuana, Mexico to determine what mechanisms are driving channel instability. A scenario analysis was conducted to quantitatively assess the impact of urban channel alterations, including hardpoint installation, slope alteration, bed composition change, and vegetation removal, on channel incision, widening, and sediment load. This paper provides a quantitative understanding of the processes that contribute to downstream instability from urban channel alterations in semi-arid, developing countries.

Chapter 4 is titled *Modeling channel sources and sinks of sediment in a semi-arid urbanizing environment: CONCEPTS-AnnAGNPS integrated model for Los Laureles Canyon watershed* and uses a watershed-scale model of hillslope processes, AnnAGNPS, integrated with a computational channel evolution model, CONCEPTS to determine the spatial pattern of channel sources and sinks of sediment in LLCW and evaluate the overall importance of channel processes on the sediment budget for future sediment mitigation plans. This paper demonstrates the utility of integrating an empirically-based watershed scale model of hydrology and hillslope processes with a physically-based channel evolution model to evaluate watershed sediment budgets in a rapidly developing, semi-arid region.

This research contributes to an EPA Regional Applied Research Effort (RARE) Project, Sediment Load Estimation of the Tijuana River Watershed Under Existing Conditions and the Future Alternative Scenarios for Best Management Practice Implementation (Interagency Agreement ID # DW-12-92390601-0) in collaboration with the US Department of Agriculture (USDA, Agreement # 58-6408-4-015), San Diego State University (SDSU), Centro de Investigación Científica y de Educación Superior de Ensenada

(CICESE), and University of Córdoba (Spain). This dissertation provides insight to management on the impacts of urbanization and in-channel alterations on stream channel erosion in semi-arid, rapidly developing nations. This insight will allow for a better understanding of the driving mechanisms to channel instability in such environments, and to identify hotspots of erosion for targeted sediment and erosion mitigation practices.

REFERENCES

Balbo, M. (1993). Urban-Planning and the Fragmented City of Developing-Countries. *Third World Planning Review*, *15*(1), 23–35.

Biggs, T. W., Atkinson, E., Powell, R., & Ojeda-Revah, L. (2010). Land cover following rapid urbanization on the US-Mexico border: Implications for conceptual models of urban watershed processes. *Landscape and Urban Planning*, *96*(2), 78–87. https://doi.org/10.1016/j.landurbplan.2010.02.005

Booth, D. B., & Fischenich, C. J. (2015). A channel evolution model to guide sustainable urban stream restoration. *Area*, n/a-n/a. https://doi.org/10.1111/area.12180

Chin, A. (2006). Urban transformation of river landscapes in a global context. *Geomorphology*, *79*(3–4). https://doi.org/10.1016/j.geomorph.2006.06.033

Chin, A., & Gregory, K. J. (2001). Urbanization and Adjustment of Ephemeral Stream Channels. *Annals of the Association of American Geographers*, *91*(4), 595–608. https://doi.org/10.1111/0004-5608.00260

Coleman, D., Macrae, C., & Stein, E. D. (2005). *Effect of Increases in Peak Flows and Imperviousness on the Morphology of Southern*. Costa Mesa, CA.

Davis, M. (2006). *Planet of Slums*. New York: Verso.

Gregory, K. J. (2006). The human role in changing river channels. *Geomorphology*, *79*(3–4), 172–191. https://doi.org/10.1016/j.geomorph.2006.06.018

Grover, R. (2011). *Local perspectives on environmental degredation and community infratructure in Los Laureles Canyon, Tijuana, Mexico*. San Diego State University. https://doi.org/10.1007/s13398-014-0173-7.2

Hammer, T. R. (1972). Stream channel enlargement due to urbanization. *Water Resources Research*, *8*(6), 1530–1540. https://doi.org/10.1029/WR008i006p01530

Hawley, R. J., & Bledsoe, B. P. (2011). How do flow peaks and durations change in suburbanizing semi-arid watersheds? A southern California case study. *Journal of Hydrology*, *405*(1–2). https://doi.org/10.1016/j.jhydrol.2011.05.011

Hawley, R. J., Bledsoe, B. P., Stein, E. D., & Haines, B. E. (2012). Channel Evolution Model of Semiarid Stream Response to Urban-Induced Hydromodification. *Journal of the American Water Resources Association*, *48*(4), 722–744. https://doi.org/10.1111/j.1752-

1688.2012.00645.x

Lane, E. W. (1955). The importance of fluvial morphology in hydraulic engineering. *Proceedings of American Society of Civil Engineers*, *81*(795), 1–17.

Owens, P. (2005). Conceptual Models and Budgets for Sediment Management at the River Basin Scale. *Journal of Soils and Sediments*, *5*(4), 201–212. https://doi.org/10.1065/jss2005.05.133

Schumm, S. A., Harvey, M. D., & Watson, C. C. (1984). *Incised channels: morphology, dynamics, and control*. Water Resources Publications. Retrieved from https://books.google.com/books?id=KLoPAQAAIAAJ

Simon, A. (1989). A model of channel response in disturbed alluvial channels. *Earth Surface Processes and Landforms*, *14*(1), 11–26. https://doi.org/10.1002/esp.3290140103

Taniguchi, K., & Biggs, T. W. (2015). Regional impacts of urbanization on stream channel geometry: A case study in semi-arid southern California. *Geomorphology*, *248*, 228–236. https://doi.org/10.1016/j.geomorph.2015.07.038

Thorne, C. R., & Osman, A. M. (1988). The influence of bank stability on regime geometry of natural channels. In *International conference on river regime* (pp. 135–147).

Trimble, S. W. (1997). Contribution of stream channel erosion to sediment yield from an urbanizing watershed. *Science*, *278*(5342), 1442–1444. https://doi.org/10.1126/science.278.5342.1442

Walling, D. E., & Collins, A. L. (2008). The catchment sediment budget as a management tool. *Environmental Science and Policy*, *11*(2), 136–143. https://doi.org/10.1016/j.envsci.2007.10.004

Wolman, M. G. (1967). A Cycle of Sedimentation and Erosion in Urban River Channels. *Geografiska Annaler. Series A, Physical Geography*, *49*(2/4), 385–395. Retrieved from http://www.jstor.org/stable/520904

Zedler, J. B., & Norby, C. S. (1986). *the Ecology of Tijuana Estuary, California: An Estuarine Profile*.

CHAPTER 2

Stream channel erosion in a rapidly urbanizing region of the US-Mexico border: documenting the importance of channel hardpoints with Structure-from-Motion photogrammetry

ABSTRACT

Urbanization can lead to accelerated stream channel erosion, especially in areas experiencing rapid population growth, unregulated urban development on erodible soils, and variable enforcement of environmental regulations. A combination of field surveys and Structure-from-Motion (SfM) photogrammetry techniques were used to document spatial patterns in stream channel geometry in a rapidly urbanizing watershed, Los Laureles Canyon (LLCW), in Tijuana, Mexico. Ground-based SfM photogrammetry was used to map channel dimensions with 1 to 2 cm vertical mean error for four stream reaches (100-300 m long) that were highly variable and difficult to survey with differential GPS. Regional channel geometry curves for LLCW had statistically larger slopes and intercepts compared to regional curves developed for comparable, undisturbed reference channels. Cross-sectional areas of channels downstream of hardpoints, such as concrete reaches or culverts, were up to 64 times greater than reference channels, with enlargement persisting, in some cases, up to 230 m downstream. Percent impervious cover was not a good predictor of channel enlargement. Proximity to upstream hardpoint, and lack of riparian and bank vegetation paired with highly erodible bed and bank materials may account for the instability of the highly enlarged and unstable cross-sections. Channel erosion due to urbanization accounts for approximately 25-40% of the total sediment budget for the watershed, and channel erosion downstream of hardpoints accounts for one third of all channel erosion. Channels downstream of hardpoints should be stabilized to prevent increased inputs of sediment to the Tijuana Estuary and local hazards near the structures, especially in areas with urban settlements near the stream channel.

1. INTRODUCTION

Following urbanization and an increase in impervious cover, watersheds typically experience an increase in total and peak runoff and a decrease in hillslope sediment supply, resulting in stream channel erosion (Wolman, 1967; Hammer, 1972; Trimble, 1997; Hawley & Bledsoe, 2011). Channel erosion can lead to physical damage to the stream channel, mobilization of excess sediment, and ecological harm to aquatic ecosystems and downstream habitats (Trimble, 1997; Walsh et al., 2016). Unstable channels and subsequent infrastructure failure can also incur significant financial costs and threaten human safety (Gregory, 2006).

Many studies have documented the impact of urbanization on stream channel erosion and its relationship to watershed characteristics, such as percent impervious cover (Hawley & Bledsoe, 2013, Taniguchi & Biggs, 2015) and geology, slope, and land cover (Booth et al., 2010; Splinter et al., 2010). Although watershed characteristics may predict channel enlargement in many cases, they may not be the only factor in causing stream channel erosion. Local factors, such as proximity to hardpoints like road crossings or bridges, may also play an important role in channel erosion (Takken et al., 2008; Katz et al., 2014) and can lead to spatial variability in morphological adjustment (Chin & Gregory, 2001). Road crossings can cause channel scour immediately downstream in watersheds in arid climates due to increased runoff from the road surface (Chin & Gregory, 2001) and increased flood peak flows from channelization have caused channel instability for over 100 m downstream of such hardpoints (Brookes, 1987). A mix of local factors such as channel realignment, concrete-lined channelization of some stream reaches, addition of culverts, and an input of anthropogenic coarse particles into the channel, including wood, car parts, and pipes, have also contributed to the spatial variability in channel response to urbanization (Grable & Harden, 2006).

Urbanization processes in developing countries may differ from those in developed countries in ways that have greater impact on stream channel erosion, including the patterns and rates of establishment of impervious surfaces (Biggs et al., 2010) and the types and construction sequence of channelization and drainage infrastructure. Unauthorized or "irregular" developments account for a large fraction of the urban surface in many developing countries, including those within Latin America, Africa, and Asia (Davis, 2006).

Irregular developments may have less access to resources for infrastructure development, and the lack of a city-wide planning authority in such developments can cause spatially discontinuous infrastructure development (Balbo, 1993), including channelization and drainage. Despite decades of research on urbanization and stream channel erosion, primarily in humid environments (see reviews by Chin, 2006; Gregory, 2006) and more recently in arid environments (Chin & Gregory, 2001; Coleman et al., 2005; Hawley & Bledsoe, 2011; Hawley et al., 2012; Taniguchi & Biggs, 2015), very few studies have been conducted in semi-arid climates in developing countries experiencing rapid population growth, unregulated urban development on erodible soils, and variable enforcement of environmental regulations. The US-Mexico border presents a laboratory for investigating the impact of development level on stream channel response to urbanization, as such impacts can be quantified for cities in the United States (San Diego, CA) and Mexico (Tijuana, BC). Los Laureles Canyon watershed (LLCW) in Tijuana, Mexico, serves as a classic example of a hydrologically-flashy watershed in semi-arid southern California, but is located in a developing nation that has unregulated urban development adjacent to the stream channel and uncoordinated in-channel structure development, including concrete-lined reaches and culverts, mixed with highly erodible earthen channels.

Traditional surveys of stream channels measure channel geometry at discrete locations, but such surveys are time consuming and may not adequately document the geometry of complex channels that change rapidly over short distances. Remote sensing techniques including three-dimensional (3-D) photo-reconstruction and Structure-from-Motion (SfM) photogrammetry can be used to create detailed digital elevation models (DEMs) with open-source, or freely available, software packages and require little training and equipment (James & Robson, 2012; Castillo et al., 2015). Systematic errors such as vertical doming or the 'dome effect' can occur in SfM-derived DEMs, typically from near-parallel images acquired from unmanned aerial vehicles (UAVs) or inaccurate correction of radial lens distortion (Wackrow & Chandler, 2008, 2011; James & Robson, 2014). Doming errors can be mitigated by including more oblique images in the image network, the inclusion of additional ground control points, and/or utilization of a reliable camera model (Wackrow & Chandler, 2008, 2011; James & Robson, 2014). SfM photogrammetry techniques have been utilized in various geomorphic studies (James & Robson, 2012; Turner et al., 2012;

Westoby et al., 2012; Gómez-Gutiérrez et al., 2014; Micheletti et al., 2014) and can be used to map and extract stream channel (Javernick et al., 2014; Dietrich, 2015; Prosdocimi et al., 2015) and gully dimensions (Castillo et al., 2012).

Understanding the role of channel processes in watershed sediment budgets is vital for proper sediment management and mitigation (Walling & Collins, 2008). A sediment budget provides a valuable framework for managers to identify key erosional sources, whether from the hillslope or channel, and to make informed decisions about upstream sediment reduction practices (Owens, 2005; Walling & Collins, 2008). Detailed channel evaluations, such as that conducted in this study, can be used to identify the most vulnerable stream reaches and the magnitude and type of future instabilities for proper, sediment mitigation practices (Andrew Simon & Downs, 1995).

This study investigates urbanization and stream channel erosion in Tijuana, Mexico, through a mix of field topographic survey methods, including SfM photogrammetry and differential GPS, and a comparison of channel geometry to undeveloped and urbanized watersheds in southern California. The overall goal of this study is to quantify how channels respond to rapid urbanization and in-channel infrastructure development in a semi-arid region and developing country. More specifically, our research objectives are to: 1) utilize and validate Structure-from-Motion photogrammetry techniques to map channel morphology of highly enlarged stream reaches; 2) investigate how the type and magnitude of channel response to urbanization in Tijuana compare with urbanized areas in a neighboring developed country (San Diego, CA); 3) identify factors that impact channel change, including watershed characteristics such as impervious surface cover and local channel characteristics such as hardpoints; and 4) quantify the impact of channel erosion, including erosion downstream of hardpoints, on the sediment budget.

2. STUDY AREA

Los Laureles Canyon watershed (LLCW) is a bi-national watershed (11.6 km^2) whose main channel flows from Tijuana, Mexico, under the U.S.-Mexico border through culverts, and empties into the southern arm of the Tijuana Estuary (Figure 1). The Tijuana Estuary is located entirely in the United States, is one of the largest estuarine wetlands left in California, and provides vital habitat to an array of species (Weis et al., 2001). The watershed

contributing flow and sediment to the estuary includes the LLCW, two additional small watersheds, and the larger Tijuana River watershed (4,400 km^2), which is approximately two-thirds in Mexico. Excessive erosion in LLCW has accelerated the rate of sedimentation in the Tijuana Estuary (Webber, 2010), altering the natural ecosystem through the burial of vegetation, negatively affecting the native species and allowing exotic species to invade and thrive (Zedler & Norby, 1986). Two large sediment traps were built at the outlet of LLCW in the Tijuana Estuary to try to prevent sediment from entering into the estuary (Figure 1), but millions of dollars are spent annually on trap excavation and on extreme wet years, traps can fill up and overflow. Excessive erosion in LLCW also poses a threat to the infrastructure and people living in the watershed, many of which live adjacent to unstable stream channels or on steep, erodible slopes.

LLCW is hydrologically similar to many semi-arid watersheds in southern California with Mediterranean climate. The 30-year mean annual precipitation is 238 mm (PRISM Climate Group, Oregon State University, http://prism.oregonstate.edu, created 7 July 2010) and the flow regime is flashy with infrequent but geomorphically-significant large flow events. LLCW lies on the highly erodible San Diego Formation, which consists of fine- to medium-grained, poorly indurated and loosely consolidated sandstone and cobbly conglomerate (Kennedy & Peterson, 1975). Soils in the LLCW are classified as "highly erodible" according to Hanson's soils classification diagram (Pinettes et al., 2011), with critical shear stress ranging from 0.001 to 4.6 Pa and erodibility (k) ranging from 103 to 879 $cm^3\ N^{-1}\ s^{-1}$ (Biggs et al., 2018a). The stream channel network includes concrete-lined and earthen reaches with ten in-channel structures or hardpoints, including concrete flumes and culverts. The channel network includes one main channel ("Main") and two tributaries in the southwest (SW) and southeast (SE) (Figure 1). During urban development in the watershed, vegetation on the hillslopes, floodplain, and the channel is routinely cleared, leaving large proportions of exposed, erodible soils. During road grading, smaller channels are often filled in completely and reform during large flow events.

Reference or minimally disturbed channels were surveyed at Spring Canyon to serve as a baseline comparison to LLCW. Spring Canyon is located just north of the US-Mexico border near San Ysidro, approximately 8 km northeast of LLCW, and is the only minimally developed (<3% impervious) watershed entirely on the San Diego Formation (Figure 1).

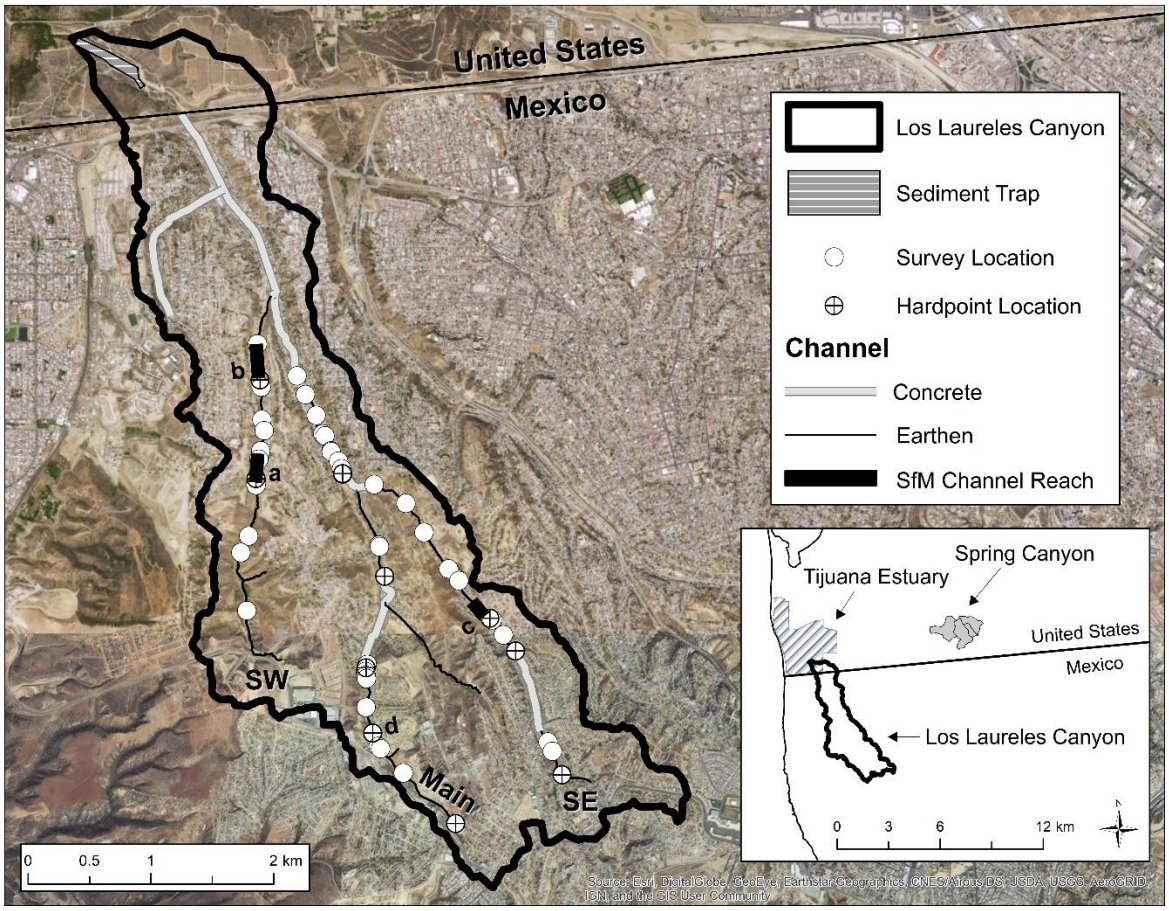

Figure 1. Study area of Los Laureles Canyon watershed and survey locations on earthen stream reaches. The Los Laureles stream channel is composed of earthen and concrete reaches and has three tributaries (SW, Main, and SE). There is a total of ten hardpoints, four hardpoint locations are labeled: a) SW metal culvert; b) SW concrete flume; c) SE hardpoint; and d) Main culvert (San Bernardo). Reference channels were surveyed at Spring Canyon.

3. METHODS

Channel cross-sectional area at capacity was surveyed at representative stream reaches using a mix of field methods including channel surveys utilizing a differential GPS (DGPS) and Structure-from-Motion (SfM) photogrammetry techniques. The combined dataset was used to develop regional channel geometry relationships and compared to regional relationships developed for southern California (Modrick & Georgakakos, 2014) and San Diego County (K. Taniguchi & Biggs, 2015). The following subsections provide a further description of the methodology utilized in this study.

3.1 Channel cross-sections with differential GPS

The earthen stream channel network in LLCW was surveyed using differential GPS (Trimble Geo7X) at 39 representative locations, which were chosen based on changes in channel geometry, channel condition, and/or bed and bank composition over space. Although portions of the stream network were channelized with concrete, only the earthen, alluvial channels were included in this analysis. At each location, the channel cross-sectional area was surveyed with a differential GPS with sub-centimeter to 5 cm vertical accuracy, and cross-sectional area at channel capacity (*A*) was defined by the major break in slope between the defined channel and floodplain (Leopold, 1994). The particle size distribution of the surficial bed material was measured using the Wolman (1954) pebble count method and channel stability was qualitatively assessed.

3.2 Structure-from-Motion photogrammetry surveys

Structure-from-Motion (SfM) photogrammetry was utilized to create detailed digital elevation models (DEMs) (Westoby et al., 2012; Castillo et al., 2015) for three highly enlarged stream reaches (hardpoint locations a, b, and c; see Figure 1) that were difficult to survey and had complex channel dimensions. The SW concrete flume reach was relatively long (400 m), and was split into two reconstructions. The reconstructed length of each reach is approximately 200 m (SW metal culvert), 300 m (SW concrete flume, downstream), 100 m (SW concrete flume, upstream) and 155 m (SE hardpoint). A minimum of ten 20 x 20 cm colored and numbered control markers were placed along the bed and banks of the channel for the entire reach length, including at minimum four error control points (ECPs), whose locations were surveyed with the differential GPS. A modified GoPro Hero3+ camera with a non-distortion lens with 4.14 mm focal length and f/3.0 aperture (Peau Productions, CA, USA, http://www.peauproductions.com/) was mounted to a telescoping painter's pole approximately 2-3 m long. The camera was set to time-lapse capture mode (1 image per second) and images were acquired by slowly walking up and down the stream reach two times, first with the camera facing upstream and second with the camera facing downstream to ensure high degree of overlap between images and to minimize topographic shading effects (Castillo et al., 2015).

The series of overlapping images was post-processed with freely available software packages to produce a 10 cm DEM: VisualSfM (Wu, 2013, 2015), SfM_Georef (James & Robson, 2012), and CloudCompare ("CloudCompare v2.5.5.2," 2015). VisualSfM uses SfM and Multiview stereo (MVS) to automatically match image texture in various images and determine the 3-D geometry of a static environment (James & Robson, 2012) and was used to create the dense point clouds. For a subset of three out of four stream reaches, to account for potential doming effects, camera calibration was conducted using the Fraser distortion model on a calibration dataset in a freely available software package called MicMac (Deseilligny & Clery, 2011; Stöcker, 2015) and dense point clouds were reconstructed using the camera model and PMVS2 software (Furukawa & Ponce, 2010; James & Robson, 2012; Castillo et al., 2015). The point clouds were georeferenced using SfM_Georef by manually identifying the GCPs in various images and transforming the point clouds from a relative coordinate system to the coordinate system of the GCPs (Castillo et al., 2015). Each control point needs to be visible and identified in at least two images and a minimum of 3 GCPs are needed to georeference the entire point cloud. The ECPs were used only for the error analysis.

Following Castillo et al. (2015), the georeferenced point clouds were filtered, merged, and converted to a 10 cm DEM using CloudCompare. A total of eighteen cross-sections were extracted from the four DEMs in ESRI ArcMap 10.2 by drawing lines perpendicular to the channel centerline, and extracting the elevation from each DEM cell. Cross-sectional area at channel capacity was identified by plotting each cross-section and identifying the major change in slope between the channel bank and the floodplain. All extracted cross-sections had well-defined banks, making channel capacity easily identifiable.

3.3 Structure-from-Motion error analysis

The mean error (*ME*) and standard deviation of error were calculated for the horizontal (x and y) and vertical (z) dimensions for each point cloud (Table 1). The mean error (*ME*) at the ECPs ranges from -14 to 7 cm in the horizontal x-y dimensions and 1 to 2 cm in the vertical z dimension, with overall model mean error in the x-y-z dimensions from -2 to 2 cm (Table 1). The standard deviation of error for the ECPs ranges from 5 to 26 cm in the horizontal x-y dimensions and 3 to 13 cm in the vertical z dimension, with overall

standard deviation of error in the x-y-z dimensions from 12 to 25 cm (Table 1). The subset of three camera calibrated models have lower mean error (-0.5 to -0.9 cm) and standard deviation of error (2 to 7 cm) compared to the uncalibrated models, but all sixteen extracted cross-sections from the uncalibrated and calibrated models have near identical cross-sectional shape and areas, indicating that there are little to no systematic deformations or "doming" in the uncalibrated SfM-derived DEMs. Areas showing elevation changes greater than ±0.5 m were typically located on the floodplain near the periphery of the models (Figure 2). Two cross-sections extracted from the camera calibrated models had a slightly larger cross-sectional area (2 and 5% increase) compared to the uncalibrated extracted cross-sections, but the channel shape was the same for both.

Table 1. Mean error (ME) and standard deviation of error in the x, y, and z dimensions at the error control points (ECPs) and comparison of cross-sectional areas from SfM and GPS from the SW reaches. A_{SfM} is the DEM extracted cross-sectional area, A_{DGPS} is the surveyed cross-sectional area, and Absolute Diff. is the absolute difference between A_{SfM} and A_{DGPS}. Locations a-c are labeled in Figure 1.

Location	SfM Reach	Total ECPs	Mean Error (cm)				Standard Deviation of Error (cm)				Cross Section (m^2)			
			X	Y	Z	XYZ	X	Y	Z	XYZ	A_{SfM}	A_{DGPS}	Absolute Diff.	% Diff.
a	SW Metal Culvert	6	1	4	2	2	5	16	3	14	32.4	33.7	-1.3	-4
b_1	SW Concrete Flume, downstream	10	-11	6	1	-1	31	26	13	25	33.1	39.4	-7.5	-16
b_2	SW Concrete Flume, upstream	6	-1	0.4	2	1	11	13	8	12	14.9	15.8	-0.9	-6
c	SE Hardpoint	4	-14	7	1	-2	8	24	12	17	-	-	-	

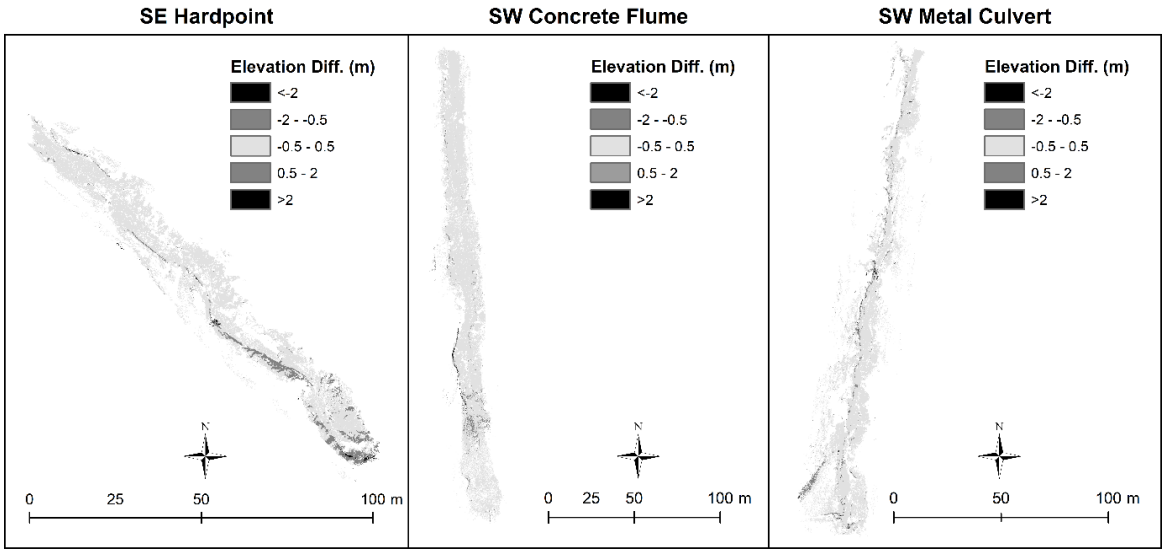

Figure 2. Digital elevation model (DEM) difference maps based on the uncalibrated and camera calibrated SfM-derived models. Mean elevation change ranged from 3 to 13 cm, with elevation changes greater than ±0.5 m located on the floodplain near the periphery of the models.

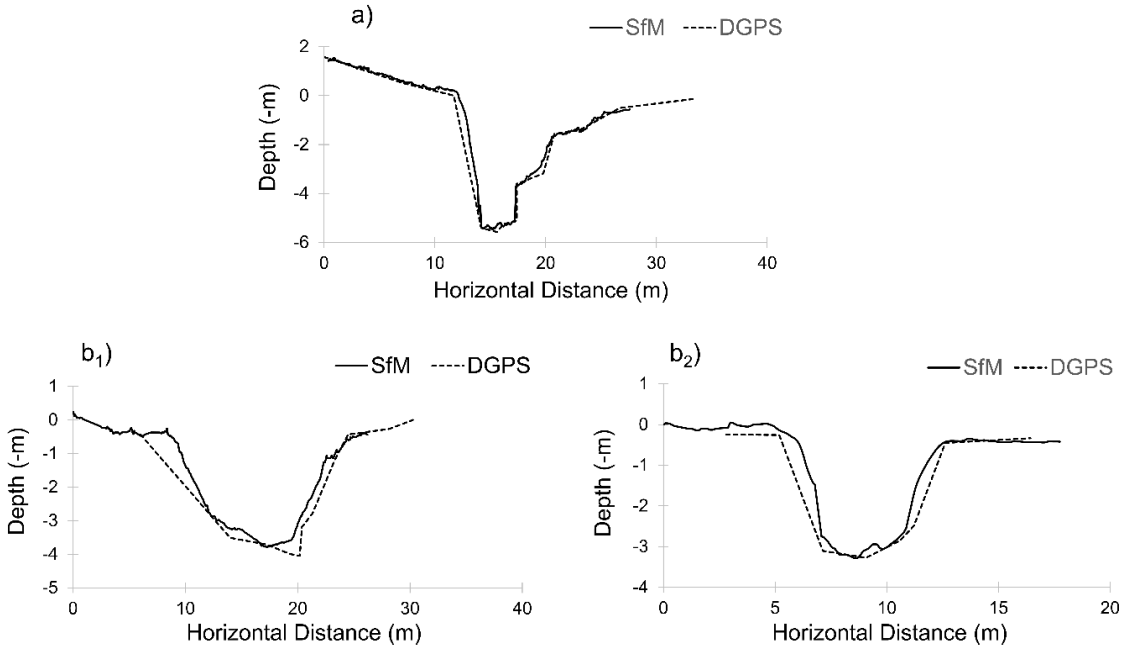

Figure 3. Comparison of surveyed cross-sections with a differential GPS (DGPS) and SfM derived DEM extracted cross-sections near two hardpoint locations in the SW channel: a) SW metal culvert; b_1) SW concrete flume, downstream; and b_2) SW concrete flume, upstream. Portions of steep banks may be cut off using a DGPS, leading to an overestimation in cross-sectional area (b_2).

The overall shape of the channel and cross-sectional area from the SfM-derived and differential GPS surveyed cross-sections match well, from -4% to -16% difference, and show that '*A'* derived from the uncalibrated SfM DEMs can be utilized with confidence (Figure 3). At the three SW locations having both SfM and GPS derived cross-sections, '*A'* from SfM is smaller than '*A'* from the GPS, but errors are relatively small, with a mean percent difference of -8%. Cross-sections extracted from SfM-derived DEMs may be more accurate than cross-sectional surveys with a differential GPS due to a higher density of topographic points represented in the 3-D models (Figure 3). When surveying the stream channel with a differential GPS, elevation points were taken at major changes in the slope, but topographic features may be smoothed over and portions of the steep banks may be cut off (i.e. cut off left and right banks in Figure 3 b_2) resulting in an overestimation in the cross-sectional area using a differential GPS or traditional survey methods. The cross-sectional comparison for the SE hardpoint was not made due to limited image overlap near the upstream end of the reach where the GPS cross-section was taken.

The largest errors in the 3-D models were found at the channel perimeter, due to the lower overlap between images and poorer convergence of perspectives. For future studies, if greater accuracies were pursued with a similar methodology, utilizing a low-cost pole with a camera and walking-pace photography, it would be advisable to calibrate the camera for each field survey with a specific image set (see recommendations in MicMac´s manual, IGN 2017) and collect the images along both channel margins to ensure better overlap and perspectives on the periphery, preferably along the upstream direction where there is better perspectives of the channel.

SfM-derived DEMs in this study results in similar or lower errors in comparison to other studies on SfM applications of rivers and gullies, despite being a highly time- and cost-efficient approach. Riverscape mapping using SfM photogrammetry and overlapping imagery from an unmanned aerial vehicle (UAV) resulted in errors from 10 cm to 1 m in the horizontal and vertical dimensions (Dietrich, 2015) and with a helicopter as low as 10 cm vertical error (Javernick et al., 2014). Ground-based SfM techniques used in this study may have lower errors due to the additional oblique camera angles in comparison to the near-parallel flight lines and viewing angles from UAV or aerial acquired images, which can lead to systematic deformations or vertical doming in the resulting DEMs (James & Robson,

2014; Dietrich, 2015). UAV and ground-based methods have been combined to create low-error topographic models of gullies with accuracy of 1 cm (Stöcker, 2015). Ground-based SfM photogrammetry techniques are a cost effective and accurate way to map river reaches that are free of vegetation, highly variable in channel dimensions, and difficult to survey with the traditional survey-level and rod or GPS.

3.4 Regional channel geometry curves and impervious surface cover

Studies investigating the impact of urbanization on stream channel geometry should ideally compare channel dimensions at discrete locations before, during, and after urbanization (Leopold, 1973), but in many cases channel dimensions prior to urbanization are unknown. A space-for-time substitution method is used in this study to compare channels in urbanized watersheds (LLCW) to channels in undeveloped watersheds (San Diego and southern California) using regional channel geometry curves (Hammer, 1972; Chin & Gregory, 2001; Navratil et al., 2013; Taniguchi & Biggs, 2015). Regional channel geometry curves (regional curves) were developed for LLCW using the surveyed cross-sectional data (N=39) and the SfM-derived cross-sections (N=18) combined. Regional curves relate channel cross-sectional area at capacity (A) to watershed area (A_w):

$$A = \alpha A_w^{\beta} \quad (1)$$

where 'A' is in m^2, A_w is in km^2, and α and β are coefficients (Dunne & Leopold, 1978).

Regional reference curves, which served as the baseline under non-urban reference conditions for comparison to the LLCW channel survey, were taken from the literature for southern California (Modrick & Georgakakos, 2014) and San Diego County (K. Taniguchi & Biggs, 2015) and supplemented by additional field surveys. Due to potential geological differences between the LLCW and the streams in the literature (Modrick & Georgakakos, 2014; K. Taniguchi & Biggs, 2015), an additional reference curve was developed from a field survey conducted in Fall 2016 in Spring Canyon, which drains the same erodible San Diego Formation as LLCW (Figure 1). In Spring Canyon, 10 channel cross-sections were surveyed with a differential GPS and had watershed areas ranging from 0.12 to 1.3 km^2. For the San Diego County regional curves, watershed area ranged from 0.3 to 1,847 km^2 (K. Taniguchi & Biggs, 2015).

The channel enlargement ratio (*ER*) was calculated as '*A'* observed at LLCW divided by '*A'* predicted from the regional reference curves. The impact of the regional reference curve on the *ER* was determined by using both the San Diego County curve from Taniguchi and Biggs (2015) and the curve from Spring Canyon to calculate the *ER* for each cross-section in LLCW.

Percent impervious cover (IC) was calculated for the watersheds draining to the surveyed cross-sections in LLCW from an updated 2003 vegetation-impervious-soil (VIS) map by Biggs et al. (2010). To account for the potential increase in impervious surfaces since 2003, Google Earth imagery from 2012 (Google Earth, 11/11/2012, 2016 DigitalGlobe) was used to update the 2003 VIS map. To do this, a land use map for 2012 was first generated by visual interpretation, on-screen digitizing and classification of the 2012 imagery into seven land use categories (agriculture, rangeland, paved urban, dispersed unpaved urban, urban unpaved, unpaved levelled land, and sediment trap). Land cover validation points (N=1000) were randomly generated within LLCW and the land cover from the 2012 imagery at each point was classified as either vegetation, impervious, or soil. IC for 2012 (IC_{2012}) was calculated as the percent of validation points that were classified as impervious for each of the seven land use categories. IC for 2003 (IC_{2003}) for each of the seven land use categories was tabulated from the 2003 VIS map. IC_{2003} and IC_{2012} were plotted and a linear regression equation was developed ($IC_{2012} = 2.2\ IC_{2003} - 11.2$; $r^2 = 0.89$). Impervious cover has increased by 2-fold over the 9-year period. For each surveyed cross-section, the IC_{2003} draining the upstream watershed was calculated from the 2003 VIS map, and IC_{2012} was calculated from the regression equation and used in this study.

To analyze the impact of hardpoints on downstream cross-sectional area, the cross-sectional area was plotted versus distance downstream from the watershed divide and stratified into two groups: within hardpoint influence (HP) and not within hardpoint influence (NHP). Cross-sections that were downstream of a hardpoint and enlarged were considered "within hardpoint influence". Downstream channel recovery distance, or the downstream distance of hardpoint-induced enlargement, was defined as the distance in which the channel recovers to the '*A'* upstream of the hardpoint and/or becomes stable, and was identified visually on the plot of downstream distance versus '*A'*. Downstream of the ten hardpoints, there were twenty-one survey locations that were within hardpoint influence (HP). In the

SW channel, the four downstream-most cross-sections near the confluence with the Main channel had high errors in the GPS and were excluded from the analysis. Channel surveys conducted in 2009 were used instead of the high error cross-sections to determine downstream recovery distance for that reach, but were excluded from all other analyses. Based on field interpretation and image comparison of the four cross-sections between 2009 and 2014, there were no signs of channel erosion and no substantial change in cross-sectional area.

Regional curves were developed for both HP and NHP cross-sections using linear regressions on the log-transformed variables. Statistical significance of the difference in slopes (β) and intercepts (α) of the HP, NHP, and reference regional curves were tested using analysis of covariance (ANCOVA) (Chaplin, 2005; Johnson & Fecko, 2008; K. Taniguchi & Biggs, 2015). The San Diego County and southern California regional reference curves included channels from a wide range of drainage areas compared to the smaller drainage areas from LLCW. Channels draining larger watersheds could potentially alter the α and β values in the regional curves. A subset of channels with smaller drainage areas ($A_w < 15$ km^2) from both San Diego County and southern California reference data was also used in the ANCOVA analysis to control for the potential impact of larger watersheds on the regional regression parameters.

3.5 Relative sediment contribution from channel erosion

The mass of sediment (tons) generated from channel erosion due to urbanization (M_{urban}) was calculated for the 57 earthen cross-sections as:

$$M_{urban} = \sum_{i=1}^{57} \rho_b \left(A_{LLCW\,i} - A_{ref\,i} \right) L_i \qquad (2)$$

where $A_{LLCW\,i}$ is the cross-sectional area (m^2) at LLCW survey location i, $A_{ref\,i}$ is the predicted cross-sectional area (m^2) prior to urbanization for survey location i, L_i is the reach length for survey location i (m), ρ_b is the estimated bulk density of the soil (1.67 tons/m^3), and 57 is the total number of earthen cross-sections, including those surveyed with GPS and SfM. $A_{ref\,i}$

was estimated using both the reference curve from Spring Canyon, and from the reference curve for San Diego County for the given watershed area at survey location *i* (K. Taniguchi & Biggs, 2015).

The mass of sediment (tons) generated from the ten hardpoints (M_{HP}) was calculated as:

$$M_{HP} = \sum_{i=1}^{10} \sum_{j=1}^{n_i} \rho_b \left(A_{HP\,i,j} - A_{NHP\,i,j} \right) L_{i,j} \qquad (3)$$

where 10 is the total number of hardpoints (*i*) and n_i is the total number of HP survey locations (*j*) at hardpoint *i*, $A_{HP\,i,j}$ is the cross-sectional area (m^2) for HP *i* at HP survey location *j*, $A_{NHP\,i,j}$ is the estimated cross-sectional area (m^2) not within hardpoint influence for HP *i* at HP survey location *j*, $L_{i,j}$ is the reach length (m) for HP *i* at HP survey location *j*, and ρ_b is the estimated bulk density of the soil (1.67 tons/m^3). The total number of hardpoint survey locations is 21. $A_{NHP\,i,j}$ was locally estimated by linearly interpolating the nearest upstream A_{NHP} to the nearest downstream A_{NHP}. M_{urban} and M_{HP} were divided by the watershed mean time since the start of urbanization, to get the sediment yield (t y^{-1}) due to urbanization and hardpoints.

The sediment supply from channel erosion (M_{urban}) may be underestimated due to additional sediment supplied to the channel directly by residents of LLCW (Figure 4). Residents fill in channels with sediment and construction debris following rainfall events to try to prevent the channel from eroding their property. The added sediment is from grading of new development zones and debris from construction sites within LLCW and nearby areas. There is large uncertainty about the volume of fill sediment added to the channel, but field observation suggests that approximately 5-10% of the channel volume is filled with sediment annually, primarily in highly eroded stream reaches downstream of channel hardpoints.

Figure 4. Residents fill in the channel with loose sediment and construction debris to prevent the channel from eroding into their homes. Picture taken in the SW channel.

Uncertainty may arise in the calculation of M_{urban} and M_{HP} due to potential errors in the surveyed cross-sections, volume estimation using the upstream cross-sectional area and reach length, mass of sediment added due to channel fill, and the regional curves used to estimate A_{ref} and A_{NHP}. Similar to Zhang et al. (2014), cumulative probable error (*PE*) can be calculated to reflect the variabilities of all components used to estimate the mass of sediment generated due to urbanization and hardpoints:

$$PE = \left\{ \left(\frac{M_{DGPS}}{M_{LLCW}} \right)^2 E_{DGPS}{}^2 + \left(\frac{M_{SfM}}{M_{LLCW}} \right)^2 E_{SfM}{}^2 + \left(\frac{M_{curve}}{M_{LLCW}} \right)^2 E_{curve}{}^2 \right\}^{\frac{1}{2}} \quad (4)$$

where M_{DGPS} and M_{SfM} are the mass of sediment (tons) calculated from cross-sections surveyed with a DGPS and SfM photogrammetry, respectively, M_{LLCW} is the total mass of sediment (tons) generated from LLCW, M_{curve} is the mass of sediment (tons) estimated from

the regional curves (SD reference for M_{urban} or NHP curve for M_{HP}), E_{DGPS} is the error for the mass calculation from cross-sections surveyed with a DGPS, E_{SfM} is the error for the mass calculation from SfM-derived cross-sections, and E_{curve} is the standard error from the regional curve (SD reference or NHP) divided by the mean. E_{curve} for the SD reference and NHP regional curves are 1.06 and 0.53, respectively.

Three components of error associated with the DGPS derived mass (E_{DGPS}) were squared and summed together, including the error from channel fill (0.05), relative error in the measurement of A_{DGPS} (0.08), from the cross-sectional comparison of DGPS and SfM-derived cross-sections, and relative error in the reach volume calculation (0.01). Errors in the reach volume calculation primarily arise if there is sinuosity between surveyed cross-sections and/or cross-sectional variation within a given reach (Castillo et al., 2012). Following Castillo et al. (2012), relative error in the reach volume (E_{vol}) was calculated for a representative stream reach in the SW channel that was 60 m long where SfM photogrammetry was conducted, as:

$$E_{vol} = \frac{V_p - V_o}{V_o} \quad (5)$$

where V_p is the predicted reach volume calculated as the upstream cross-sectional area multiplied by reach length, and V_o is the observed reach volume from the SfM-derived DEM using the cut and fill function in ArcGIS 10.5. In this study, the value for E_{vol} was relatively low (0.01) because cross-sections were surveyed at representative stream reaches to minimize the impact of cross-sectional variation between survey locations and reach sinuosity is minimal. Similarly, E_{SfM} included error from channel fill (0.05) and relative error in the reach volume calculation (0.01). The final values used for E_{DPGS} and E_{SfM} were 0.009 and 0.0026, respectively.

The mass of sediment generated by channel erosion was compared to mean annual sediment yield from LLCW, based on annual tons of sediment excavated from the sediment traps at the outlet of LLCW in the Tijuana Estuary from 2006 to 2012. The total sediment yield from LLCW includes sediment retained in the trap, and sediment that was lost through the trap and entered into the estuary. The trap efficiency, or the proportion of the total sediment yield that is retained in the sediment trap, for medium sand, fine sand, silt, and clay was estimated by following the guidelines for sedimentation under turbulent, non-ideal

conditions (Morris & Fan, 1998). See Biggs et al. (2017) for trap efficiency equations and methods used to correct the annual total sediment yield from LLCW.

4. RESULTS AND DISCUSSION

4.1 Regional hydraulic geometry curve comparison

Regional hydraulic geometry curves were developed for Spring Canyon reference channels and LLCW and compared to curves from the literature (Table 2). The regional curve for Spring Canyon is not statistically significant ($p > 0.1$; $r^2 = 0.13$) due to the small number of survey sites ($n = 10$) and small range of watershed sizes (0.1 to 1 km^2) but the curve has a statistically similar slope and intercept to southern California and San Diego County reference curves (Figure 5; Table 2). Channels in Spring Canyon are geomorphically stable, with no signs of incision or instability of the banks. The regional curve for all cross-sections at LLCW is statistically significant ($p < 0.001$; $r^2 = 0.22$). The α value from the regional curve for LLCW (6.97) is significantly larger than all reference regional curves ($p < 0.001$), suggesting that channel cross-sectional area is significantly larger in Los Laureles Canyon than in reference channels for a given watershed area. All cross-sections surveyed in LLCW are larger than the predicted regional reference cross-sectional areas for southern California (Modrick & Georgakakos, 2014), San Diego County (Taniguchi & Biggs, 2015), and Spring Canyon for a given watershed area. The slope (β) from Los Laureles regional curve (0.76) is significantly larger ($p < 0.01$) than the β value from San Diego County (0.16) reference curve, but not significantly different ($p > 0.1$) from Spring Canyon (0.29) and southern California (0.387) reference curve β values.

LLCW cross-sections were split into two groups (HP and NHP) based on downstream recovery distance (Figure 6) and regional curves were developed for each group (Table 2). Twenty-one cross-sections are within hardpoint influence, with downstream channel recovery distance varying from 50 to 230 m downstream of the channel hardpoint. Regional curves for HP and NHP locations (Table 2**;** Figure 5) are statistically significant ($p < 0.01$) and the HP α value is statistically larger than the NHP α value ($p < 0.05$), indicating that channels downstream of hardpoints are significantly larger than channels that are not within the hardpoint influence distance downstream. Additionally, both HP and NHP curves have

statistically larger α values ($p < 0.001$) compared to all reference curves. The α and β of the NHP regional curve for LLCW are statistically larger than the San Diego County reference curve, indicating that urbanization has led to channel erosion even without the downstream impact of hardpoints. In comparison to the San Diego County urban curve, the HP curve has statistically larger α ($p < 0.01$) and β ($p < 0.05$) values, while the NHP curve has a significantly larger β ($p < 0.05$). All ANCOVA results were the same using the subset of channels draining watersheds less than 15 km^2 for San Diego County and southern California reference regional datasets. This indicates that the range of drainage area does not significantly impact the slope or intercept of the reference regional curves.

Table 2. Regional curves for Los Laureles Canyon (this study), Spring Canyon (this study), San Diego County (Taniguchi & Biggs, 2015) and southern California (Modrick & Georgakakos, 2014). 'A' is cross-sectional area (m^2) and A_w is watershed area (km^2)

Location	Equation	r^2	p-value	N
Los Laureles Canyon:				
All	$A = 6.97\ A_w^{0.76}$	0.22	<0.001	57
Within hardpoint influence	$A = 11.26\ A_w^{1.05}$	0.42	<0.001	21
Not within hardpoint influence	$A = 4.60\ A_w^{0.84}$	0.36	<0.001	36
Reference Channels:				
Spring Canyon	$A = 0.81\ A_w^{0.29}$	0.13	>0.1	10
San Diego County	$A = 0.76\ A_w^{0.16}$	0.08	0.04	46
Southern California	$A = 0.53\ A_w^{0.39}$	0.29		54

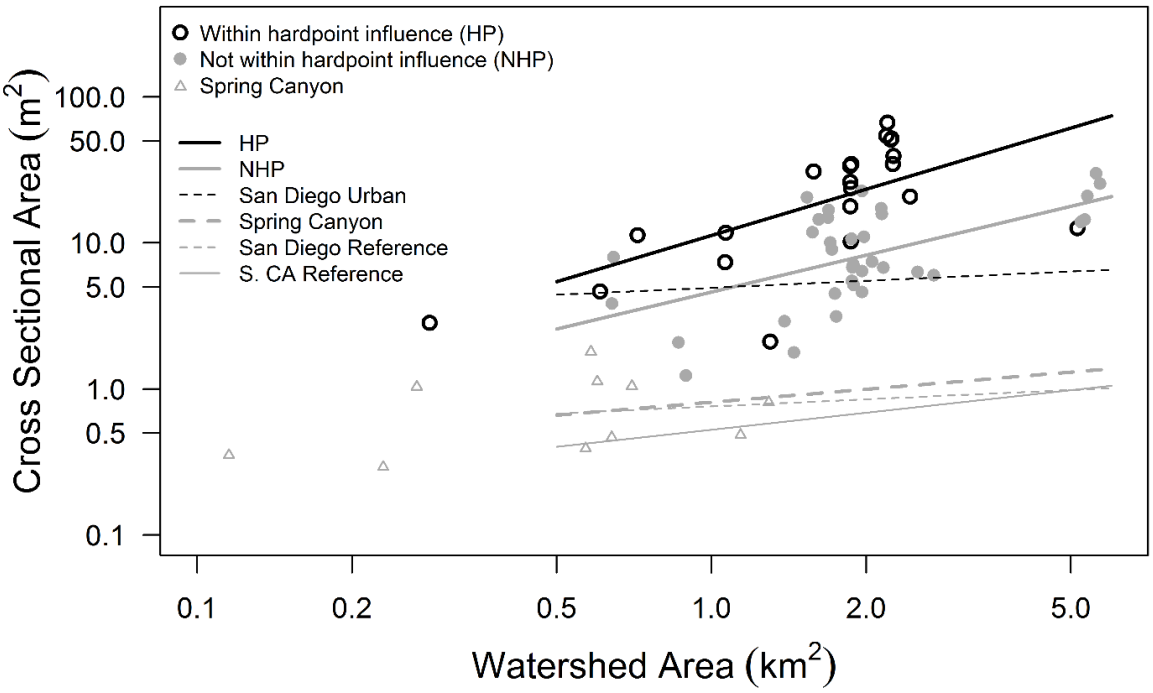

Figure 5. Regional curve comparison of surveyed cross-sections at LLCW stratified by: within hardpoint influence distance (HP) and not within hardpoint influence distance (NHP); and regional curves developed for San Diego County urban watersheds (San Diego Urban) (Taniguchi & Biggs, 2015) and minimally developed watersheds in San Diego County (San Diego Reference) (Taniguchi & Biggs, 2015), southern California (S.CA Reference) (Modrick & Georgakakos, 2014), and the surveyed Spring Canyon reference cross-sections.

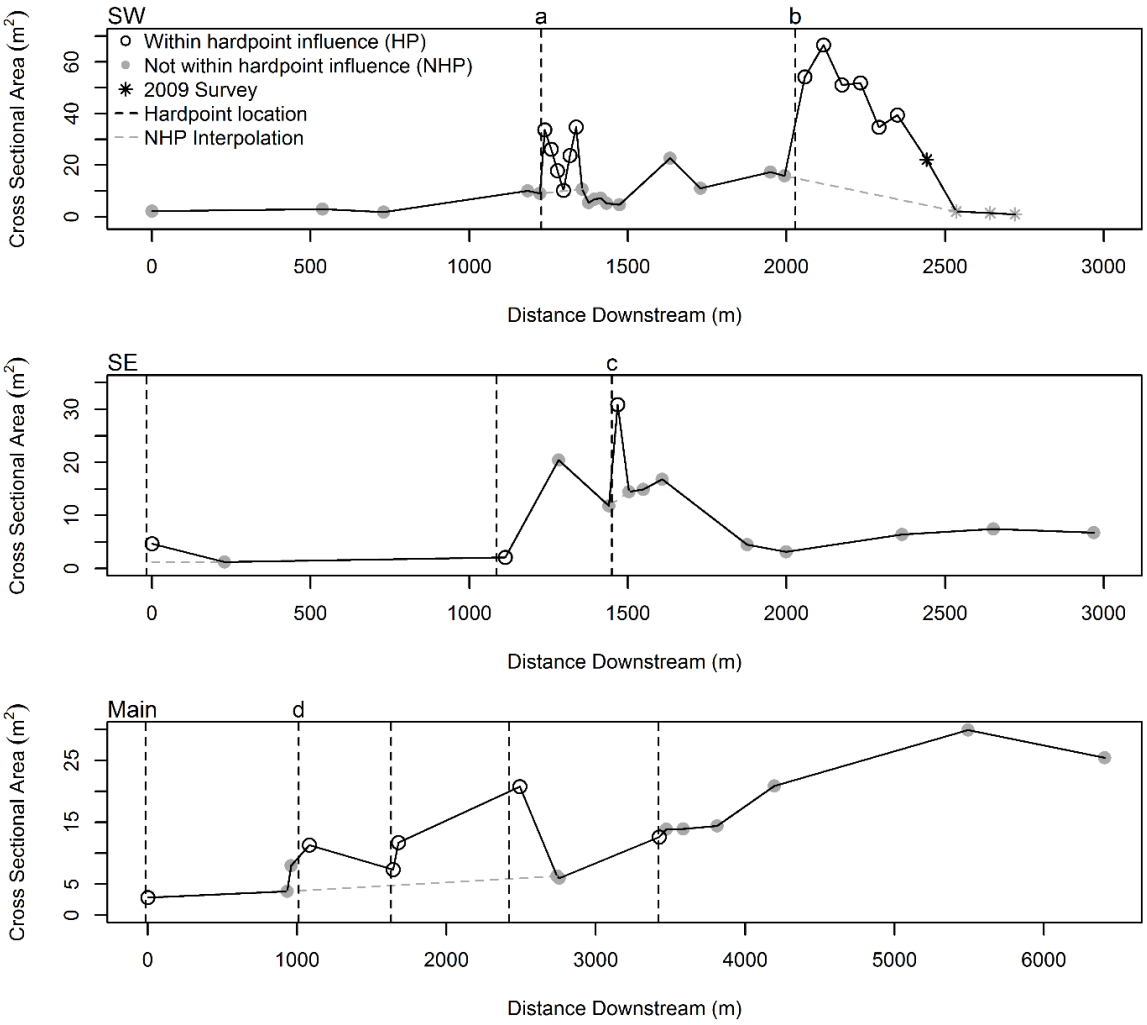

Figure 6. Distance downstream and cross-sectional area for the SW and SE tributaries and the Main channel. Open circles fall within hardpoint influence distance. Four hardpoint locations are labeled: a) SW metal culvert; b) SW concrete flume; c) SE hardpoint; and d) Main culvert (San Bernardo). The SW concrete flume (b) caused the most enlargement downstream. The GPS had high degree of error for the four downstream-most points in SW, so cross-sections surveyed in 2009 were plotted instead, but were not used in the regression analysis. NHP interpolated cross-sections are shown as the grey dashed line.

4.2 Spatial variability of downstream effects from hardpoints

Channel enlargement tends to decrease with increasing distance downstream from channel hardpoints in the SW and SE tributaries (Figure 6) and varies spatially (Figure 7). The SW

concrete flume is a 50 m long concrete-lined rectangular stream reach, 3 m deep by 1.3 m wide, and shows a downstream channel recovery distance of 230 m with the channel stabilizing downstream of this distance threshold (Figure 6). This stream reach is the most enlarged in the watershed with approximately 5 m of incision (Figure 7 b) and a scour hole immediately downstream of the structure. Incision and widening occurred beyond the dimensions of the concrete flume, which caused portions of the concrete sides to collapse (Figure 8). The small width-to-depth ratio of the structure may have created large water depths, which would have normally spread overbank but are now confined in the channel, causing higher channel velocities and downstream channel enlargement (Brookes, 1987). The SW metal culvert also caused over 2 m of incision downstream (Figure 7 a). Downstream of the SE hardpoint there is over 1 m of incision with little channel widening, but the incision is confined to within a few meters of the hardpoint and did not propagate downstream (Figure 7 c).

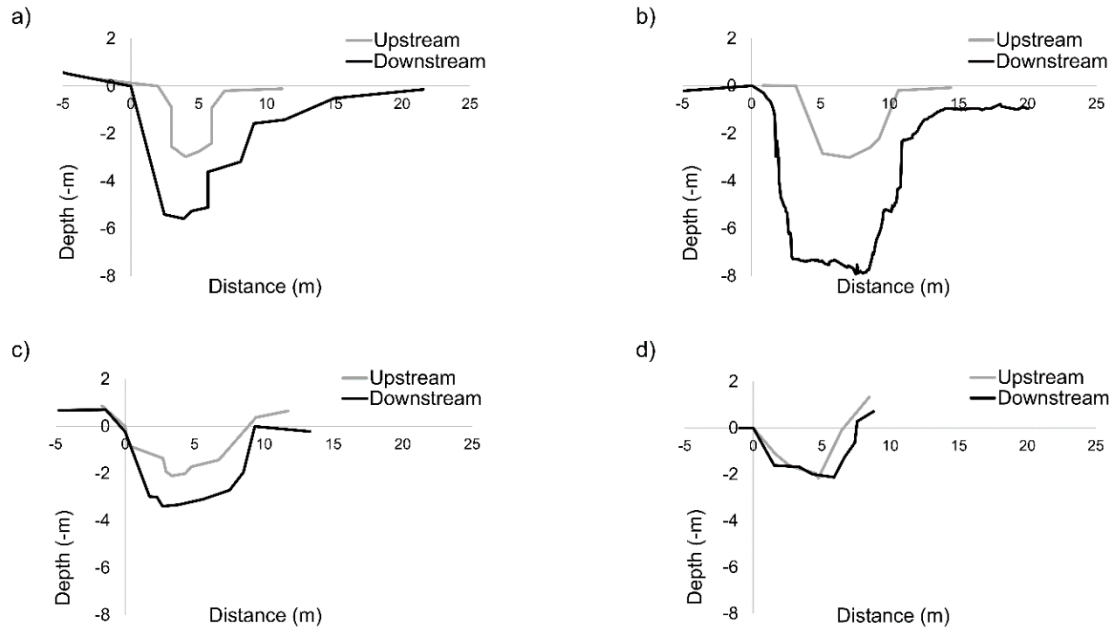

Figure 7. Channel cross-sections upstream and downstream of hardpoints for: a) SW metal culvert; b) SW concrete flume; c) SE hardpoint; and d) Main culvert (San Bernardo).

The most enlarged cross-sections are downstream of channel hardpoints, but not every hardpoint causes downstream instability. The upstream-most hardpoints in Main and SE are concrete-lined and drain into earthen channels but show little or no signs of

downstream channel erosion. Due to the small drainage area (< 0.7 km^2) and potentially lower amounts of runoff to these non-enlarged cross-sections, the downstream impacts of hardpoints may be negligible. In the Main channel, two culverts beneath roads in San Bernardo, a neighborhood with massive gully erosion of the sandy dirt roads, show little signs of enlargement downstream of them (Figure 7 d). High amounts of sediment supply from the hillslopes may account for the lack of channel erosion downstream of hardpoints in San Bernardo, but the mechanisms resulting in the stable cross-sections are unknown.

Figure 8. SW concrete flume facing upstream where portions of the concrete sides and bottom collapsed due to excess incision and widening. Fallen concrete pieces labelled (A).

Many studies on the impacts of hardpoints on channel morphology focus on the upstream migration of headcuts (Schumm et al., 1984) or local scour holes downstream of hydraulic structures (Bormann & Julien, 1991; Hoffmans & Pilarczyk, 1995). For the channel evolution model developed for southern California urban streams (Hawley et al., 2012), the importance of hardpoints and upstream propagation of headcuts were highlighted,

but did not stress the downstream impact of hardpoints, although they acknowledge that downstream scour may occur. Road crossings have caused downstream channel scour in ephemeral stream channels in Arizona, resulting in channels that were deeper and narrower than channels upstream of the road crossings (Chin & Gregory, 2001). Hardpoints in LLCW, in contrast, cause both incision and widening in the downstream direction for up to 230 m, creating persistent enlargement beyond the local scour holes. Brookes (1987) documented similar downstream impacts of hardpoints and found that the downstream effects from channelization varied between 120 and 1952 m, but downcutting was mainly observable immediately downstream of the channelization (i.e. within 135 m). Hardpoints in highly erodible, hydrologically flashy environments have the potential to cause major downstream enlargement, especially in areas with urban settlements adjacent to the stream channel.

4.3 Impervious cover and channel enlargement

Channel enlargement varied widely for a given watershed impervious cover percentage (IC) (Figure 9), indicating that IC may not be a good predictor of enlargement and is not the main factor contributing to spatial variability in channel enlargement. Although an increase in IC typically results in a decrease in sediment supply to the stream system, this may not always be the case in developing countries. In LLCW, some areas that had the highest impervious cover (IC>30%) also contained large proportions of unpaved roads and bare hillslopes. Despite the increase in IC during urbanization, channels can stay the same or even aggrade if there is sufficient sediment supply from upstream or from hillslopes. In Tijuana, only the oldest urban areas (>40 years) have a high percentage of impervious cover (Biggs et al., 2010). The developed areas near the outlet of LLCW that have been urbanized for more than 45 years have a significantly larger proportion of paved roads in comparison to newly urbanized areas. However, channel erosion is not a problem in the older urban areas, despite the higher proportions of impervious cover, because the stream channels have also been channelized and paved over with concrete for nearly 4 km of stream length (Figure 1).

Channel cross-sectional area downstream of hardpoints is up to 64 times larger than the predicted cross-sectional area under reference conditions for LLCW and up to 32 times larger than the enlargement predicted for San Diego County urban streams. All of the cross-sections that have enlargement ratios larger than 25 (n = 9) are impacted by

hardpoints. Although hillslope sediment supply rates were not quantified in this study, hardpoints may cause the most enlargement in areas where the unpaved roads are compacted and cobbly and therefore generate less sediment (i.e. the SW and SE). The cobbly, compacted roads may also have lower infiltration rates and could potentially generate higher volume and velocity of runoff compared to the less-consolidated, sandy dirt roads in San Bernardo.

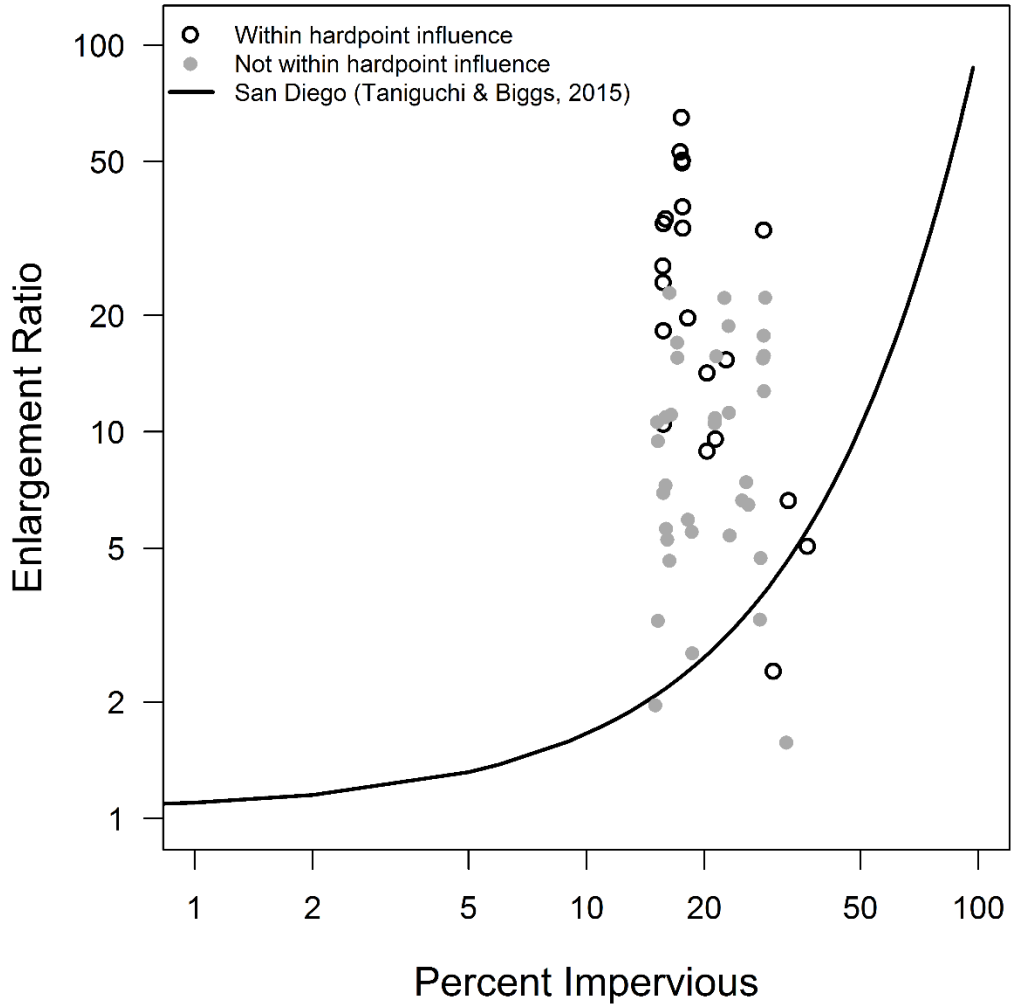

Figure 9. Percent impervious versus channel enlargement ratio for Los Laureles Canyon, stratified by points within hardpoint influence and points not within the hardpoint influence downstream distance.

Channels in Tijuana may start to erode with lower proportions of impervious cover compared to San Diego County urban channels (Taniguchi & Biggs, 2015), despite similar rainfall patterns, due to the lack of riparian and bank vegetation in urban areas of LLCW. Urbanization in Tijuana is characterized by the clearing and levelling of land, but in contrast

to developed countries, urban settlements are often built within meters of the stream channel, leaving little, if any, room for a riparian buffer zone between the channel and the urban development. Locally, riparian and bank vegetation can create added roughness to the channel boundary and floodplain, which increases flow resistance and decreases near-bank velocities and shear stresses exerted on the banks, promoting sediment deposition and channel accretion (Hickin, 1984; Clifton, 1986; Rhoads, 1992; Friedman et al., 1996). The lack of a riparian zone and bank vegetation can lead to stream channel erosion, as well as degradation to the ecological well-being of the river system (Boothroyd et al., 2004).

4.4 Sediment generation from channel erosion

The amount of sediment generated from urban-induced channel erosion is approximately 143,000 and 144,000 tons, or 8,400 to 8,500 t y^{-1}, based on the mean time since the start of urbanization for the entire watershed (17 years). The estimate of urban-induced channel erosion is based on the assumption that the pre-development cross-sections at LLCW followed the same regional reference curves as those from San Diego County (K. Taniguchi & Biggs, 2015) and Spring Canyon. This channel erosion estimate does not account for the timing and interactions among storm events, urbanization, and channel erosion, and instead represents the long-term mean rate of erosion from channels that we use to compare with rates of total sediment load observed at the outlet of the watershed. Channel erosion due to hardpoints (~3,000 t y^{-1}), accounts for more than 1/3 of the total sediment contribution from channel erosion. Cumulative probable error (PE) for M_{urban} and M_{HP} are 0.11 and 0.09, respectively.

The channel contribution (M_{urban}) based on a channel survey conducted in 2009 was approximately 183,000 tons, which is larger than what we estimated from this study (143,000 – 144,000 tons), primarily due to the fact that a large portion of the Main channel that was earthen and highly eroded in 2009 was channelized and lined with concrete by the time of the 2014 survey. Concrete lined channels, although they may have supplied sediment prior to channelization, are excluded from this analysis and assumed to have zero contribution to the overall sediment budget. If we assume that 5-10% of the entire channel volume gets filled by residents and eroded away every year, we estimate an added sediment supply of

approximately 7,000 to 14,000 t y^{-1}, which more than doubles the channel erosion rate to 15,400 to 22,500 t y^{-1}.

The average annual sediment yield from the entire LLCW, based on measured annual sediment excavated from the Los Laureles sediment traps at the outlet from 2006-2012 and corrected for trap efficiency, is approximately 58,000 t y^{-1} or 5,000 t km^{-2} y^{-1}. Depending on the estimate of channel fill, channel erosion accounts for 25 to 40 percent of the total sediment budget for the watershed, which implies that the contribution of hillslope sediment supply is substantial (60-75%) in LLCW. Infrastructure failure, such as broken water main pipes, cause large gullies to form on the hillslopes and could be a significant source of sediment in LLCW. Trimble (1997) found that channel erosion accounted for more than 2/3 of the total sediment budget in an urbanized watershed in southern California, which may be due to high amounts of impervious surfaces and low hillslope sediment supply. In developing countries, large fractions of bare soil persist for decades following urbanization, and the soil fraction decreases only slightly from newly urbanized areas to areas that have been urbanized for up to 40 years (Biggs et al., 2010). Given that LLCW has only been urbanized for 17 years on average, hillslope sediment supply from unpaved roads may be the dominant source of sediment for decades to come.

5. CONCLUSION

Urbanization and channel structures have led to extreme channel enlargement in the rapidly urbanizing Los Laureles Canyon watershed in Tijuana, Mexico. Channel cross-sectional area for a given watershed area were significantly larger in Los Laureles Canyon compared to reference channels. Impervious cover in the watershed doubled within a 9-year time period. Although percent impervious cover is typically a good indicator of channel enlargement (Coleman et al., 2005; Hawley & Bledsoe, 2013), impervious cover was a poor predictor of channel enlargement in LLCW and is not the only variable for explaining spatial variability in channel enlargement in a rapidly developing watershed like Los Laureles Canyon. Local channel hardpoints have caused channel enlargement of up to 64 times the predicted cross-sectional area under reference conditions and have caused enlargement for up to 230 m downstream. Additionally, the lack of a riparian buffer zone and bank vegetation in urbanized areas could decrease flow resistance and reduce channel stability.

Channel erosion accounts for approximately 25-40% of the total sediment yield from Los Laureles Canyon, with erosion downstream of channel hardpoints contributing more than one third of all channel erosion. Channels downstream of hardpoints should be stabilized to prevent increased inputs of sediment to the Tijuana Estuary and local hazards near the structures, especially in areas with urban settlements near the stream channel. If the erosion is allowed to continue, bank failure can cause homes or bridges to collapse, channels can erode into adjacent dirt roads, and infrastructure damage, such as water main breaks, can occur. Future studies on the sediment budget of the watershed and modelling the impact of land use changes and management practices, such as road paving, on flooding, channel erosion, and sediment loadings to downstream ecosystems can help managers make informed decisions on erosion and sediment mitigation practices.

ACKNOWLEDGEMENTS

This study was funded by the US Environmental Protection Agency (EPA) (Interagency Agreement ID # DW-12-92390601-0) in collaboration with the US Department of Agriculture (USDA, Agreement # 58-6408-4-015), Centro de Investigación Científica y de Educación Superior de Ensenada (CICESE), and University of Córdoba (Spain). This article has been subjected to the USEPA review and approved for publication. The authors are grateful for the valuable comments and suggestions provided by Dr. Ronald Bingner (USDA), Dr. Douglas Stow (San Diego State University), Dr. Thomas Dunne (University of California, Santa Barbara), and Dr. Oliver Chadwick (University of California, Santa Barbara). Dr. Robert J. Hawley (Sustainable Streams, LLC), two anonymous reviewers, and an Associate Editor at ESPL provided helpful comments that greatly improved the manuscript. Please note that although this work was reviewed by USEPA and approved for publication, it may not necessarily reflect official Agency policy. Mention of trade names or commercial products does not constitute endorsement or recommendation for use.

REFERENCES

Balbo, M. (1993). Urban-Planning and the Fragmented City of Developing-Countries. Third World Planning Review, 15(1), 23–35.

Biggs, T. W., Atkinson, E., Powell, R., & Ojeda-Revah, L. (2010). Land cover following rapid urbanization on the US-Mexico border: Implications for conceptual models of urban watershed processes. Landscape and Urban Planning, 96(2), 78–87. http://doi.org/10.1016/j.landurbplan.2010.02.005

Biggs, T. W., Taniguchi, K. T., Gudino-Elizondo, N., Yongping, Y., Bingner, R. L., Langendoen, E. J., & Liden, D. (2018). Field measurements to support sediment and hydrological modeling in Los Laureles Canyon (EPA/600/X-18/0XX). Washington, DC.

Booth, D. B., Dusterhoff, S. R., Stein, E. D., & Bledsoe, B. P. (2010). Hydromodification screening tools: GIS-based catchment analyses of potential changes in runoff and sediment discharge. Southern California Coastal Water Research Project, (Technical Report 605).

Boothroyd, I. K. G., Quinn, J. M., Langer, E. R., Costley, K. J., & Steward, G. (2004). Riparian buffers mitigate effects of pine plantation logging on New Zealand streams: 1. Riparian vegetation structure, stream geomorphology and periphyton. Forest Ecology and Management, 194(1–3), 199–213. http://doi.org/10.1016/j.foreco.2004.02.018

Bormann, N. E., & Julien, P. Y. (1991). Scour downstream of grade-control structures. J. Hydraul. Eng., 117(5), 579–594.

Brookes, A. (1987). River channel adjustments downstream from channelization works in England and Wales. Earth Surface Processes and Landforms, 12(4), 337–351. http://doi.org/10.1002/esp.3290120402

Castillo, C., James, M. R., Redel-Macías, M. D., Pérez, R., & Gómez, J. a. (2015). SF3M software: 3-D photo-reconstruction for non-expert users and its application to a gully network. Soil, 1(2), 583–594. http://doi.org/10.5194/soil-1-583-2015

Castillo, C., Perez, R., James, M. R., Quinton, J. N., Taguas, E. V, & Gomez, J. A. (2012). Comparing the Accuracy of Several Field Methods for Measuring Gully Erosion. Soil Science Society of America Journal, 76(4), 1319–1332. http://doi.org/10.2136/sssaj2011.0390

Chaplin, J. J. (2005). Development of Regional Curves Relating Bankfull-Channel Geometry and Discharge to Drainage Area for Streams in Pennsylvania and Selected Areas of Maryland - Scientific Investigations Report. Development, 34. Retrieved from http://pubs.usgs.gov/sir/2005/5147/SIR2005-5147.pdf

Chin, A. (2006). Urban transformation of river landscapes in a global context. Geomorphology, 79(3–4). http://doi.org/10.1016/j.geomorph.2006.06.033

Chin, A., & Gregory, K. J. (2001). Urbanization and Adjustment of Ephemeral Stream Channels. Annals of the Association of American Geographers, 91(4), 595–608. http://doi.org/10.1111/0004-5608.00260

Clifton, C. (1986). Effects of Vegetation and Land Use on Channel Morphology. Geography, 2(1), 121–129.

CloudCompare v2.5.5.2. (2015). Retrieved from http://www.danielgm.net/cc/

Coleman, D., Macrae, C., & Stein, E. D. (2005). Effect of Increases in Peak Flows and Imperviousness on the Morphology of Southern. Costa Mesa, CA.

Davis, M. (2006). Planet of Slums. New York: Verso.

Deseilligny, M., & Clery, I. (2011). Apero, an open source bundle adjustment software for automatic Calibration and orientation of set of images. In F. Remondino & S. ElHakim (Eds.), 4th ISPRS International Workshop 3d-Arch 2011: 3d Virtual Reconstruction and Visualization of Complex Architectures (pp. 269–276). Gottingen: Copernicus Gesellschaft Mbh.

Dietrich, J. T. (2015). Riverscape mapping with helicopter-based Structure-from-Motion photogrammetry. Geomorphology, 252, 144–157. http://doi.org/10.1016/j.geomorph.2015.05.008

Dunne, T., & Leopold, L. B. (1978). Water in Environmental Planning. San Francisco, CA: W.H. Freeman and Co.

Friedman, J. M., Osterkamp, W. R., & Lewis, W. M. (1996). The role of vegetation and bed-level fluctuations in the process of channel narrowing. Geomorphology, 14(4 SPEC. ISS.), 341–351. http://doi.org/10.1016/0169-555X(95)00047-9

Furukawa, Y., & Ponce, J. (2010). Accurate, dense, and robust multiview stereopsis. IEEE Transactions on Pattern Analysis and Machine Intelligence, 32(8), 1362–1376. http://doi.org/10.1109/TPAMI.2009.161

Gómez-Gutiérrez, Á., de Sanjosé-Blasco, J., de Matías-Bejarano, J., & Berenguer-Sempere, F. (2014). Comparing Two Photo-Reconstruction Methods to Produce High Density Point Clouds and DEMs in the Corral del Veleta Rock Glacier (Sierra Nevada, Spain). Remote Sensing, 6(6), 5407–5427. http://doi.org/10.3390/rs6065407

Grable, J. L., & Harden, C. P. (2006). Geomorphic response of an Appalachian Valley and Ridge stream to urbanization. Earth Surface Processes and Landforms, 31(13), 1707–1720. http://doi.org/10.1002/esp.1433

Gregory, K. J. (2006). The human role in changing river channels. Geomorphology, 79(3–4), 172–191. http://doi.org/10.1016/j.geomorph.2006.06.018

Hammer, T. R. (1972). Stream channel enlargement due to urbanization. Water Resources Research, 8(6), 1530. http://doi.org/10.1029/WR008i006p01530

Hawley, R. J., & Bledsoe, B. P. (2011). How do flow peaks and durations change in suburbanizing semi-arid watersheds? A southern California case study. Journal of Hydrology, 405(1–2). http://doi.org/10.1016/j.jhydrol.2011.05.011

Hawley, R. J., & Bledsoe, B. P. (2013). Channel enlargement in semiarid suburbanizing watersheds: A southern California case study. Journal of Hydrology, 496, 17–30. http://doi.org/10.1016/j.jhydrol.2013.05.010

Hawley, R. J., Bledsoe, B. P., Stein, E. D., & Haines, B. E. (2012). Channel Evolution Model of Semiarid Stream Response to Urban-Induced Hydromodification. Journal of the American Water Resources Association, 48(4), 722–744. http://doi.org/10.1111/j.1752-1688.2012.00645.x

Hickin, E. J. (1984). Vegetation and River Channel Dynamics. Canadian Geographer / Le Geographe Canadien, 28(2), 111–126. http://doi.org/10.1111/j.1541-0064.1984.tb00779.x

Hoffmans, G. C. M., & Pilarczyk, K. W. (1995). Local scour downstream of hydraulic structures. J. Hydraul. Eng., 121(4), 326–340.

James, M. R., & Robson, S. (2012). Straightforward reconstruction of 3D surfaces and topography with a camera: Accuracy and geoscience application. Journal of Geophysical Research-Earth Surface, 117, 17. http://doi.org/10.1029/2011jf002289

James, M. R., & Robson, S. (2014). Mitigating systematic error in topographic models derived from UAV and ground-based image networks. Earth Surface Processes and Landforms, 39(10), 1413–1420. http://doi.org/10.1002/esp.3609

Javernick, L., Brasington, J., & Caruso, B. (2014). Modeling the topography of shallow braided rivers using Structure-from-Motion photogrammetry. Geomorphology, 213, 166–182. http://doi.org/10.1016/j.geomorph.2014.01.006

Johnson, P. A., & Fecko, B. J. (2008). Regional channel geometry equations: A statistical comparison for physiographic provinces in the eastern US. River Research and Applications, 24(6), 823–834. http://doi.org/10.1002/rra.1080

Katz, H. A., Daniels, J. M., & Ryan, S. (2014). Slope-area thresholds of road-induced gully erosion and consequent hillslope-channel interactions. Earth Surface Processes and Landforms, 39(3), 285–295. http://doi.org/10.1002/esp.3443

Kennedy, M. P., & Peterson, G. L. (1975). Geology of the San Diego Metropolitan Area, California. San Diego, CA.

Leopold, L. B. (1973). River channel change with time - Example. Geological Society of America Bulletin, 84(6), 1845–1860. http://doi.org/10.1130/0016-7606(1973)84<1845:rccwta>2.0.co;2

Leopold, L. B. (1994). A View of the River. Harvard University Press. Retrieved from http://books.google.com/books?id=QWDQ7ezcjbcC

Micheletti, N., Chandler, J. H., & Lane, S. N. (2014). Investigating the geomorphological potential of freely available and accessible structure-from-motion photogrammetry using a smartphone. Earth Surface Processes and Landforms, 486(October 2014), n/a-n/a. http://doi.org/10.1002/esp.3648

Modrick, T. M., & Georgakakos, K. P. (2014). Regional bankfull geometry relationships for southern California mountain streams and hydrologic applications. Geomorphology, 221, 242–260. http://doi.org/10.1016/j.geomorph.2014.06.004

Morris, G. L., & Fan, J. (1998). Reservoir Sedimentation Handbook: Design and Management of Dams, Reservoirs and Watersheds for Sustainable Use. New York: McGraw-Hill Companies, Inc.

Navratil, O., Breil, P., Schmitt, L., Grospretre, L., & Albert, M. B. (2013). Hydrogeomorphic adjustments of stream channels disturbed by urban runoff (Yzeron River basin, France). Journal of Hydrology, 485, 24–36. http://doi.org/10.1016/j.jhydrol.2012.01.036

Owens, P. (2005). Conceptual Models and Budgets for Sediment Management at the River Basin Scale. Journal of Soils and Sediments, 5(4), 201–212. http://doi.org/10.1065/jss2005.05.133

Pinettes, P., Courivaud, J., Fry, J., Mercier, F., & Bonelli, S. (2011). First introduction of Greg Hanson's «Jet Erosion Test» in Europe: return on experience after 2 years of testing. In USSD Annual Meeting and Conference. San Diego, CA. Retrieved from http://www.researchgate.net/publication/259193239_FIRST_INTRODUCTION_OF_GREG_HANSON'S__JET_EROSION_TEST__IN_EUROPE__RETURN_ON_EXPERIENCE_AFTER_2_YEARS_OF_TESTING/file/e0b4952a5976804314.pdf

Prosdocimi, M., Calligaro, S., Sofia, G., Dalla Fontana, G., & Tarolli, P. (2015). Bank erosion in agricultural drainage networks: new challenges from structure-from-motion photogrammetry for post-event analysis. Earth Surface Processes and Landforms, 40(14), 1891–1906. http://doi.org/10.1002/esp.3767

Rhoads, B. L. (1992). Fluvial geomorphology. Progress in Physical Geography, 16(4), 456–477. http://doi.org/10.1177/030913339201600404

Schumm, S. A., Harvey, M. D., & Watson, C. C. (1984). Incised channels: morphology, dynamics, and control. Water Resources Publications. Retrieved from https://books.google.com/books?id=KLoPAQAAIAAJ

Simon, A., & Downs, P. W. (1995). An interdisciplinary approach to evaluation of potential instability in alluvial channels. Geomorphology, 12(3), 215–232. http://doi.org/10.1016/0169-555X(95)00005-P

Splinter, D. K., Dauwalter, D. C., Marston, R. A., & Fisher, W. L. (2010). Ecoregions and stream morphology in eastern Oklahoma. Geomorphology, 122(1–2), 117–128. http://doi.org/10.1016/j.geomorph.2010.06.004

Stöcker, C. (2015). Measuring gullies by synergetic application of UAV and close range photogrammetry - A case study from Andalusia, Spain. Catena, 132, 1–11. http://doi.org/10.1016/j.catena.2015.04.004

Takken, I., Croke, J., & Lane, P. (2008). Thresholds for channel initiation at road drain outlets. Catena, 75(3), 257–267. http://doi.org/10.1016/j.catena.2008.07.001

Taniguchi, K., & Biggs, T. W. (2015). Regional impacts of urbanization on stream channel geometry: A case study in semi-arid southern California. Geomorphology, 248, 228–236. http://doi.org/10.1016/j.geomorph.2015.07.038

Trimble, S. W. (1997). Contribution of stream channel erosion to sediment yield from an urbanizing watershed. Science, 278(5342), 1442–1444. http://doi.org/10.1126/science.278.5342.1442

Turner, D., Lucieer, A., & Watson, C. (2012). An automated technique for generating georectified mosaics from ultra-high resolution Unmanned Aerial Vehicle (UAV) imagery, based on Structure from Motion (SFM) point clouds. Remote Sensing, 4(5), 1392–1410. http://doi.org/10.3390/rs4051392

Wackrow, R., & Chandler, J. H. (2008). A convergent image configuration for DEM extraction that minimises the systematic effects caused by an inaccurate lens model. Photogrammetric Record, 23(121), 6–18. http://doi.org/10.1111/j.1477-9730.2008.00467.x

Wackrow, R., & Chandler, J. H. (2011). Minimising systematic error surfaces in digital elevation models using oblique convergent imagery. Photogrammetric Record, 26(133), 16–31. http://doi.org/10.1111/j.1477-9730.2011.00623.x

Walling, D. E., & Collins, A. L. (2008). The catchment sediment budget as a management tool. Environmental Science and Policy, 11(2), 136–143. http://doi.org/10.1016/j.envsci.2007.10.004

Walsh, C. J., Roy, A. H., Feminella, J. W., Cottingham, P. D., Groffman, P. M., Ii, R. P. M., & Ii, R. A. P. M. O. (2016). The urban stream syndrome: current knowledge and the search for a cure Source: Journal of the North American Benthological Society, Vol. 24, No. 3 (Sep., 2005), Published by: The University of Chicago Press on behalf of the Society for Freshwater, 24(3), 706–723.

Webber, S. R. (2010). The role of local watersheds on sediment accumulation in the Tijuana Estuary Reserve. San Diego State University.

Weis, D. A., Callaway, J. C., & Gersberg, R. M. (2001). Vertical accretion rates and heavy metal chronologies in wetland sediments of the Tijuana Estuary. Estuaries, 24(6A), 840–850. http://doi.org/Doi 10.2307/1353175

Westoby, M. J., Brasington, J., Glasser, N. F., Hambrey, M. J., & Reynolds, J. M. (2012). "Structure-from-Motion" photogrammetry: A low-cost, effective tool for geoscience applications. Geomorphology, 179, 300–314. http://doi.org/10.1016/j.geomorph.2012.08.021

Wolman, M. G. (1954). A method of sampling coarse river-bed material. Eos, Transactions American Geophysical Union, 35(6), 951–956. http://doi.org/10.1029/TR035i006p00951

Wolman, M. G. (1967). A Cycle of Sedimentation and Erosion in Urban River Channels. Geografiska Annaler. Series A, Physical Geography, 49(2/4), 385–395. Retrieved from http://www.jstor.org/stable/520904

Wu, C. (2013). Towards Linear-time Incremental Structure From Motion. In International Conference on 3D vision publication (3DV Conference) (pp. 127–134). Seattle, WA.

Wu, C. (2015). VisualSFM: A Visual Structure from Motion System. Retrieved from http://ccwu.me/vsfm/

Zedler, J. B., & Norby, C. S. (1986). the Ecology of Tijuana Estuary, California: An Estuarine Profile.

Zhang, Z., Hu, H., Tian, F., Yao, X., & Sivapalan, M. (2014). Groundwater dynamics under water-saving irrigation and implications for sustainable water management in an oasis: Tarim River basin of western China, 3951–3967. http://doi.org/10.5194/hess-18-3951-2014

CHAPTER 3

Quantifying the Relative Effects of Compounded Channel Alterations on Stream Channel Evolution in a Rapidly Urbanizing, Semi-arid Region

ABSTRACT

The process of urbanization in developing regions, such as Tijuana, Mexico, often involves direct manipulation of the stream channel, installation of hardpoints, and subsequent channel enlargement. Spatial and temporal trends of channel evolution were simulated for the period of 2001 to 2048 to evaluate the impact of in-channel alterations of a highly enlarged stream reach upstream and downstream of a concrete flume in Tijuana, Mexico. The analysis was conducted to identify which processes generated the observed channel instabilities, and to determine if the channel can be stabilized under current land cover conditions. Seven model simulations representing an incremental naturalization of the stream system were assessed: 1) 'actual' (2001) channel conditions; 2) larger concrete flume geometry; 3) no concrete flume; 4) historical slope downstream of the flume; 5) coarsening the bed downstream of the flume; 6) vegetated stream banks and floodplain; and 7) all cross sections reverted to an estimated reference channel geometry. Overall, the concrete flume caused enlargement immediately downstream, but prevented channel enlargement upstream. Channel erosion is caused mainly by the destruction of the natural channel, including channel burial, straightening, steepening, and removal of riparian vegetation, often performed in the process of turning channels into roads. Reformation of an enlarged river reach that is disconnected from the floodplain, leads to higher flow depths constrained in the channel, larger shear stresses, and accelerated channel incision. The largest reduction in sediment yield at the outlet of the watershed was achieved by reverting the enlarged cross sections back to the reference channel geometry (5,700 tons $year^{-1}$). Although channel incision was estimated to cease after 2020, channel widening is estimated to continue beyond the year of 2050 if bank stabilization measures are not implemented.

1. INTRODUCTION

Stream channels evolve based on the balance between sediment load and sediment size to a river's slope and discharge (Lane, 1955). A state of equilibrium can be achieved if sediment discharge balances stream power. However, changes to the sediment or discharge can cause the channel to aggrade or degrade and may alter the driving or resisting forces to erosion. The driving forces of channel instability include an increase in discharge and slope and a decrease in sediment load from the watershed. Resisting forces include cohesion, roughness, and armoring of the bed and banks, decrease in the slope or discharge, and an increase in sediment load to the channel. Human activities can alter both the resisting or driving forces to channel erosion by altering the land surface and/or the stream channel characteristics.

Urbanization impacts both the discharge and sediment supply of a watershed in ways that can lead to stream channel erosion. The theory describing the impact of urbanization on stream morphology is based on field sites in developed countries, where urbanization typically involves watershed-scale land cover changes, such as an increase in impervious surfaces, which leads to an increase in total and peak discharge and a decrease in hillslope sediment supply (Wolman, 1967; Trimble, 1997; Hawley & Bledsoe, 2011). Alterations in the discharge and sediment supply in urban watersheds, also referred to as hydromodification, can lead to stream channel erosion (Hammer, 1972; Trimble, 1997; Booth & Henshaw, 2001; Hawley et al., 2011; Hawley & Bledsoe, 2013; Taniguchi & Biggs, 2015). However, channel morphology can be impacted by direct channel and floodplain alterations including channelization (Brookes, 1987), road crossings (Chin & Gregory, 2001), and in-channel structures (Segura & Booth, 2010). The process of urbanization in developing countries typically involves direct manipulation of the stream channel which can lead to changes in the resisting and driving forces to erosion and subsequent channel instabilities, independent of watershed land cover. For example, the process of urbanization in Tijuana, Mexico involves complete vegetation removal of the hillslopes, and riparian buffer, and stream channels are often filled in with loose sediment, graded, and turned into unpaved roads. After the landscape is graded, straightened, steeper channels re-form along the unpaved roads during the wet season. The newly formed channels are typically

composed of highly erodible, unconsolidated sediment with little to no vegetation protecting the banks and a steeper slope, all of which favor further incision and widening. Additionally, stream reaches located downstream of hardpoints or non-erodible features, such as concrete flumes and culverts, were statically larger than reaches located away from hardpoints in Tijuana (Taniguchi et al., 2018). However, it remains unclear whether the geometry and flow characteristics of the hardpoints themselves were generating the instabilities, or if the urban channel alterations led to excess enlargement. It is necessary to gain a mechanistic understanding of channel evolution in such areas, including the driving mechanisms of channel instabilities, to ensure proper sediment and erosion mitigation practices are implemented to reduce excess sedimentation of downstream ecosystems.

Channel evolution models (CEMs) have been developed to qualitatively describe the sequence of channel changes over time in response to a disturbance (Schumm et al., 1984; Thorne & Osman, 1988; Simon, 1989; Bledsoe et al., 2012; Booth & Fischenich, 2015). The classic CEM for incised, single-thread streams include evolutionary stages of a pre-disturbed stable channel (stage I) followed by a disturbance that leads to degradation via incision (stage II), bank failure and widening (stage III), aggradation (stage IV), and an establishment of a quasi-equilibrium state (stage V) (Schumm et al., 1984). CEMs can be used to predict the likely response of the channel to a disturbance or to diagnose the sequence of events leading to the current channel condition (Booth & Fischenich, 2015). Although CEMs can provide a valuable foundation in understanding urban processes and channel evolution, these models cannot be used to quantitively assess channel evolution over time, nor predict the timescales of the evolutionary stages.

With an increase in computing power and better knowledge on fluvial hydraulics, computer models can be utilized to investigate how channels evolve over long periods of time (FISRWG, 1998; Langendoen & Alonso, 2008). Additionally, scenario analyses using alluvial channel models and numerical simulations can evaluate the impact of various boundary conditions on channel morphology (Darby & Thorne, 1996; Simon & Darby, 1997) and the impact of in-channel disturbances on channel evolution over time (Niezgoda & Johnson, 2005, 2006; Simon & Rinaldi, 2006; Rowley & Hotchkiss, 2014). Although there are a range of advanced alluvial channel models that can simulate hydraulics, sediment

transport, and channel evolution, including HEC-6 (USACE, 1993), FLUVIAL-12 (Chang, 2006), SRH-1D (Huang & Greimann, 2010) and CONCEPTS (CONservational Channel Evolution and Pollutant Transport System; Langendoen & Alonso, 2008; Langendoen & Simon, 2008), a majority of models do not consider channel width adjustment via mass wasting, which can be the primary source of sediment in many stream systems (Simon & Rinaldi, 2006). The CONCEPTS model accounts for bank failure via mass wasting, is the only model that uses actual bank geometry, as opposed to idealized bank geometry (Langendoen & Simon, 2008), and can simulate flow processes influenced by in-stream grade stabilization structures (Langendoen & Alonso, 2008).

This study utilizes CONCEPTS to quantitatively describe the channel evolution of a highly enlarged stream reach following the installation of a concrete flume to assess the impacts of urban channel alterations, identify the processes governing channel adjustment, and determine if a highly unstable stream reach can be stabilized under current land cover conditions in a semi-arid developing watershed in Tijuana, Mexico, Los Laureles Canyon watershed (LLCW). The overarching management goal is to understand mechanisms driving channel erosion to ultimately reduce sediment load to the aggrading Tijuana Estuary. The research question to be addressed in this paper is:

What mechanisms drive channel enlargement in a rapidly developing watershed, including hardpoint characteristics, slope alteration, bed composition change, vegetation removal, and floodplain storage removal?

The primary hypotheses tested are: 1) the size and geometry of hardpoint structures impact downstream incision and widening, with the deep and narrow concrete flume causing more channel enlargement due concentrated flows with large flow depths compared to a wider concrete flume; 2) channel incision downstream of hardpoints is dependent on channel boundary materials of the bed; and 3) channel alterations during the process of urbanization including vegetation removal and channel straightening impact channel enlargement and can disconnect the channel from the floodplain.

2. STUDY SITE

This study focuses on a highly erodible tributary (SW channel; drainage area of 2.5 km^2) of the semi-arid Los Laureles Canyon watershed (LLCW; drainage area of 11.6 km^2) located in Tijuana, Mexico (Figure 1). The LLCW lies on the San Diego formation, which includes marine and fluvial sediment deposits of conglomerate, sandy-conglomerate, and siltstone geologic units. Erosion in LLCW has led to accelerated sedimentation of the Tijuana Estuary, one of the largest estuarine habitats left in California, and millions of dollars are spent annually on excavation of sediment basins at the outlet of LLCW. Channel instabilities, in particular, can impact residents of LLCW through infrastructure failure of homes and bridges. Taniguchi et al. (2018) found that the major hotspots of channel erosion in LLCW were located downstream of two hardpoints in the SW channel: 1) a circular metal culvert in the central portion of the watershed and 2) a concrete flume in the northern portion of the watershed. This paper focuses on the channel evolution of the reach upstream and downstream of the concrete flume because it is representative of typical urban channel alterations in Tijuana, Mexico and potentially other semi-arid developing countries.

The valley floor of the SW watershed is primarily composed of erodible, sandy-conglomerate. In the southern half of the watershed, the mesa tops and steep hillsides are comprised of coarser conglomerate "red caps" with weathered rock and soils, which are often underlain by sandy-conglomerate sediment. The coarser material that are embedded in the valley fill sediment likely originated from the conglomerate hillslopes and mesa tops. Detailed channel stability surveys conducted in 2014 indicate that there are spatial differences in bed composition and riparian woody vegetative cover in the SW watershed, which coincide with the spatial arrangement of urban development. The northern portion of the watershed is densely urbanized, with urban development extending from the steep mesa tops all the way to the stream channel. Unpaved roads in the northern watershed border both the left and right banks of the stream channel, leaving a less than 10 m distance between the banks and the homes. Subsequently, woody riparian vegetative cover is low (category of 0-10%) and the median grain size of the channel bed (D_{50}) is 5.4 mm (fine gravel). In the central portion of the watershed, the right valley margin has been cleared and graded but urban development is relatively sparse and riparian vegetative cover is relatively low. The

southern third of the watershed is primarily undeveloped, except for the mesa tops, and riparian vegetative cover is higher (categories of 11-25% to 50-75%). In both the central and southern watershed, bed composition is coarser (D_{50} = 32 mm, or coarse gravel) than in the northern watershed.

Historical Google Earth imagery of the northern watershed from 1994 (Google Earth, 5/30/1994, U.S. Geologic Survey), 2000 (Google Earth, 4/1/2000, 2018 DigitalGlobe), 2001 (Google Earth, 7/9/2001, 2018 DigitalGlobe), 2008 (Google Earth, 6/25/2008, 2018 DigitalGlobe), and 2014 (Google Earth, 12/22/2014, 2018 DigitalGlobe) portray the typical sequence of urban development and channel alterations in Tijuana, Mexico (Figure 2). In 1994, prior to the construction of the concrete flume, the stream reach was undisturbed with a slightly meandering and vegetated stream channel and vegetated hillslopes. Urban development started in spring of 2000, with complete vegetation removal, grading of the hillslopes and filling of the stream channel. By July 2001, the channel reformed along the unpaved road, with a straighter planform and steeper slope compared to the pre-altered 1994 condition, and the concrete flume was constructed to provide a road crossing. The flume is approximately 50 m long with a top width of 1.5 m and vertical sides of 3 m. The top width of the channel in July 2001 was approximately 4.5 m. Aerial photographs from 2008 and 2014 show a fairly straight, re-formed channel compared to the 1994 digitized stream and enlargement of the stream reach downstream of the flume, with a top width of approximately 11 m.

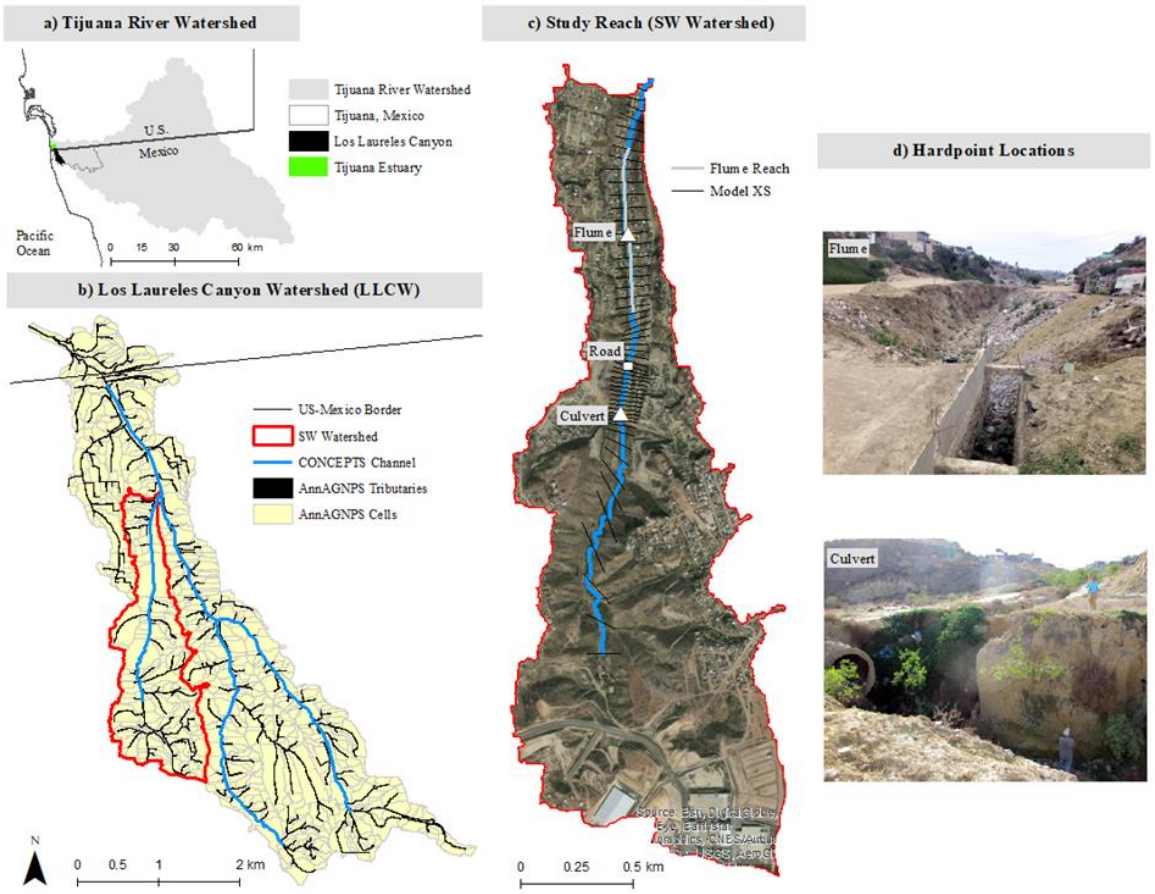

Figure 1. Study area map showing a) Tijuana River watershed, b) Los Laureles Canyon Watershed (LLCW) with AnnAGNPS tributaries and cells, CONCEPTS channel, and red watershed boundary of SW, c) SW watershed aerial basemap with indication of the CONCEPTS model reach and cross sections, flume reach that this study focuses on, concrete flume, metal culvert, and road crossing (downstream of culvert), and d) pictures of channel enlargement downstream of concrete flume and metal culvert.

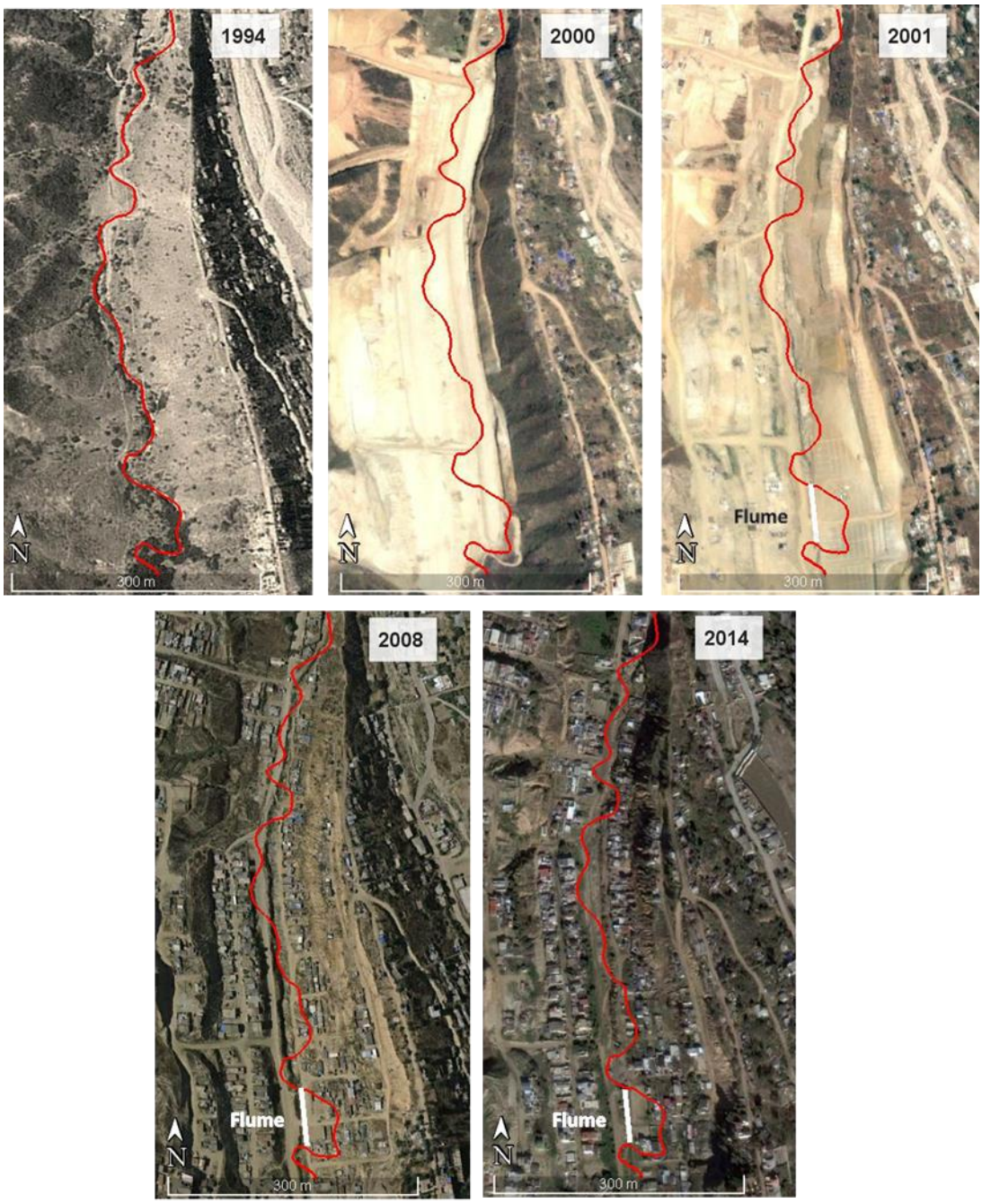

Figure 2. Aerial imagery showing the reach downstream of the concrete flume. Image from 1994 shows the pre-urban channel digitized in red, 2000 shows the initial start of urbanization with vegetation removal, grading of land and filling in the channel with loose sediment, 2001 shows the re-formation of a straight channel along the unpaved, graded road and concrete flume installed for a road crossing, and 2008 and 2014 show the straightened and enlarged channel downstream of the flume.

3. METHODS

A channel hydraulic model (CONCEPTS) linked to a watershed model, annualized agricultural nonpoint source pollutant loading model (AnnAGNPS; Bingner & Theurer, 2001), was developed for the entire LLCW and calibrated for discharge and sediment yield at the outlet of the watershed (Figure 1b). The CONCEPTS model was used to gain insight on the mechanisms driving channel instability and to simulate the impact of urban channel alterations on channel morphology. A channel sub-model for the SW watershed based on channel conditions in 2001, the time the concrete flume was installed, was developed to simulate channel evolution from 2001 to 2014 and was validated with the longitudinal bed elevation surveyed in 2014 and a surveyed cross section downstream of the concrete flume. An extended simulation period from 2001 to 2048 was conducted to determine if and/or when the SW channel will reach a steady-state condition. Finally, a scenario analysis was conducted to determine the impact of various factors on channel instability, including hardpoint geometry, steepening of the channel slope, changes in bed composition through grading, removal of vegetation, and feedbacks resulting from initial channel enlargement.

3.1 CONCEPTS Model Overview

CONCEPTS is a one-dimensional computational hydraulic and channel evolution model that uses a distributed flow routing scheme where the flow is computed as a function of time simultaneously at all cross-sections in the model (Langendoen & Alonso, 2008). Unsteady, one-dimensional flow is calculated using the Saint Venant equations (Chaudhry, 2008), which include continuity and momentum equations. Sediment transport and bed erosion are based on the conservation of sediment mass by size class, entrainment rate for each size class, and a sediment mass balance is calculated at each cross-section (Langendoen & Alonso, 2008). Entrainment of bed and bank materials via fluvial erosion is based on the critical boundary shear stress and the shear stress exerted on the bed or bank materials. CONCEPTS calculates bank erosion for both fluvial erosion and mass failure. For mass failure, the banks are treated as potential failure blocks and divided into slices; the factor of safety is estimated through a limit-equilibrium method (e.g., Morgenstern & Price, 1965), which accounts for soil pore-water effects on soil shear strength and the hydrostatic force exerted by the surface water on the bank face. The CONCEPTS bank erosion algorithms are

widely accepted and have recently been incorporated into various computer models such as HEC-RAS v5 (Gibson et al., 2015), SRH-2D (Lai et al., 2015), and TELEMAC2D v7p3 (Langendoen et al., 2016).

3.2 CONCEPTS Input Data and Setup

Required input data for CONCEPTS includes: channel geometry, channel boundary roughness (Manning's *n*) of the bed, banks, and floodplain, grain size distribution of the bed and bank materials, critical shear stress (τ_c) and erodibility of bed and bank material, and water and sediment inflows. A CONCEPTS channel model was first developed for the entire LLCW, based on field data collected in 2014 (Taniguchi et al., 2018) at 57 earthen and 32 concrete channel locations, including stream channel geometry, particle size distribution of the channel bed (D_{50} ranging from 5.4 mm to 32 mm), and jet-test erodibility measurements of cohesive banks following Hanson (1990). In the CONCEPTS model, critical shear stress was set as 6 Pa and erodibility (*k*) was 1.0E-7 m s^{-1} Pa^{-1}. Concrete flume roughness was set to 0.015 and earthen, sandy-gravel channel roughness was set to 0.035, which are typical values for the observed channel conditions (e.g., Chow, 1959; Barnes & Barnes Jr., 1987).

To simulate hydraulics and channel evolution of the model reach, hydrographs and sedigraphs from all storm events of the simulation period need to be imposed at the upstream boundary (river km 0) and at the mouths of all minor tributaries. Hydrographs and sedigraphs were not available for the SW watershed, and were only available at the outlet of LLCW for thirteen storm events from 2014 to 2017. Therefore, a watershed-scale model, AnnAGNPS (Bingner & Theurer, 2001), was developed for LLCW to provide sediment and hydrologic inflow to the CONCEPTS channel model. AnnAGNPS provides event-wise runoff volume, peak discharge, and sediment load (clay, silt, and sand) for 462 reaches and 1,142 cells draining into the CONCEPTS channel model (Figure 1b). The transition from AnnAGNPS reaches to the CONCEPTS reach was determined by the cross-sectional survey from 2014, along the main stem of the channel network extending to the channel head. For the SW watershed, the channel head was inaccessible due to restricted access, so the upstream-most model cross section started at the upstream-most surveyed location. Triangular hydrographs were constructed for the downstream end of each cell or reach using

the event total runoff, peak discharge and time-to-peak. AnnAGNPS outputs the event total sediment load of sand (including very coarse sand to very fine sand), silt, and clay. The sand load is reported as one value per event and is not split by size class. Therefore, the total sand reported by AnnAGNPS was parsed into fine sand (90%), medium and coarse sand (8%) and very coarse sand (2%) categories, based on the hillslope average particle size distribution of sand from the Los Flores soil (Biggs et al., 2018b). The AnnAGNPS daily sediment mass delivered to the channel for sand, silt, and clay were converted to triangular sedigraphs based on time to peak, total storm duration, and total sediment load. The peak sediment discharge was assumed to occur at the time of peak discharge.

Rainfall data were collected at one station on the Mexican side of the border from 2014-2016 but were not available for the whole simulation period (2001-2016), so rain gauges in the US were analyzed for their correlation with the Mexico rain gauge (Biggs et al, 2018a). The measured daily precipitation at the Brownfields climate station in San Diego was applied uniformly over the entire watershed using a type-II, 24-hour rainfall distribution (TR-55). The storm type-II was determined by comparing cumulative rainfall observed at the rain gauge in Mexico (Biggs et al., 2018a) with the cumulative distribution functions from TR-55.

The LLCW AnnAGNPS model was first calibrated and validated for discharge at the outlet of the LLCW based on thirteen observed rainfall events from 2014 to 2017 (Biggs et al., 2018a). Then the AnnAGNPS model was calibrated for sediment production and validated against gully surveys following storm events (Gudino-Elizondo et al., 2018) and total annual sediment yield calculated from the tons of sediment excavated from the sediment traps at the outlet of LLCW from 2009 to 2012, corrected for trap efficiency (Biggs et al., 2018a). A sensitivity analysis was conducted to determine the most sensitive parameters on sediment load, constrain parameter values, and to develop the most suitable parameter combinations for the watershed (Gudino-Elizondo et al., 2018). Model calibration and validation were conducted for the entire LLCW, but discharge and sediment yield were not available to do so for the SW watershed.

A CONCEPTS sub-model of the SW tributary was developed and utilized in this study (Figure 1c) with a focus on the concrete flume reach, including 311 m upstream and 662 m downstream of the flume (Figure 1c). The concrete flume reach study extent starts at the upstream-most stable cross section and ends at the downstream-most stable cross section from the flume. In order to simulate channel evolution following straightening and initial channel formation along the flume reach (year 2001, Figure 2), a 2001 initial model was constructed using estimated channel conditions from 2001. The SW model contained 57 cross sections with an average spacing of 49 m. Initial channel geometry from 2001 was determined for all cross-section locations in the model. Upstream of the flume reach (Figure 1c), the initial channel geometry was linearly interpolated between the surveyed stable cross-sections that showed little to no signs of enlargement. For the flume reach, the initial 2001 thalweg elevation for each cross-section was linearly interpolated based on the thalweg elevation of the stable cross-section upstream of the flume to the thalweg elevation of the stable cross-section downstream of the flume. For the initial channel geometry of the flume reach, "historical" channel geometry from 2001 was utilized with an estimated top width of 4.5 m measured from historical imagery from 2001, bottom width of 1.5 m (width of the flume), and depth of 3 m (depth of the flume). The initial trapezoidal channel geometry was inserted at the interpolated thalweg elevation for each cross-section location along the flume reach. The two most downstream cross sections are located at a concrete-lined channel that stabilizes the confluence with the main stem of LLCW. It is assumed that the bed and bank material of these cross sections are not erodible, though deposition could occur.

3.3 CONCEPTS Model Simulation Period

The concrete flume and metal culvert were installed between April 2000 and July 2001. Model scenario for the SW channel starts after the hardpoints were installed and the channel reformed (2001) and ends at the time of the channel survey in 2014. Channel cross-sectional geometry and thalweg longitudinal elevation surveyed in 2014 are utilized as model validation and compared to simulated channel geometry and thalweg elevation in 2014 for the reach downstream of the concrete flume. Additionally, an extended timeseries from 2001 to 2048 was simulated to determine if and how long it will take for the channel to reach a steady-state condition. The AnnAGNPS time series of rainfall, runoff, and sediment yield

from 2001 to 2016 was extended by 32 years by copying the 16-year period and pasting it to the end of the time series two times to get an extended scenario period of 2001 to 2048.

A total of 323 rainfall events were simulated between 2001 and 2014. Total annual rainfall ranged from 76 mm to 450 mm for the scenario period, with mean annual rainfall of 198 mm. The scenario period included one 10-year event (~60 mm daily total), one 5-year event (~50 mm daily total), and three 2-year events (~40 mm daily total), with the majority (98%) of the storm events smaller than the 2-year storm (ranging from 36 mm to 0.3 mm; mean of 8 mm). The extended timeseries, which included observed rainfall from 2001 to 2016, had relatively low rainfall with total annual of 196 mm and 177 mm, respectively. However, one additional 5-year storm occurred in 2016. The entire extended 2001-2048 scenario period included 24 storm events between the 2-year to 10-year recurrence intervals.

3.4 CONCEPTS Scenario Analysis

Seven CONCEPTS model scenarios were conducted to test the impact of various channel alterations on channel stability, under current land cover conditions for the scenario period of 2001 to 2048. The analysis was conducted to identify what processes generated the instability observed in the channel, and to determine if the SW channel can be stabilized under current land cover conditions. Therefore, the focus was on in-channel alterations as opposed to returning the watershed back to natural conditions.

The first scenario represents current channel conditions from 2001 described in section 3.2, and every subsequent scenario represents an incremental “naturalization” of the stream system towards historical channel conditions. We hypothesized that a combination of hardpoint characteristics and reach characteristics led to channel instability, including hardpoint geometry, hardpoint prevention of upstream incision, steepening of the channel slope, changes in bed composition through grading, removal of vegetation and feedbacks resulting from initial channel enlargement. The seven scenarios build upon the previous scenario and are as follows: 1) observed (2001) channel conditions; 2) larger concrete flume geometry; 3) no concrete flume; 4) historical slope downstream of the flume; 5) coarsening the bed downstream of the flume; 6) vegetated stream banks and floodplain; and 7) reference channel geometry based on the reference regional geometry curve for an undisturbed watershed with similar lithology (Spring Canyon, Taniguchi et al., 2018). Scenario 2 was

conducted to test if the 2001 concrete flume geometry (rectangular, narrow and deep) impacts downstream channel instability, so the flume geometry in scenario 2 was set as the historical 2001 channel geometry (trapezoidal, with bottom width of 1.5 m and top width of 4.5 m). Scenario 3 represents a scenario without the concrete flume, which allows channel incision and widening at the flume reach with bed and bank boundary conditions set as the boundary conditions at the cross-section upstream of the flume. Scenario 4 tests if straightening and subsequent increase in slope impacted channel enlargement. Historical channel elevation data were not available for 1994, therefore historical valley-averaged channel slope in 1994 (S_{1994}) was estimated for the reach downstream of the flume based on historical aerial imagery from 1994 as:

$$S_{1994} = S_{2001} \times \frac{L_{\text{valley},1994}}{L_{\text{channel},1994}} \quad (1)$$

where S_{2001} is the estimated slope from initial 2001, $L_{\text{channel},1994}/L_{\text{valley},1994}$ is the 1994 channel sinuosity, $L_{\text{valley},1994}$ is the straight-lined valley length in m from 1994, and $L_{\text{channel},1994}$ is the channel length along the stream reach in m from 1994 (red line, Figure 2). The channel gradient of the reach downstream of the concrete flume was adjusted to S_{1994} (0.0327) for scenario 4.

For scenario 5, the bed of the reach downstream of the flume (D_{50} = 5.4 mm) was coarsened and set to the bed composition upstream of the flume (D_{50} = 32 mm), which is assumed to reflect the historic bed composition. To simulate vegetated stream banks for scenario 6, bank and floodplain roughness downstream of the metal culvert to the end of the concrete flume reach were increased from 0.035 to 0.07 (Chow, 1959) and cohesion of the banks was increased from 1 kPa to 10 kPa (Bankhead et al., 2013). The final scenario (7) represents channel conditions close to "reference", including reference channel geometry width (3.5 m) and depth (0.5 m) based on hydraulic width and depth equations from an undisturbed channel on similar lithology (Spring Canyon; Taniguchi et al., 2018).

The results of the modeled scenarios were analyzed by plotting cumulative bed change and top width change over the scenario period for each scenario at the cross-sections immediately upstream and downstream of the concrete flume. Cumulative channel-derived sediment load (tons) over the scenario period at the outlet of the SW watershed was

compared across the seven scenarios. Cumulative channel-derived sediment load was calculated by subtracting the total cumulative daily hillslope contribution from AnnAGNPS, from the cumulative daily sediment load simulated by CONCEPTS.

4. RESULTS AND DISCUSSION

4.1 Hillslope Coarse Sediment Uncertainty

A major uncertainty in this study is the relative contribution of coarse sediment from the hillslopes (>0.25 mm), given that AnnAGNPS only simulates hillslope-derived fine sediments (silt and clay) and reports a single value for sand. The estimation of coarser sediment added to the hillslope timeseries may differ from the actual coarse sediment load delivered to the channel and was based on two assumptions. The first assumption was that the coarsest sediment size that gets delivered to the stream channel is 2 mm. Although particles coarser than sand may get delivered to the stream channel, it is assumed that gravel that has accumulated in the valley fill alluvium has been transported from the hillslopes during large, episodic flow events. The simulation period includes relatively dry water years where this assumption may be more valid. The second assumption was that hillslope-derived sand reflect the hillslope soil texture of the sand size classes, including very coarse to very fine sand, from the non-cobbly Los Flores soil. Using the sand texture from Los Flores alone may not capture the heterogeneity of soil texture in the SW watershed. There are coarser, cobbly soils in LLCW, but field observation suggests that the majority of the coarse sediment from the hillslopes gets transported to the channel via gullies that form almost exclusively on the Los Flores soil formation.

Simulated thalweg elevation from 2001 to 2014 for the reach downstream of the concrete flume was compared to surveyed thalweg elevation in 2014 for two model simulations: 1) assuming all of the sand from AnnAGNPS is fine sand (or washload) and 2) partitioning the AnnAGNPS sand to reflect the hillslope soil texture (Figure 3). Simulated thalweg elevation from 2014 with coarser sand added from the hillslopes (dotted line) matched the 2014 surveyed thalweg elevation (grey line), while simulated 2014 thalweg elevation without coarser sand added overpredicted incision (red line). Therefore, the model with the coarser sand added was utilized in this study.

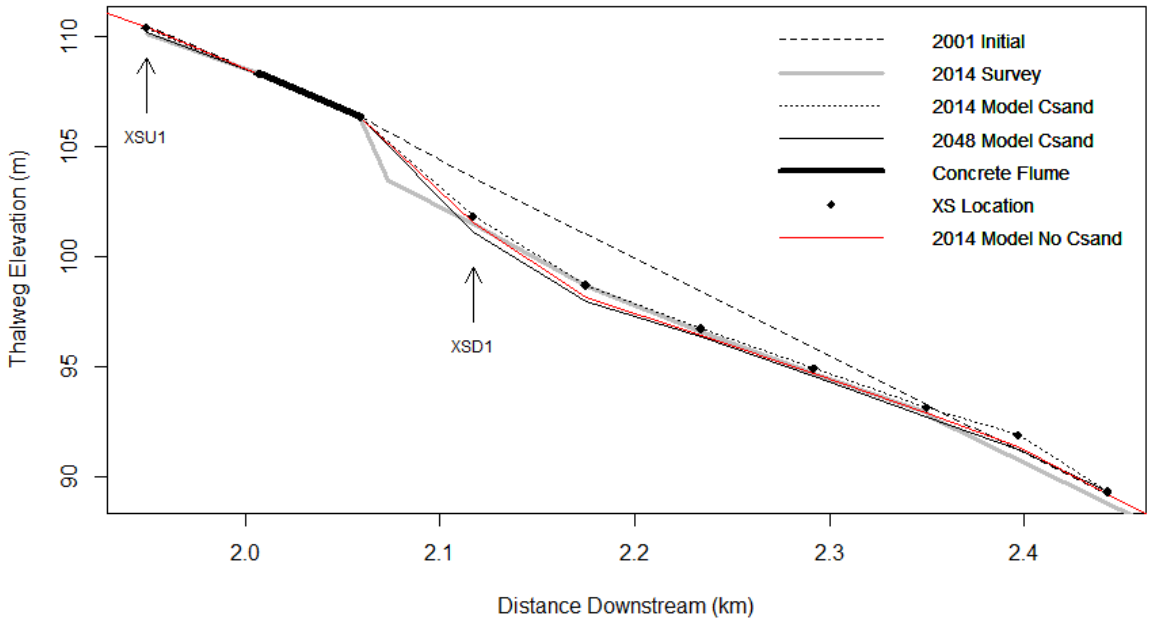

Figure 3. Thalweg elevation plot for the reach downstream of the concrete flume. Simulated thalweg elevation from 2014 with coarser sand added from the hillslopes (dotted line) matched the 2014 surveyed thalweg elevation (grey line), while simulated 2014 thalweg elevation without coarser sand added overpredicted incision (red line). Channel incision continues slightly until 2048 (solid black line). The 2001 initial (dashed line) represents the estimated thalweg elevation at the start of the simulation, soon after the flume was installed and the channel reformed. Arrows indicate cross-sectional locations immediately upstream (XSU1) and downstream (XSD1) of the concrete flume.

4.2 Simulated Channel Evolution

CONCEPTS accurately simulated bed incision from 2001 to 2014 for the reach downstream of the concrete flume (Figure 3). Mean absolute error in the simulated and surveyed thalweg elevations for seven cross sections downstream of the flume and one cross section immediately upstream of the flume was 0.09 m. In January 2001, bed incision was initiated following a series of four consecutive rainfall events, all less than the 2-year flood. Maximum incision was located at river km 2.3. As the channel bed downstream of the flume incised, the channel gradient decreased until it matched the approximate historical 1994 slope (0.0327 m/m). Downstream of the flume, from XSD1 to river km 2.4, the channel gradient decreased from the initial 2001 slope of 0.044 m/m to 0.0367 m/m (2014 simulated, 0.037

m/m observed) and finally to 0.033 m/m in 2048. As the slope declined, coarse particles started to deposit and the D_{50} of the bed increased from 6 mm to 70 or 90 mm.

The incision relaxation distance downstream of the flume (291 m) observed in the field survey and model scenario occur at river km 2.4 (Figure 3). Incision relaxation distance refers to the downstream reach length from the hardpoint (i.e. concrete flume) in which there is no incision. A scenario turning off an AnnAGNPS tributary that drains into river km 2.4 was conducted to determine if the source of coarse sediment depositing at this location was the adjacent hillslope or the incising channel. Simulated results indicated that channel deposition was due to excess coarse sediment generated from upstream channel erosion that deposits downstream at river km 2.4. The relaxation distance is therefore governed by the distance in which coarse sediment from channel erosion is in equilibrium with local transport capacity of the stream.

Simulated channel cross-sectional geometry 15 m downstream of the flume (XSD1) in 2014 matched observed cross sections surveyed in 2014 using a combination of a differential GPS and a 10 cm digital elevation model created using structure-from-motion (SfM) photogrammetry techniques (Figure 4). The 2014 surveyed cross-section includes road fill near the banks and floodplain (dotted area); the pre-road bank is identifiable in the field and in the cross section (Figure 4). Channel cross sectional area matched well between simulated and observed, with 2.8% difference. Model results from 2014 to 2048 indicate that incision will continue after 2014 for 0.7 m and failure of the banks will occur. There was observed channel widening at XSD1 in 2016, but residents and city officials fill in the

channel with loose debris following bank failure to protect the unpaved road and adjacent homes.

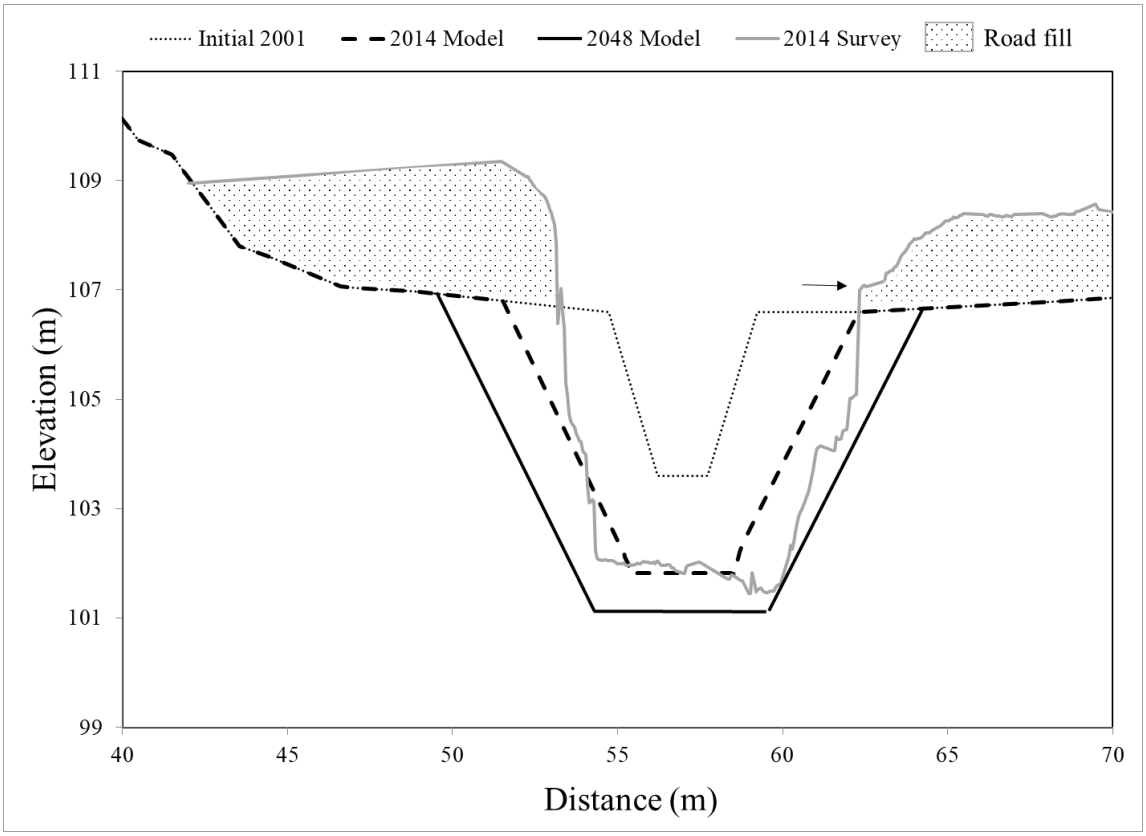

Figure 4. Cross-sectional geometry comparison downstream of the concrete flume at XSD1 from modelled output geometry from 2014 and 2048 compared to surveyed cross-section from 2014. Surveyed 2014 cross-section includes road fill that was added to the floodplain (dotted area). Arrow indicates true initial bank elevation. By 2048, there was simulated bed incision, bank failure, and subsequent widening.

Cumulative bed elevation and top width changes were plotted over a 48-year simulation period following the installation of the concrete flume to determine the approximate timescale of incision and widening at XSD1 (Figure 5). Bed incision exponentially increases for 20 years, reflective of the incision CEM stage II, after which the bed slope declines, deposition of coarse particles occurs, and the channel bed stabilizes. After 10 years of simulation, incision of 1.8 m causes the banks to become unstable and to collapse, leading to channel widening, or CEM stage III. Although bed elevation stabilized after 20 years, the channel continues to widen exponentially, without apparent stabilization.

Future model runs will include an additional 20 years of simulation to determine the time in which channel widening starts to decline.

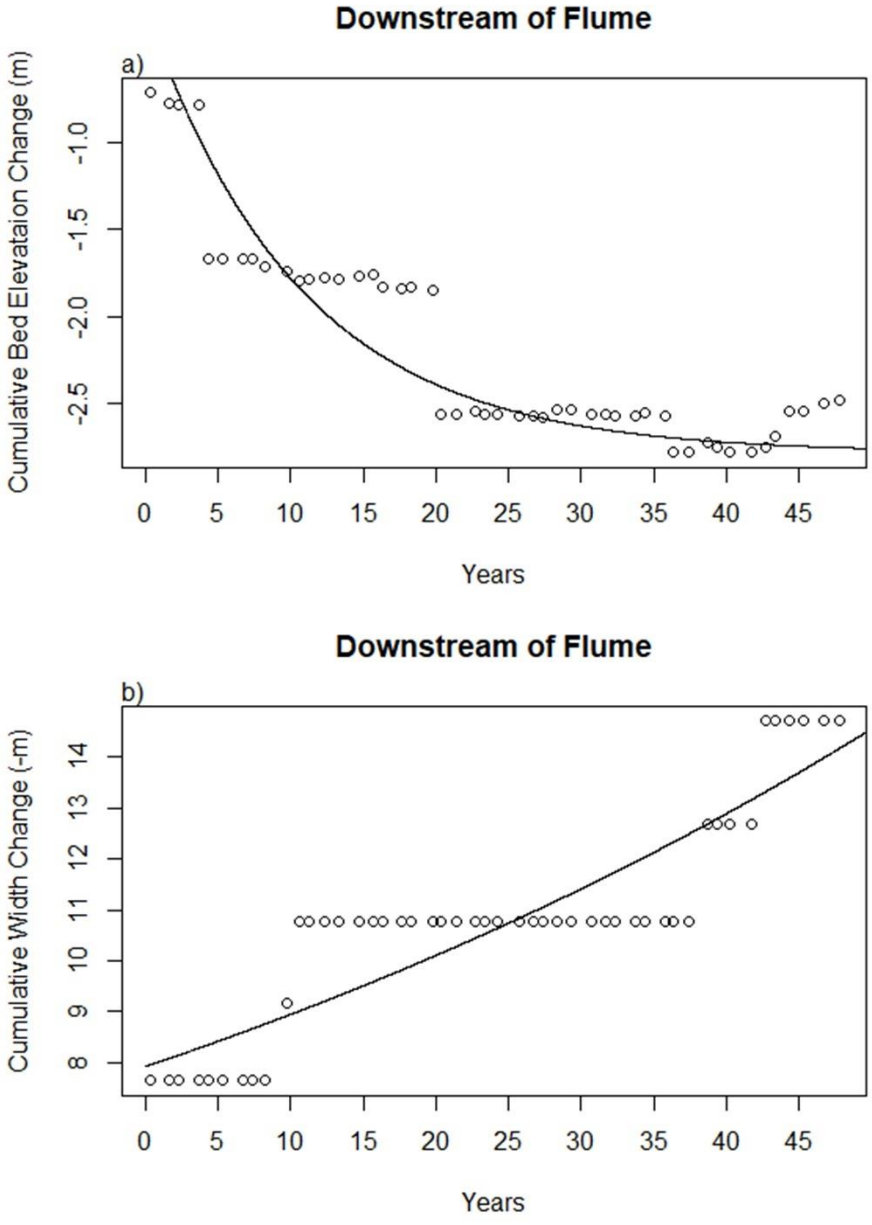

Figure 5. Cumulative bed elevation change and width change downstream of the flume under 2001 conditions. Bed lowering occurs rapidly for the first twenty years after the hardpoint was installed in 2001, with stabilization and deposition following. The channel continues to widening throughout the simulation period.

4.3 Scenario Analysis

4.3.1 BED ELEVATION ADJUSTMENT

The hardpoint geometry only had a minor impact on bed incision, while the alterations to the resisting forces, including the bed particle size and bank cohesion and roughness from vegetation, had the largest impact on bed incision. The cross-section 15 m downstream of the current concrete flume (XSD1) incised less with each modeled scenario (Figure 6a). Note that each subsequent scenario represents a stepwise return to estimated historic (pre-1994) conditions. Under 2001 channel conditions (scenario1), ~2 m of incision occurred within the first 5 years of the scenario period, and incision exponentially decreased as the scenario period extended to 2048. Total incision from the 2001 conditions was 2.5 m. Scenario 2 indicates that with a larger flume, incision will only be reduced by 0.1 m at XSD1, suggesting that the narrow and deep current geometry of the flume is not governing downstream instability, and that alterations of this geometry would not be sufficient to stabilize the channel. Under scenario 3, where the larger flume is removed, the incision propagates upstream, but incision is reduced by <0.5 m at the downstream XSD1, and the channel bed reaches a relatively steady-state condition 3 years sooner than scenario 1. The concrete flume has caused an increase in incision at XSD1, but has also prevented the reach upstream of the flume from incising. For scenario 4 (no flume and with the historical slope from 1994), 2.2 m of incision occurs by the end of the scenario period and there is only a minimal reduction in incision (-0.04 m) compared to scenario 3. Altering the slope back to historical conditions, however, caused the initial rate of incision to decrease.

The largest reduction in incision occurred by altering the resisting forces to erosion. Coarsening the bed downstream of the flume to pre-disturbed conditions (scenario 5) has led to 0.5 m of deposition by 2048. This indicates that filling the channel with highly erodible, fine sediment during the process of urbanization has caused a reduction in the bed armoring and played a large role on downstream incision. Adding bank vegetation (scenario 6) through increased bank cohesion and roughness has led to 1 m of deposition downstream of the flume. However, throughout the simulation period, the channel bed was actively adjusting with incision and deposition occurring following a large storm that occurs every 20 years. Returning to the reference channel geometry (scenario 7), all cross-section locations

in the SW model experienced relatively stable beds for the entire scenario period. The shallower reference channel geometry may experience less channel instability due to a smaller channel capacity and more frequent inundation of the floodplain compared to an enlarged channel geometry. In enlarged channels, flows that have formerly inundated the floodplain may be confined in the channel, leading to larger flow depths, excess energy and stream channel enlargement (Brookes, 1987). Channel enlargement has therefore disconnected the stream channel from the floodplain storage.

In contrast to downstream of the concrete flume, the bed elevation 12 m upstream of the concrete flume at XSU1 remained relatively stable throughout the entire scenario under the initial 2001 channel conditions (scenario 1), with incision ranging from 0.04 m to 0.35 m (Figure 6b). However, with a larger flume slightly more incision occurred at XSU1 (~0.2 m) due to a decrease in water depth at the downstream wider flume and thus a local increase in friction slope. A comparison of scenarios 2 and 3 show that the concrete flume also serves as grade control and prevents upstream migration of a knickpoint into the upstream reach; without the concrete flume (scenario 3), the XSU1 incises a total of 1.4 m. Without the concrete flume and with the 1994 historical slope (scenario 5), cumulative incision is reduced by 67% at XSU1. The reduction in channel slope reduces the available stream power for a given discharge. Coarsening the bed, adding vegetation, and reverting back to the natural channel geometry all caused net deposition by 2048. At both XSU1 and XSD1, reverting back to a natural geometry caused less deposition compared to solely vegetating the banks. Floodplain inundation will be more frequent with smaller channel geometries, and therefore sediment that may have deposited in the channel with a larger geometry, can be deposited on the floodplain.

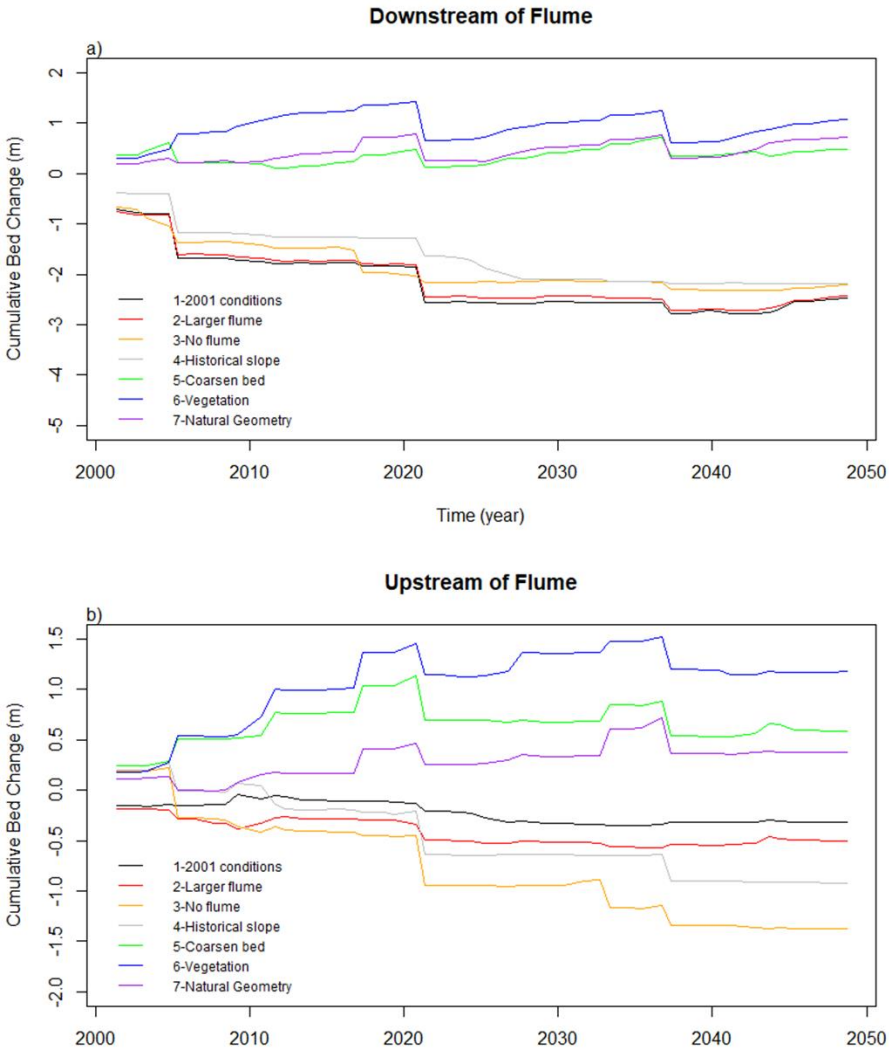

Figure 6. Cumulative bed elevation changes over the model scenario time period (2001-2048) for seven scenarios at two cross-sectional locations: a) 15 m downstream of the concrete flume (XSD1) and b) 12 m upstream of the concrete flume (XSU1). Scenarios 2-5 relate to in-channel changes to the reach downstream of the concrete flume and scenarios 6 (added vegetation) and 7 (natural geometry) relate to the reach downstream of the metal culvert to the downstream most earthen cross section in the SW channel.

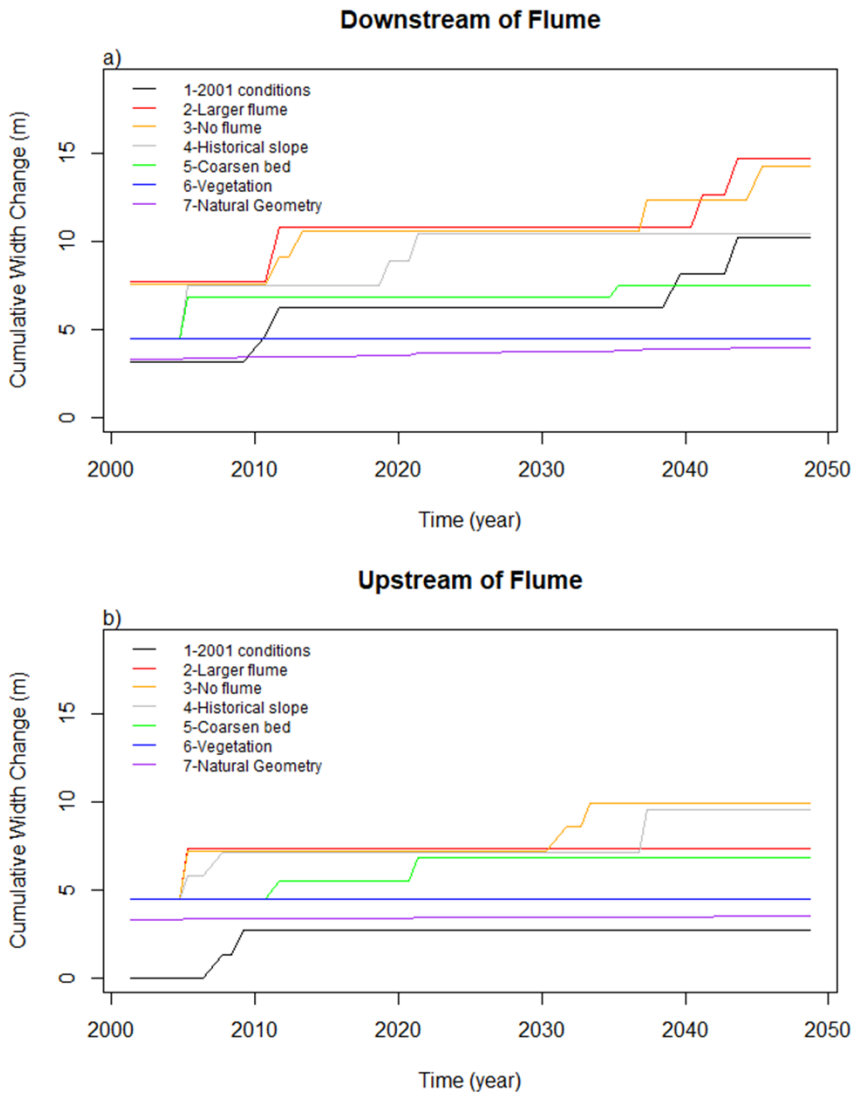

Figure 7. Cumulative change in top width over the model simulation time period (2001-2048) for seven scenarios at two cross-sectional locations: a) downstream of the concrete flume (XSD1) and b) upstream of the concrete flume (XSU1).

4.3.2 CHANNEL WIDENING

Although the bed is actively incising during the simulation period, bank failure upstream and downstream of the concrete flume occurs less frequently (Figure 7). With a larger flume and without the flume (scenarios 2 and 3), widening at the downstream XSD1 increased by 4 and 4.5 m, respectively, compared to the 2001 conditions (scenario 1). All scenarios excluding revegetating the banks (scenario 6) and reverting to a natural channel geometry (scenario 7) show that XSD1 may still be actively widening throughout the

simulation period. Channel width upstream of the flume remained relatively stable across all scenarios except removal of the concrete flume (scenario 3). Without the presence of the concrete flume, channel widening at XSU1 increased by ~5 m compared to scenario 1. This indicates that the concrete flume has prevented both incision and widening in the upstream direction.

4.3.3 SEDIMENT LOAD

The long-term cumulative channel-derived sediment load at the outlet of the SW watershed decreased with every scenario except for altering the flume geometry (Figure 8). Although each scenario caused a reduction in sediment load, the magnitude of reduction from scenarios 2 to 6 remained relatively the same (range of 26,000 tons to 38,000 tons) and the largest reduction (~150,000 tons) was caused by reverting to reference channel geometries (scenario 7). Although coarsening the bed, adding bank vegetation, and reverting to reference geometries (scenarios 5 to 7) caused relatively little changes in the channel geometry upstream and downstream of the flume (Figure 6 and 7), sediment load reduction was greatest for scenario 7 because the entire channel was connected to the floodplain storage. Figure 6 and 7 reflect change in width and depth plots at two cross section locations (XSU1 and XSD1) and do not portray how the majority of stream reaches in the channel network stabilized following scenario 7. With a smaller channel capacity and cross-sectional area, floodplain inundation is more likely to occur and sediment is able to deposit on the floodplain, all of which can lead to more stable channels and a reduction in sediment load to the outlet.

Although reverting to reference channel geometries and reconnecting the channel to the floodplain storage shows the largest reduction in sediment load to the outlet, this is a highly infeasible management practice that would require alterations of extensive reach lengths, subsequent high costs and may lead to frequent flooding of homes adjacent to the stream channel. Aside from reverting back to a natural channel geometry, the largest reduction in cumulative channel-derived sediment load was from removing the flume (38,000 tons) and coarsening the bed downstream of the flume (35,000 tons). Coarse gravel augmentation can be implemented to prevent or reduce incision of incising streams (Arnaud

et al., 2017), including downstream reaches below dams (Ock et al., 2013), and may be the most cost-effective and feasible management practice in the study watershed.

Sediment is collected in two traps at the outlet of LLCW in the Tijuana Estuary in the United States and excavated annually prior to the wet season (i.e. the fall). Total annual sediment excavated from the traps and corrected for trapping efficiency are available from 2006 to 2012 (Biggs et al., 2018a). From 2006 to 2012, the corrected mean annual sediment excavated from the traps of 52,190 tons yr^{-1}. The mean annual sediment load from the SW watershed based on the integrated CONCEPTS-AnnAGNPS model was approximately 36,686 tons yr^{-1}, which implies that the SW watershed supplied about 70% of the total sediment to the Tijuana Estuary from 2006 to 2012. Channel erosion accounted for 73 to 83% of the total sediment load from the SW watershed. If the SW channel had not incised, mean annual sediment load from the SW watershed would have reduced by 5,700 tons $year^{-1}$, estimated from the natural channel scenario 7.

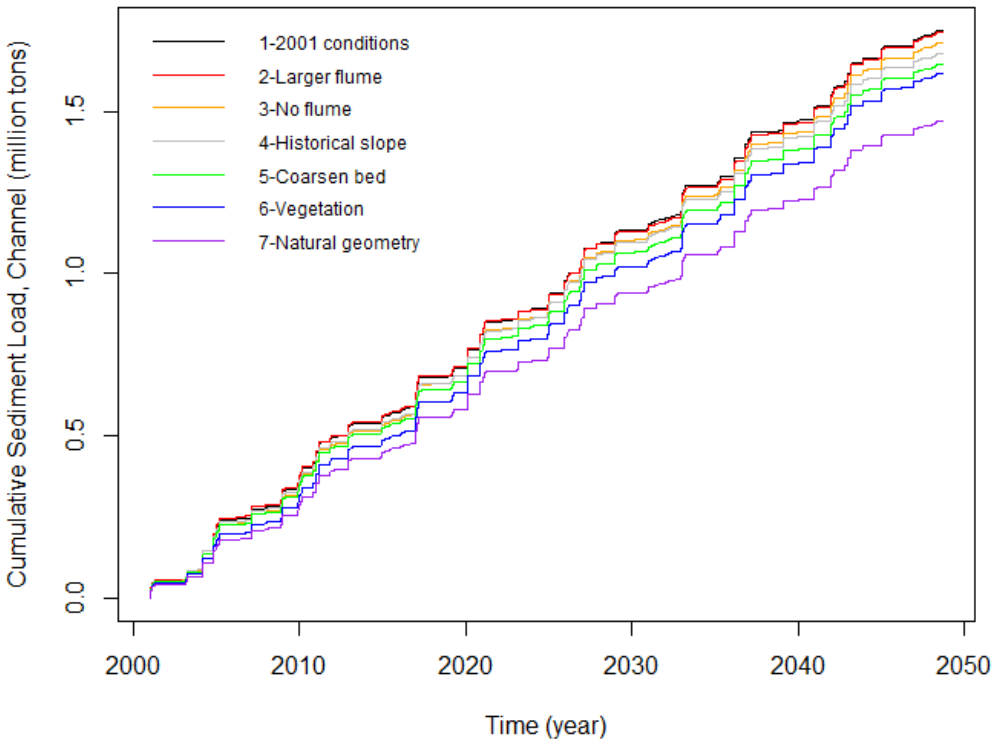

Figure 8. Cumulative channel-derived sediment load at the outlet of the SW watershed for 7 scenarios. Scenarios 1-3 show similar sediment load. Coarsening the bed downstream of the flume, adding vegetation along the bed and floodplain, and reverting back to a natural channel geometry all served to progressively lower channel-derived sediment load at the outlet of the watershed.

4.4. Spatial Patterns of Erosion and Deposition

Complex spatial patterns of erosion and deposition were observed in this study (Figure 9). Downstream of the concrete flume, degradation of the channel bed flattens the channel gradient and reduces the available stream power for a given discharge, similar to the channel evolution model described by Simon and Hupp (1986). The channel downstream of the flume, which has altered bed material of unconsolidated loose sediment and lacks vegetation along the channel banks, incises until it reaches the historical valley averaged slope from 1994 by scenario year 2048. As bank heights are increased and bank angles are steepened by fluvial undercutting, banks become unstable and channel widening via mass wasting occurs. Coarse sediment is mobilized from the banks and deposits downstream (i.e. at river km 2.4) where the channel becomes stable and incision diminishes.

A slightly different spatial pattern of erosion and deposition is observed downstream of the metal culvert and the road crossing. Both the metal culvert and the road crossing serve as artificial grade control and promote upstream deposition, similar to the concrete flume. These structures have disrupted the downstream transmission of bed materials, which leads to an increase in channel degradation downstream of the structures, similar to the findings of Simon and Darby (2002) and Chin & Gregory (2001). The incision relaxation distance downstream of the metal culvert is governed by the downstream road crossing, which promotes deposition of the coarse material from channel erosion downstream of the culvert.

Although incision is exacerbated downstream of the metal culvert and concrete flume, these structures are not the sole reason for channel instabilities. Scenarios with and without both structures indicate that downstream incision would still occur without the presence of both structures, although downstream incision is reduced. The process of urbanization, which includes complete development of the valley floor that oftentimes extends to the stream channel, have created enlarged channels that are completely removed from floodplain storage. Moreover, vegetation removal and grading of the channel into an unpaved road during the process of urbanization have decreased the resistance to erosion.

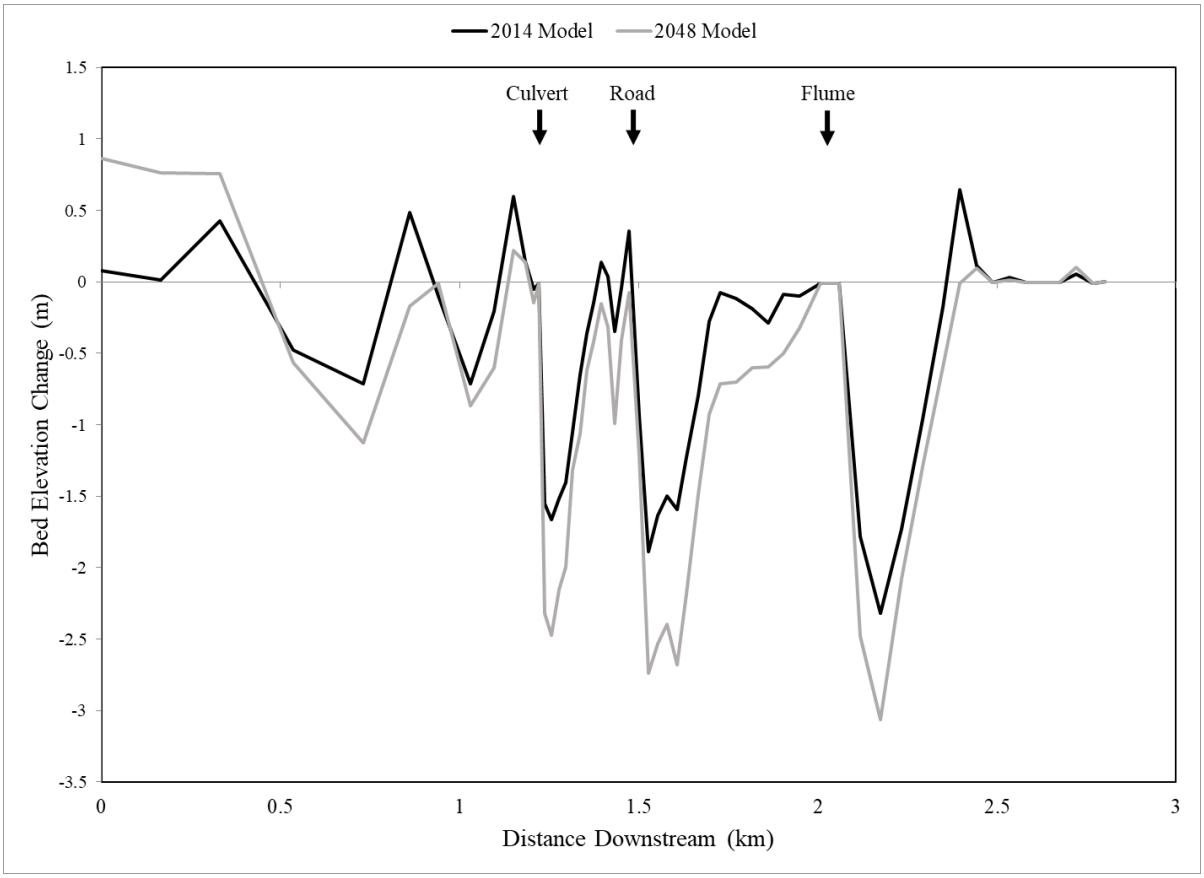

Figure 9. Bed elevation changes for the entire SW channel model. Observed patterns of incision downstream of three channel disturbances: culvert, road crossing, and concrete flume.

5. CONCLUSIONS

CONCEPTS was used to quantitively assess channel evolution following the installation of a concrete flume and to assess the relative importance of compounded channel alterations on stream channel instability in a rapidly urbanizing, semi-arid region. Model simulations from 2001 to 2048 indicate that the reach downstream of the flume actively incised from 2001 to 2020, until the slope decreased and coarse material deposited on the bed. Channel widening, in contrast, has not diminished and is predicted to continue beyond the year 2048. However, local channel filling of loose sediment is implemented following large storm events to prevent damage of the adjacent unpaved road and failure of homes and can limit channel widening.

The geometry and presence of the flume only accounted for local downstream scour. The concrete flume, instead, prevented incision in the upstream direction by serving as grade control. Channel erosion is caused mainly by the destruction of the natural channel, including channel burial, straightening, steepening, and removal of riparian vegetation, often performed in the process of turning channels into roads. Enlarged, unprotected channels reform and are subsequently disconnected from the floodplain storage.

Urban development of the valley floor, including direct manipulation of the stream channels and channel confinement, have caused excessive channel enlargement and subsequent floodplain storage removal. Although the largest reduction in sediment yield at the outlet of the SW watershed was achieved by reverting the enlarged cross sections back to the reference channel geometry, this management practice would likely cause more frequent floodplain inundation of the homes adjacent to the stream channel. Gravel augmentation downstream of the flume may be a cost-effective management practice that can stabilize the incising bed and reduce sediment load to the Tijuana Estuary.

Future research needs to be conducted on better characterizing the medium-coarse sediment load off of the hillslopes to add confidence in the model results. Although model results with and without the addition of coarser sediment was conducted, a sensitivity analysis utilizing the area-weighted spatial distribution of hillslope soil texture would greatly improve model uncertainty. Additionally, model scenarios at the watershed scale for LLCW need to be conducted to fully understand the contribution of the sediment supplied from the SW watershed on the overall sediment budget to the Tijuana Estuary.

ACKNOWLEDGMENTS

This study was funded by the US Environmental Protection Agency (EPA) (Interagency Agreement ID # DW-12-92390601-0) in collaboration with the US Department of Agriculture (USDA, Agreement # 58-6408-4-015), and Centro de Investigación Científica y de Educación Superior de Ensenada (CICESE).

REFERENCES

Arnaud, F., Piégay, H., Béal, D., Collery, P., Vaudor, L., & Rollet, A. J. (2017). Monitoring gravel augmentation in a large regulated river and implications for process-based restoration. In *Earth Surface Processes and Landforms* (Vol. 42, pp. 2147–2166). https://doi.org/10.1002/esp.4161

Bankhead, N., Simon, A., & Thomas, R. E. (2013). *Experiments, model development and bank stability simulations to assess bank erosion rates and potential mitigation strategies*. Davis, CA.

Biggs, T. W., Taniguchi, K. T., Gudino-Elizondo, N., Yongping, Y., Bingner, R. L., Langendoen, E. J., & Liden, D. (2018a). *Field measurements to support sediment and hydrological modeling in Los Laureles Canyon* (EPA/600/X-18/0XX). Washington, DC.

Biggs, T. W., Taniguchi, K. T., Gudino-Elizondo, N., Yongping, Y., Bingner, R. L., Langendoen, E. J., & Liden, D. (2018b). *Geology, soil properties and erosion on marine terraces along the US-Mexico Border* (XXXX). Washington, DC.

Bingner, R. L., & Theurer, F. D. (2001). AnnAGNPS: Estimating sediment yield by particle size for sheet and rill erosion. In *paper presented at Seventh Federal Interagency Sedimentation Conference, Subcomm. on Hydrol. and Sediment., Advis. Comm. on Water Inf.* Reno, Nev., 25-29 March.

Bledsoe, B. P., Stein, E. D., Hawley, R. J., & Booth, D. (2012). Framework and Tool for Rapid Assessment of Stream. *JAWRA Journal of the American Water Resources Association*, *48*(4), 788–808. https://doi.org/DOI: 10.1111/j.1752-1688.2012.00653.x

Booth, D. B., & Fischenich, C. J. (2015). A channel evolution model to guide sustainable urban stream restoration. *Area*, *47*(4), 408–421. https://doi.org/10.1111/area.12180

Booth, D. B., & Henshaw, P. C. (2001). Rates of channel erosion in small urban streams. *Land Use and Watersheds: Human Influence on Hydrology and Geomorphology in Urban and Forest Areas*, *2*, 17–38. https://doi.org/10.1029/WS002p0017

Brookes, A. (1987). River channel adjustments downstream from channelization works in England and Wales. *Earth Surface Processes and Landforms*, *12*(4), 337–351. https://doi.org/10.1002/esp.3290120402

Chang, H. (2006). *Generalized computer program FLUVIAL-12, Mathematical Model for Erodible Channels Users Manual*. San Diego, CA.

Chaudhry, M. H. (2008). *Open Channel Flow*. *Springer Science & Business Media*. https://doi.org/10.1007/978-0-387-68648-6

Chin, A., & Gregory, K. J. (2001). Urbanization and Adjustment of Ephemeral Stream Channels. *Annals of the Association of American Geographers*, *91*(4), 595–608. https://doi.org/10.1111/0004-5608.00260

Chow, V. T. (1959). *Open-channel Hydraulics*. New Jersey: Blackburn Press. Retrieved from https://books.google.com/books?id=JG9_PwAACAAJ

Darby, S. E., & Thorne, C. R. (1996). Modelling the Sensitivity of Channel Adjustments in Destabilized Sand-Bed Rivers. *Earth Surface Processes and Landforms*, *21*, 1109–1125. https://doi.org/10.1002/(SICI)1096-9837(199612)21:12<1109::AID-ESP655>3.0.CO;2-F

Federal Interagency Stream Restoration Working Group (FISRWG). (1998). *Stream Corridor Restoration: Principles, Processes, and Practices*. *U.S. Dept. of Agriculture, Natural Resources Conservation Service*. Washinton, D.C. https://doi.org/-0-934213-59-3

Gibson, S., Simon, A., Langendoen, E., Bankhead, N., & Shelley, J. (2015). A Physically-Based Channel-Modeling Framework Integrating HEC-RAS Sediment Transport Capabilities and the USDA-ARS Bank-Stability and Toe-Erosion Model (BSTEM). *Federal Interagency Sediment Conference, SedHyd Proceedings*.

Gudino-Elizondo, N., Biggs, T., Castillo, C., Bingner, R., Langendoen, E., Taniguchi, K. T., … Liden, D. (2018). Measuring Ephemeral Gully Erosion Rates and Topographical Thresholds in an Urban Watershed Using Unmanned Aerial Systems and Structure from Motion Photogrammetric Techniques. *Land Degradation & Development*, 1–10. https://doi.org/10.1002/ldr.2976

Gudino-Elizondo, N., Biggs, T. W., Bingner, R. L., Yuan, Y., Langendoen, E. J., Taniguchi, K. T., … Liden, D. (2018). Modeling ephemeral gully erosion from unpaved urban roads: Equifinality and implications for scenario analysis. *Geosciences*, *137*(8). https://doi.org/10.3390/geosciences8040137

Hammer, T. R. (1972). Stream channel enlargement due to urbanization. *Water Resources*

Research, *8*(6), 1530. https://doi.org/10.1029/WR008i006p01530

Hanson, G. J. (1990). SURFACE ERODIBILITY OF EARTHEN CHANNELS AT HIGH STRESSES PART II - DEVELOPING AN IN SITU TESTING DEVICE. *Transactions of the ASAE*, *33*(1), 0132–0137. https://doi.org/10.13031/2013.31306

Harry, H., Barnes, J., & Barnes Jr., H. H. (1987). Roughness Characteristics of Natural Channels. *Technical Report, Geological Survey Water-Supply, United States Government Printing Office, Washington, U.S.A*, 219. https://doi.org/10.1016/0022-1694(69)90113-9

Hawley, R. J., & Bledsoe, B. P. (2011). How do flow peaks and durations change in suburbanizing semi-arid watersheds? A southern California case study. *Journal of Hydrology*, *405*(1–2). https://doi.org/10.1016/j.jhydrol.2011.05.011

Hawley, R. J., & Bledsoe, B. P. (2013). Channel enlargement in semiarid suburbanizing watersheds: A southern California case study. *Journal of Hydrology*, *496*, 17–30. https://doi.org/10.1016/j.jhydrol.2013.05.010

Hawley, R. J., Bledsoe, B. P., & Stein, E. D. (2011). *Hydromodification Effects on Flow Peaks and Durations in Southern California Urbanizing Watersheds*.

Huang, J. V, & Greimann, B. (2010). *User's Manual for SRH-1D 2.6, Sedimentation and River Hydraulics, One Dimension, Version 2.6*. U.S. Department of the Interior, Bureau of Reclamation, Technical Service Center, Sedimentation and River Hydraulics Group.

Lai, Y. G., Thomas, R. E., Ozeren, Y., Simon, A., Greimann, B. P., & Wu, K. (2015). Modeling of multilayer cohesive bank erosion with a coupled bank stability and mobile-bed model. *Geomorphology*, *243*, 116–129. https://doi.org/10.1016/j.geomorph.2014.07.017

Lane, E. W. (1955). The importance of fluvial morphology in hydraulic engineering. *Proceedings of American Society of Civil Engineers*, *81*(795), 1–17.

Langendoen, E. J., & Alonso, C. V. (2008). Modeling the Evolution of Incised Streams: I. Model Formulation and Validation of Flow and Streambed Evolution Components. *Journal of Hydraulic Engineering*, *134*(6), 749–762. https://doi.org/10.1061/(ASCE)0733-9429(2008)134:6(749)

Langendoen, E. J., Mendoza, A., Abad, J. D., Tassi, P., Wang, D., Ata, R., … Hervouet, J. M. (2016). Improved numerical modeling of morphodynamics of rivers with steep

banks. *Advances in Water Resources*, *93(Part A)*, 4–14. https://doi.org/10.1016/j.advwatres.2015.04.002

Langendoen, E. J., & Simon, A. (2008). Modeling the Evolution of Incised Streams. II: Streambank Erosion. *Journal of Hydraulic Engineering*, *134*(7), 1094–1100. https://doi.org/10.1061/(ASCE)0733-9429(2008)134

Morgenstern, N. R., & Price, V. E. (1965). The analysis of the stability of general slip surfaces. *Géotechnique*, *15*(1), 79–93. https://doi.org/https://doi.org/10.1680/geot.1965.15.1.79

Niezgoda, S. L., & Johnson, P. A. (2005). Improving the urban stream restoration effort: Identifying critical form and processes relationships. *Environmental Management*, *35*(5), 579–592. https://doi.org/10.1007/s00267-004-0088-8

Niezgoda, S. L., & Johnson, P. A. (2006). Modeling the long term impacts of using rigid structures in stream channel restoration. *Journal of the American Water Resources Association*, *42*(6), 1597–1613. https://doi.org/10.1111/j.1752-1688.2006.tb06023.x

Ock, G., Sumi, T., & Takemon, Y. (2013). Sediment replenishment to downstream reaches below dams: implementation perspectives. *Hydrological Research Letters*, *7*(3), 54–59. https://doi.org/10.3178/hrl.7.54

Rowley, K., & Hotchkiss, R. (2014). Sediment Transport Conditions Near Culverts. *World Environmental and Water Resources Congress 2014*, 1402–1411. https://doi.org/10.1061/9780784413548.141

Schumm, S. A., Harvey, M. D., & Watson, C. C. (1984). *Incised channels: morphology, dynamics, and control*. Water Resources Publications. Retrieved from https://books.google.com/books?id=KLoPAQAAIAAJ

Segura, C., & Booth, D. B. (2010). Effects of geomorphic setting and urbanization on wood, pools, sediment storage, and bank erosion in puget sound streams. *Journal of the American Water Resources Association*, *46*(5), 972–986. https://doi.org/10.1111/j.1752-1688.2010.00470.x

Simon, A. (1989). A model of channel response in disturbed alluvial channels. *Earth Surface Processes and Landforms*, *14*(1), 11–26. https://doi.org/10.1002/esp.3290140103

Simon, A., & Darby, S. E. (1997). Process-form interactions in unstable sand-bed river channels: A numerical modeling approach. *Geomorphology*, *21*(2), 85–106.

https://doi.org/10.1016/S0169-555X(97)00043-3

Simon, A., & Darby, S. E. (2002). Effectiveness of grade-control structures in reducing erosion along incised river channels: The case of Hotophia Creek, Mississippi. *Geomorphology*, *42*(3–4), 229–254. https://doi.org/10.1016/S0169-555X(01)00088-5

Simon, A., & Hupp, C. (1986). Channel evolution in modified Tennessee channels. In *Proceedings of the 4th Federal Interagency Sedimentation Conference* (pp. 571–582). Washington DC: Las Vegas US Government Printing Office.

Simon, A., & Rinaldi, M. (2006). Disturbance, Evolution and the Roles of Excess Transport Capacity and Boundary Materials in Controlling Channel Response. *Treatise on Geomorphology*, *79*, 574–594. https://doi.org/10.1016/B978-0-12-374739-6.00255-4

Taniguchi, K., & Biggs, T. W. (2015). Regional impacts of urbanization on stream channel geometry: A case study in semi-arid southern California. *Geomorphology*, *248*, 228–236. https://doi.org/10.1016/j.geomorph.2015.07.038

Taniguchi, K. T., Biggs, T. W., Langendoen, E. J., Castillo, C., Gudino-Elizondo, N., Yongping, Y., & Liden, D. (2018). Stream channel erosion in a rapidly urbanizing region of the US-Mexico Border: Documenting the importance of channel hardpoints with Structure-from-Motion photogrammetry. *Earth Surface Processes and Landforms (ESPL)*, *43*(7), 1465–1477.

Thorne, C. R., & Osman, A. M. (1988). The influence of bank stability on regime geometry of natural channels. In *International conference on river regime* (pp. 135–147).

Trimble, S. W. (1997). Contribution of stream channel erosion to sediment yield from an urbanizing watershed. *Science*, *278*(5342), 1442–1444. https://doi.org/10.1126/science.278.5342.1442

US Army Corps of Engineers (USACE). (1993). *HEC-6: Scour and deposition in rivers and reservoirs: Users Manual*. Davis, CA.

Wolman, M. G. (1967). A Cycle of Sedimentation and Erosion in Urban River Channels. *Geografiska Annaler. Series A, Physical Geography*, *49*(2/4), 385–395. Retrieved from http://www.jstor.org/stable/520904

CHAPTER 4

Modeling Channel Sources and Sinks of Sediment in a Semi-arid Urbanizing Environment: CONCEPTS-AnnAGNPS Integrated Model for Los Laureles Canyon Watershed

ABSTRACT

Channel erosion may be a dominant source of sediment following urbanization in semi-arid regions that are characterized by steep terrain and highly erodible soils. This study investigates a rapidly developing, semi-arid watershed in Tijuana, Mexico, Los Laureles Canyon watershed (LLCW), where channel erosion contributes to the excessive sedimentation of a downstream estuary. A linked watershed-scale hillslope model, AnnAGNPS, and channel evolution model, CONCEPTS, are used to document the spatial pattern of channel sources and sinks of sediment and to evaluate the overall importance of channel processes on the sediment budget for future sediment mitigation plans. Channel erosion in LLCW accounts for approximately 60% of the total sediment budget to the Tijuana Estuary. About one third of the entire earthen channel network contributes 90% of the channel-derived sediment load. This indicates that if effective channel stabilization measures are implemented on a third of the river network length, it could provide up to a 90% reduction in channel-derived sediment yield, or a 54% reduction on the total sediment yield for the watershed. Coarsening the bed alone reduces incision but may not be efficient in reducing annual channel-derived sediment load as it increases channel widening. With high discharges, enlarged channels that are disconnected to the floodplain storage, and subsequent high transport capacity in stream reaches, both the channel bed and bank must be stabilized and discharge from urban areas should be reduced to effectively decrease channel erosion.

1. INTRODUCTION

Identifying erosional processes that contribute to sediment yield is vital for implementing erosion mitigation plans to reduce sediment yield and decrease degradation of downstream ecosystems. Watershed scale mitigation plans require knowledge of the basin-

wide sediment budget, including sediment sources and sinks, and how the sediment is transported across the landscape and through the river network (Reid & Dunne, 1996). A sediment budget provides a valuable framework for managers to identify key erosional sources, whether from hillslopes or channels, and to make informed, targeted decisions about upstream sediment reduction practices (Owens, 2005; Walling & Collins, 2008). Although human activities on hillslopes, such as agricultural practices and removal of vegetation, can lead to increased sediment load to the channel, it is important to understand the sediment transport and erosional processes of the river network, as riverine deposition and stream bank erosion may be critical factors in determining catchment sediment budgets (Prosser et al., 2001). Sediment budgets can shed light on the importance of channel erosion on the total sediment yield, especially in urban settings where enhanced peak discharges increase channel scour (Trimble, 1997).

Traditional watershed assessments that document the spatial pattern of erosion and sediment transport often require extensive field data, which can be costly and time-consuming. Measuring suspended sediment flux at multiple stream reaches in the downstream direction is an effective way to understand the downstream patterns of sediment yield (Singer & Dunne, 2001), but the spatial extent of such a study may be limited by the availability of funds. Additionally, in semi-arid regions or during times of drought, there may be limited rainfall events or opportunities to collect suspended sediment samples during the period of study. Sediment tracers for identifying source areas and key erosional processes have been used in a variety of studies (see review by Collins et al., 2017), but can be expensive to implement and possess key uncertainties in the current methodological techniques.

Computer modeling can be used to map spatial patterns in the sources and sinks of sediment and sediment yield at the watershed scale (Wilkinson et al., 2009). In many watershed scale models, hillslope erosion is based on empirical relationships that require calibrated input parameters and oftentimes the channel erosion component is excluded (de Vente & Poesen, 2005). Integration of an empirically-based watershed model of hillslope erosion with a physically-based channel evolution and sediment transport model can be useful for studying areas where both hillslope and channel erosional processes are dominant. The U.S. Department of Agriculture (USDA) has developed various computer models to

evaluate the impact of hillslope erosion and restoration measures on stream morphology and downstream sediment loads (Shields et al., 2006). Two of these models, AnnAGNPS (Annualized Agricultural Non-Point Source; Bingner & Theurer, 2001; Bingner et al., 2015) and CONCEPTS (CONservational Channel Evolution and Pollutant Transport System; Langendoen & Alonso, 2008; Langendoen & Simon, 2008), simulate pollutant loading from the hillslopes (AnnAGNPS) and channel evolution of incising streams (CONCEPTS). AnnAGNPS simulated hydrology has served as inflow to the CONCEPTS channel model in watersheds where discharge measurements were unavailable and the linked models can accurately simulate channel hydraulics, sediment transport, and stream channel evolution within a stream system (Langendoen et al., 2002; Langendoen & Simon, 2008). However, no studies have utilized both the hydrology and sediment load simulated from AnnAGNPS as input into the CONCEPTS channel model. In rapidly developing regions, such as Tijuana, Mexico and similar environments, ephemeral gully erosion of unpaved roads and stream channel erosion are dominant sources of sediment at the watershed scale. The CONCEPTS-AnnAGNPS linked model may be appropriate in such regions because there is a strong connectivity between hillslopes and stream channels due to floodplain vegetation removal (Bracken et al., 2015) during the process of urbanization.

In highly altered environments, where human activities that impact hillslopes and channels may be unpredictable and implemented at various spatial scales, the fate of sediment may be harder to model because sediment may move in and out of storage in ways that cannot be predicted with physics alone (Meade, 1982). Many models do not incorporate socio-geomorphic processes (Urban, 2002; Ashmore, 2015), such as human intervention at the resident-scale (i.e. channel stabilization measures at highly eroded, discrete locations) or community-scale (i.e. construction of check dams or bank stabilization of stream reaches). Such practices may decrease channel erosion and lead to a reduction in sediment load to the outlet of the watershed, leading to an overestimation of simulated channel erosion on the sediment budget. In socio-hydrology, the community sensitivity loop describes how human behavior and water management decisions are directly driven by a community's social and environmental values, local action, and lobbying and all reflect on community sensitivity to hydrologic or geomorphic change (Elshafei et al., 2014). The community sensitivity state variable, refers to a community's perceived level of threat to the community's quality of life

(Elshafei et al., 2014) and provides the key linkage between human intervention or action to hydrologic and/or geomorphic changes. In tightly coupled human-environmental systems, computational models may be improved with the utilization of socio-geomorphic processes, such as implementation of sediment reduction practices, via the community sensitivity state variable.

This study investigates a rapidly developing, semi-arid watershed in Tijuana, Mexico, Los Laureles Canyon watershed (LLCW), where hillslope and channel erosion contribute to the excessive sedimentation of a downstream estuary. An understanding of the overall sediment budget is necessary for management action in LLCW and sediment reduction to the Tijuana Estuary. A linked watershed-scale hillslope model, AnnAGNPS, and channel evolution model, CONCEPTS, are used to answer the following research questions:

(i) Where are the channel sources and sinks of sediment for Los Laureles Canyon watershed and;
(ii) What is the overall importance of channel processes on the sediment budget?

The overall objectives of this study are to: 1) document channel changes from repeat surveys conducted from 2009 and 2014; 2) develop a spatially-linked watershed scale model of hillslope and channel erosion to determine the spatial pattern of channel sources and sinks of sediment; 3) evaluate the overall importance of channel processes on the sediment budget for future sediment mitigation plans; and 4) discuss limitations of the integrated modeling scheme for a rapidly developing, semi-arid region.

2. STUDY AREA

Los Laureles Canyon watershed (LLCW) is a binational semi-arid watershed (11.6 km^2) whose main channel drains from Tijuana, Mexico under the US-Mexico border through culverts and empties into the Tijuana Estuary, one of the largest estuarine habitats left in California (Weis et al., 2001). In LLCW, rapid urbanization on steep, erodible slopes has led to excessive hillslope and stream channel erosion during rainfall events and issues of sedimentation in the Tijuana Estuary (Gudino-Elizondo et al., 2018; Taniguchi et al., 2018). During the process of urbanization, the floodplain is fully developed, stream channels are stripped of vegetation and oftentimes filled with unconsolidated sediment and converted into unpaved roads, and an enlarged stream channel reforms following rain events. With a constrained stream channel and developed floodplain, floodplain storage is removed, flow

depths increase, and channel erosion is exacerbated. Additionally, large ephemeral gullies form on unpaved roads in urban areas located on the highly erodible Los Flores soil unit (Gudino-Elizondo et al., 2018). The large inputs of sediment transported to the Tijuana Estuary alter the natural ecosystem through the conversion of lowlands to uplands, impacting inundation and salinity levels, and negatively affecting the native species and allowing exotic species to thrive (Zedler & Norby, 1986). Hillslope and stream channel erosion in the watershed also impact the quality of life for the upstream residents of LLCW due to infrastructure failure of homes, buildings, water/sewage mains, and unpaved roads (Gudino-Elizondo et al., 2018).

LLCW is a semi-arid watershed with Mediterranean climate and a flashy flow regime. Long-term mean annual precipitation is 238 mm (PRISM Climate Group, Oregon State University, http://prism.oregonstate.edu, created 7 July 2010). LLCW is located on the erodible San Diego Formation which is comprised of fine-to medium-grained, loosely consolidated sandstone and cobbly conglomerate. According to maps from the Mexican Geological Survey, there are four main geologic units in LLCW, which includes marine and fluvial sediment deposits of conglomerate, sandy conglomerate, and a small fractional coverage of a silt unit and alluvial unit that is mostly paved or channelized. The conglomerate occurs in the southern end of the watershed, mainly on the upper parts of hillslopes and along interfluves. Conglomerates often have “red caps” of weathered rock and soil, which are sometimes underlain by sandy conglomerate unit. The valley floor of LLCW and the northern portion of the watershed are comprised primarily of the sandy conglomerate unit. Soils in LLCW have critical shear stress ranging from 0.001 to 4.6 Pa and erodibility (k) ranging from 103 to 879 cm3 N-1 s-1 (Biggs et al., 2018b).

There are two minor tributaries that drain into the mainstem (Main) of LLCW: southwest (SW) and southeast (SE) tributaries. The upper reaches of Main drains a primarily sparsely urbanized, unpaved and levelled land that was cleared for future development with a predominantly paved southern-most portion of the watershed. The central reaches of Main pass through primarily dense and a small portion of sparsely urbanized, unpaved areas of land. Large gullies form in several neighborhoods along the steep, unpaved roads. The lower reaches of Main are channelized with concrete and drain through densely urbanized and paved land. The land use in the SE watershed is dominated by unpaved urban areas, with

a concrete channel in the upper portion of the watershed. Soils in the SE watershed are cobbly, which prevents gullies from forming in the unpaved roads, and D_{50} of the bed ranges from 32 to 45 mm. The lower portion of the SW watershed is primarily characterized by unpaved urban land and the upper portion is primarily undeveloped. The major hotspots of channel enlargement are located in the SW watershed downstream of a concrete flume and metal culvert (Chapter 2, and Taniguchi et al., 2018). Although cross sections were statistically larger downstream of in channel hardpoints, hardpoints only caused local downstream incision and prevented enlargement in the upstream direction (Chapter 3).

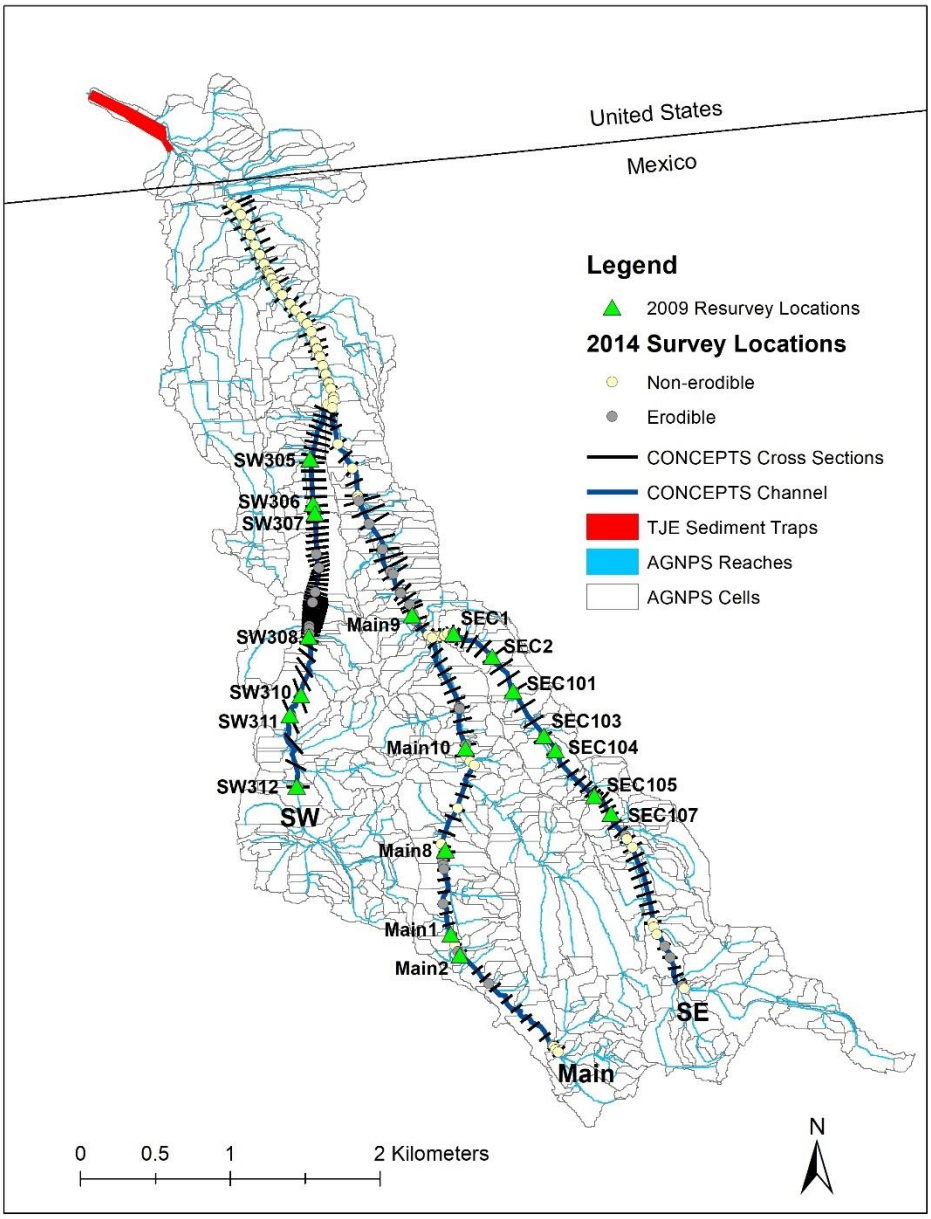

Figure 1. Los Laureles Canyon Watershed (LLCW) with AnnAGNPS cells and reaches and spatially-linked CONCEPTS channel model and cross sections. Eighteen earthen cross sections were resurveyed from 2009 to 2014.

3. METHODS

3.1 Channel Changes from 2009 to 2014

Stream channel geometry surveys were conducted in the summer of 2009 at 38 earthen locations along the Main, SE, and SW tributaries of LLCW. In the summer of 2014,

19 earthen locations were resurveyed with a differential GPS and a total of 71 cross sections were surveyed at representative stream reaches, which were chosen based on along-stream changes in channel geometry, channel condition, and/or bed and bank composition (Taniguchi et al., 2018). The 2014 survey included cross sections on both earthen (n=39) and concrete reaches (n=32). A total of 18 additional earthen cross sections were extracted from Structure-from-Motion (SfM) derived digital elevation models (DEMs) (Taniguchi et al., 2018). Repeat survey locations were based on GPS points surveyed in 2009, in addition to field notes and field pictures used for location indicators (i.e. using proximity to homes and features that did not change).

Changes in bankfull width and depth from 2009 to 2014 were calculated from the repeat surveys. At locations showing the largest changes in width, historical aerial imagery from 2009 and 2014 was used to validate changes in width at locations where the banks were clearly identifiable in both images. The observed change in width and depth and mass of erosion from channel change were used as validation of the changes in bed elevation and top width simulated by the CONCEPTS model. Root mean square error (RMSE) between simulated and observed changes in width and depth were calculated.

3.2 CONCEPTS Model Set-up

3.2.1 CONCEPTS Channel Evolution Model

CONCEPTS is a numerical computer model that simulates unsteady, one-dimensional flow, sediment transport by size class, and channel incision and widening (Langendoen & Simon, 2008). CONCEPTS uses a distributed flow routing scheme where discharge is calculated simultaneously at all cross sections along the stream network using the Saint Venant equations (Cunge et al., 1980), including the continuity and momentum equations. The governing equations are solved using the generalized Preissman scheme. Sediment transport is calculated for 14 predefined sediment size classes, ranging from 10 μm to 64 mm, with a corresponding transport equation for each class: Laursen (1958) for silts; Yang (1973) for sands; and Meyer-Peter & Mueller (1948) for gravels. Width adjustment is simulated via fluvial erosion and bank mass failure (Langendoen & Simon, 2008). Required input data include channel and floodplain geometry and hydraulic roughness at specified cross sections, water and sediment inflows to the channel cross sections, grain size

distribution and stratigraphy of bed and bank material, and critical shear stress and erodibility of bed and bank material.

Field data collected in 2014 (Taniguchi et al., 2018) at 89 channel cross sections (57 earthen and 32 concrete) were used as input for the LLCW CONCEPTS model, including stream channel geometry, particle size distribution of the earthen channel bed, and jet-test erodibility measurements of cohesive banks (Hanson, 1990). Eighteen of the earthen cross sections were extracted from an SfM-derived DEM and 39 of the earthen cross sections were surveyed with a differential GPS (Taniguchi et al., 2018). Manning's roughness of concrete was set to 0.015 and of earthen, sandy, gravel-bedded channels was set to 0.035, which are typical values for the observed channel conditions (e.g., Chow, 1959; Barnes, & Barnes Jr., 1987). The median grain size of the bed (D_{50}) ranged from 2 mm to 45 mm. A total of 195 cross sections are used in the CONCEPTS model; 89 cross sections were surveyed in the field in 2014 and 106 cross sections were spatially interpolated between surveyed cross sections in order to maintain consistent cross section spacing throughout the model. Average cross section spacing was 63 m. The floodplain topography at each cross section was extracted from a 2007 USGS National Elevation Dataset (NED) 3 m DEM.

To simulate channel hydraulics and morphological change in CONCEPTS, hydrographs of all runoff events between 2009 and 2014 for SE and Main and between 2001 and 2014 for SW were imposed at the upstream boundary (model km 0) and at the mouths of major tributaries and lateral inflow cells. Observed hydrographs were available at the outlet of the watershed for 13 storms from 2014 to 2017 but were not available at the upstream boundaries. Therefore, AnnAGNPS was used to generate the water and sediment inflow from the cells and reaches draining into the CONCEPTS channels for the simulation time period. See section 3.2.2 for a description of the AnnAGNPS model.

Channel bed particle counts and sieve analyses of four cross section locations and in the sediment trap at the outlet (TJE sediment trap in Figure 1) indicate that about 70-90% of the bed material is coarser than fine sand, and fine sand comprises a large proportion (40%) of the sediment delivered to and deposited in the sediment traps at the outlet of LLCW (Figure 2). Therefore, all particles <0.25 mm (fine sand and finer) were treated as washload in CONCEPTS. Critical shear stress was set to 6 Pa and erodibility (k) was set as 1e-7 m/(s Pa).

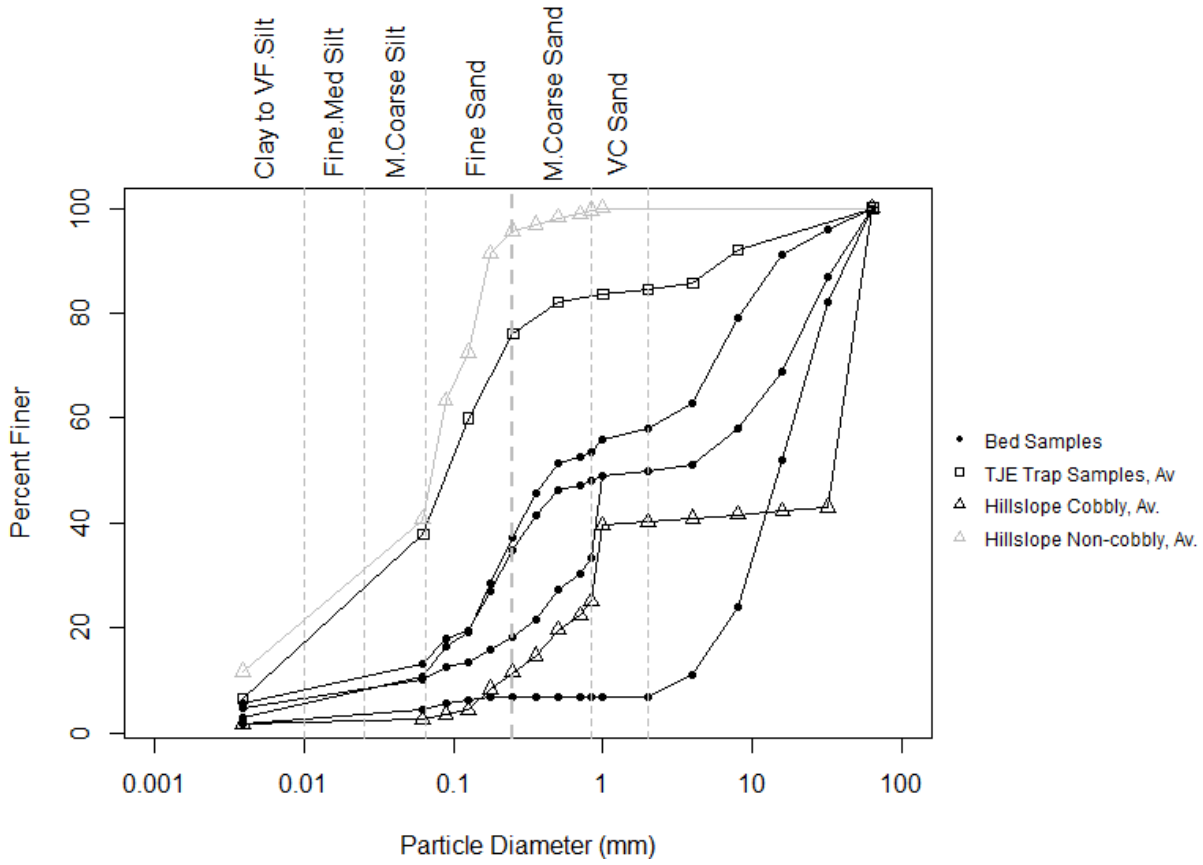

Figure 2. Percent finer by particle diameter size (mm) from 4 samples of the bed, average from 36 samples in the Tijuana Estuary sediment traps, and average from 4 hillslope soil samples (2 from cobbly soils and 2 from non-cobbly soils). Dashed vertical lines indicate upper boundaries of CONCEPTS size classes of sand, silt, and clay, with darker dashed line indicating the upper boundary for washload. Bed samples include proportion of particles coarser than sand (>2mm) from D50 pebble counts characterizing the coarse particles and particles <2 mm from a sieve analysis.

To simulate channel changes from 2009 to 2014, the stream channel cross sectional geometry surveyed in 2009 was inserted into the CONCEPTS cross section locations for the SE and Main tributaries, and the 2014 surveys were used for validation. The 2009 survey was conducted with a total station and only contained relative elevation, so it was assumed that the top bank elevation between survey dates remained the same, and the channel geometry from 2009 was inserted at the 2014 bank elevation. Cross sections were linearly interpolated between the 2009 survey locations. In concrete reaches and areas that were not surveyed in 2009 but showed little signs of enlargement in aerial comparisons between dates, cross sectional geometry from 2014 was utilized for the 2009 model geometry. For the SW sub-watershed, channel hardpoints, including a concrete flume and metal culvert, were

installed in 2001. In Chapter 3, a CONCEPTS model was developed for 2001 conditions that uses estimated historical channel geometry from 2001 based on historical aerial imagery. For the SW sub-model, both the 2009 and 2014 surveyed channel geometry were used as validation.

To test the sensitivity of channel boundary conditions of the bed and banks on simulated long-term mean annual sediment load, a scenario removing all cobble from the banks and a scenario coarsening the bed of all cross sections to predominantly coarse gravel, as observed in the SE channel (D_{50} of 45 mm), were conducted and compared to model runs using observed channel conditions.

3.2.2 AnnAGNPS Hillslope Model

AnnAGNPS is a continuous, daily time-step, watershed-scale model that simulates water and sediment loads from discretized sub-watersheds, or cells, of homogenous land use, soils, and topography. AnnAGNPS simulates the contribution of different erosion processes, including sheet, rills, gullies, and channel erosion, but does not simulate mass wasting processes, which may be important watersheds with steep hillslopes like the LLCW. Ephemeral gullies form on unpaved roads in LLCW and are filled in with sediment following rain events. AnnAGNPS is utilized in this study because of its ability to simulate ephemeral gully formation and management practices on the hillslope. Runoff processes in AnnAGNPS are predominantly infiltration excess overland flow, which is the dominant runoff process in this semi-arid, urban watershed. AnnAGNPS uses the Natural Resources Conservation Service (NRCS) curve number (NRCS, 1972) to calculate runoff and the NRCS Technical Release 55 (TR-55) to compute peak discharge (Bingner & Theurer, 2001). Triangular hydrographs were constructed for the downstream end of each cell or reach using the event total runoff, peak discharge and time-to-peak, which is based on topography and roughness of the landscape. For this study, the hydrology and hillslope generated sediment load from sheet, rills, and gullies were linked to the CONCEPTS model channels.

Los Laureles Canyon watershed was discretized into 1,142 cells and 462 reaches using the TOPAGNPS tool based on the 2007 USGS NED 3m DEM. Cell size ranged from 9E-6 to 0.1 km^2. Soil properties were taken from the SSURGO database (NRCS, 2018) for soils near the US/Mexico border, and soils in LLCW were sampled and analyzed for particle

size (Biggs et al., 2018b). A land use map was generated by visual interpretation using the GoogleEarth™ imagery (11 November 2012, 2017 DigitalGlobe) into seven land use categories: (agriculture, rangeland, paved urban, dispersed unpaved urban (5-15% urbanized), urban unpaved (15-30% urbanized), unpaved graded land, and sediment trap). The land use map was validated by comparing aerial imagery with ground-based photography and field surveys. Curve number values were determined based on the percent impervious cover by (Biggs et al., 2010) and updated by Taniguchi et al. (2018) for each land use category (Gudino-Elizondo et al., 2018). Eight samples of cohesive soils were collected in the field to estimate critical shear stress (τ_c) and soil erodibility (k) using a mini-jet erosion test following Hanson (Hanson, 1990). Rainfall data were collected at one station on the Mexican side of the border from 2014-2016 but were not available for the whole simulation period (2009-2014), so rain gauges in the US were analyzed for their correlation with the Mexico rain gauge (Biggs et al, 2018a). The measured daily precipitation at the Brownfields climate station in San Diego was applied uniformly over the entire watershed using a type-II, 24-hour rainfall distribution (TR-55). The storm type-II was determined by comparing cumulative rainfall observed at the rain gauge in Mexico (Biggs et al., 2018a) with the cumulative distribution functions from TR-55. For a complete description of AnnAGNPS model set-up and input parameters see (Gudino-Elizondo et al., in prep.).

3.2.3 CONCEPTS-ANNAGNPS MODEL INTEGRATION, CALIBRATION, AND VALIDATION

AnnAGNPS cells and reaches were linked to the CONCEPTS model channels (Figure 1). The CONCEPTS channel represents the main stem of the stream channel network, where cross sections were surveyed, and AnnAGNPS reaches are sub-tributaries that drain into the main stem. For the SW watershed, the channel head was inaccessible due to restricted access, so the upstream-most cross section started at the upstream-most surveyed location. AnnAGNPS outputs of daily discharge were converted to triangular hydrographs based on daily event peak discharge, time to peak, and total discharge, and served as either upstream or lateral inflow into the CONCEPTS model. The AnnAGNPS daily sediment mass delivered to the channel for sand, silt, and clay were converted to triangular sedigraphs based on time to peak, total storm duration, and total sediment load. It was assumed that the peak sediment discharge occurred at the time of peak discharge. AnnAGNPS outputs the

event total sediment load of sand (including very coarse sand to very fine sand), silt, and clay. Sediment load for sand is reported as one value per event and is not split by size class. The total sand reported by AnnAGNPS was parsed into fine sand (90%), medium and coarse sand (8%) and very coarse sand (2%) categories, based on the average particle size distribution of sand from the hillslope non-cobbly soil, Los Flores (Figure 2). Simulated sediment yield was compared for scenarios with and without the addition of coarser sand (including very coarse, coarse, and medium sand) from the hillslopes. For discussion of limitations and assumptions of this study, see Section 5.2.

The AnnAGNPS integrated model was first calibrated for hydrology (total and peak runoff) using observed data collected at the outlet of LLCW during 13 storm events from 2014 to 2017. Then the AnnAGNPS model was calibrated for sediment production and validated against a combination of a) ground-based and Unmanned Aerial Vehicle (UAV) gully surveys following storm events (Gudino-Elizondo et al., 2018), and b) total annual sediment yield calculated from the tons of sediment excavated from the sediment traps at the outlet of LLCW from 2009 to 2012, corrected for trap efficiency (Biggs et al., 2018a). The trap efficiency, or the proportion of the total sediment yield that is retained in the sediment basin, for medium sand, fine sand, silt, and clay was estimated by following the guidelines for sedimentation under turbulent, non-ideal conditions (Morris & Fan, 1998) and was estimated as a function of the settling velocity ratio for each size class (Urbonas & Stahre, 1993). A sensitivity analysis was conducted on the LLCW AnnAGNPS sub-model to determine the most sensitive parameters on sediment load, constrain AnnAGNPS parameter values, and develop the most suitable parameter combinations or "behavioral models" for the watershed (Gudino-Elizondo et al., 2018). Although extensive calibration was necessary for the AnnAGNPS model, calibration of CONCEPTS was not necessary because unknown parameters for erodibility and critical shear stress were based on field measurements. However, Manning's n was adjusted from 0.035 to 0.025 at a few depositional earthen cross sections. The channel geometry survey from 2014 was used as CONCEPTS model validation for the SE and Main tributaries, and geometry surveys from 2009 and 2014 were used as validation for the SW tributary.

The watershed sediment budget was calculated using simulated hillslope contribution from AnnAGNPS and total sediment yield at the outlet from CONCEPTS. Simulated

sediment yield between excavation dates in 2010 to 2012 were compared to observed total excavated sediment. To include the full range of excavation data (2006 to 2012), an extended model simulation from WY 2006 to 2012 was also used for model validation. Comparison between simulated sediment yield from 2010 to 2012 were compared between the extended model simulation and the model starting in 2010. The long-term mean annual sediment contributions for hillslope and channel erosion were calculated for the entire simulation period (11/28/2009 to 02/26/2017, or WY 2010 to 2017) and compared to the observed mean annual sediment excavated from the sediment traps from (2006 to 2012).

Sediment sources and sinks were mapped using ArcGIS by first segmenting the CONCEPTS modeled stream channel into reach segments at cross section locations. Then, cross sectional area was calculated at each cross section from the start of the simulation (11/28/2009) and at the approximate date of the 2014 channel survey (07/14/2014). Change in cross-sectional area was calculated for each cross section. The mean change in cross sectional area for the upstream and downstream cross section of every reach was multiplied by the reach length to get volume of sediment (m^3). Volume of sediment, either eroded or deposited, was multiplied by the estimated bulk density of soil (1.67 tons m^{-3}) to get total tons of sediment for each stream reach.

4. RESULTS

4.1 Observed Channel Changes from 2009 to 2014

Changes in channel width and depth were observed between 2009 and 2014 (Table 1). The Main and SE tributaries experienced the largest bankfull channel changes. The maximum changes in width for the Main and SE cross sections were 10 m and 12 m, respectively, and 5 m in the SW tributary. The maximum changes in depth, or incision, for the Main and SE cross section locations were 1.4 m and 2.4 m, respectively, and 0.7 m for the SW cross sections. Four cross-section locations, all located in the SW channel, experienced deposition from 0.2 m to 0.5 m. This indicates that the Main and SE tributaries may have been in adjustment phase during 2009 to 2014, while the SW channel may have been in an aggradational or stabilization phase.

Table 1. Observed channel changes in bankfull width (m) and depth (m) from 2009 to 2014. River KM indicates the distance downstream from the channel head of the corresponding reach (Main, SE, or SW).

Site	River KM	Reach	Width (m)		Depth (m)		Width Change (m)	Depth Change (m)
			2009	2014	2009	2014	2009 to 2014	2009 to 2014
Main1	1.1	Main	8.2	7.6	2.0	2.3	-0.6	0.3
Main2	1.0	Main	5.2	3.7	1.0	1.4	-1.5	0.4
Main8	1.7	Main	1.8	12.1	1.0	1.6	10.3*	0.7
Main9	3.6	Main	9.0	9.0	0.8	2.2	0.0	1.4
Main10	2.5	Main	7.0	6.2	3.9	4.0	-0.8	0.1
SEC1	3.0	SE	3.0	5.3	1.4	2.0	2.3	0.6
SEC2	2.7	SE	5.6	6.1	1.3	1.5	0.5	0.2
SEC101	2.4	SE	4.4	7.0	1.4	1.4	2.7	0.0
SEC103	2.0	SE	3.5	4.7	0.5	1.0	1.2	0.4
SEC104	1.9	SE	5.6	4.2	1.5	1.9	-1.4	0.4
SEC105	1.5	SE	11.5	10.7	2.6	3.7	-0.8	1.2
SEC107	1.3	SE	3.4	15.4	1.0	3.3	12.0	2.4
SW305	2.4	SW	13.6	18.5	4.0	3.6	4.9	-0.4
SW306	2.1	SW	20.0	19.3	5.3	4.7	-0.8	-0.5
SW307	2.0	SW	8.1	7.4	3.4	2.9	-0.7	-0.4
3.xs3	1.24	SW	8.5	9.1	5.0	4.8	0.6	-0.2
SW308	1.18	SW	5.8	6.3	2.1	2.7	0.5	0.6
SW310	0.7	SW	3.0	3.9	0.4	1.1	0.9	0.7
SW311	0.5	SW	4.3	5.3	0.5	0.8	1.1	0.4
SW312	0.0	SW	3.5	4.3	1.0	1.0	0.8	0.0

*****Difference in survey location between dates. Width change from aerial imagery is 2.2 m.

To validate the change in width at the cross sections with the most observed widening (Main8, SEC107, and SW305), historical aerial imagery was used to measure and compare the top width from 2009 to that of 2014 (Figure 3). The 10 m of widening observed at Main8 was due to differences in survey location in 2009 and 2014. Based on aerial imagery and field notes from 2014, the elevation of the left bank at Main8 in 2014 was artificially raised to prevent flooding into the adjacent home, so the cross-section survey in 2014 for Main 8 was located 10 m upstream from the 2009 survey location. Based on aerial imagery and visible changes in vegetation and soil along the right bank and floodplain, the top width of Main 8 in 2014 is approximately 4 m. Change in width from 2009 to 2014 at Main 8 using the same location was ~2.2 m. At SEC107, surveyed (12 m) and image-extracted (12.3 m)

change in width match. At SW305 surveyed (4.7 m) and image-extracted (4.9 m) change in width match.

Figure 3. Color aerial imagery indicating channel width for a) Main8, b) SEC107, and c) SW305. Although surveyed bankfull width in 2014 at Main 8 was estimated to be 12 m, 2015 aerial imagery indicates that bankfull width was ~4m. Bankfull width in 2014 was incorrectly estimated because it was based on matching the top elevation a structure on the left bank (white polygon), which was artificially raised, to the right bank elevation. At SEC107 and SW305, change in width from aerial imagery validates that there was approximately 12 m (SEC107) and 5 m (SW305) of widening.

4.2 Simulated Hydrology and Channel Changes

Simulated event peak discharge ($m^3 s^{-1}$ or cms) and total event discharge (mm) were compared to observed values (Figure 4). Peak discharge tended to be underpredicted for peak discharges up to 20 cms. One storm event that had an observed peak of 5 cms, was overpredicted by 5-fold (~25 cms). The r^2 value of the peak discharge trendline is 0.12 and p-value is 0.25. In contrast, simulated and observed total event discharge had higher agreement (r^2 = 0.84, p-value <0.001). Differences in simulated versus observed peak discharges may be attributed to rain events that had rainfall intensities different than the utilized TR-55 storm type-II or storm events that had high temporal variations in rainfall intensity. AnnAGNPS uses a daily time step, so it cannot model temporal variations in rainfall intensity.

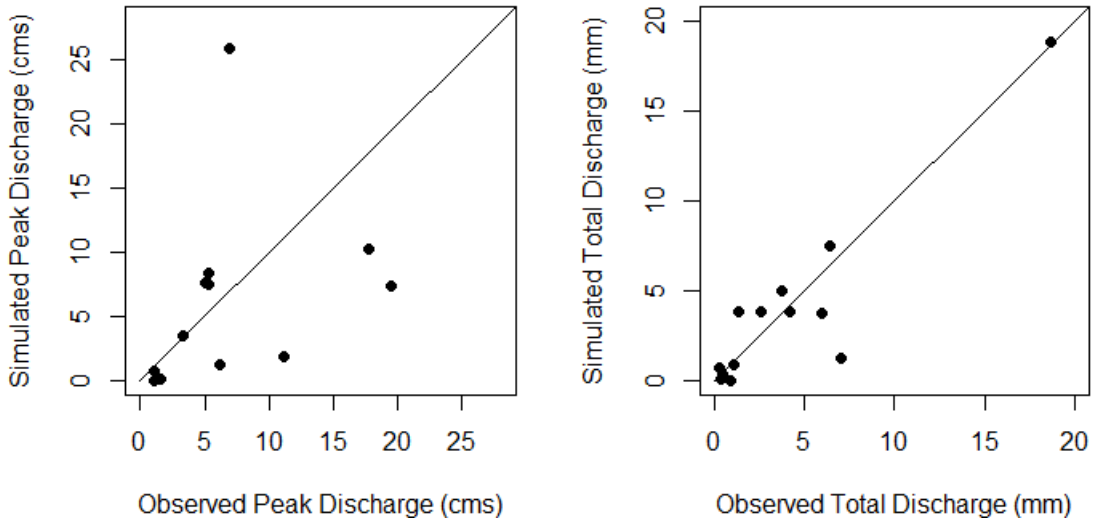

Figure 4. Comparison of observed and simulated storm event peak discharge and total discharge from 13 storms in 2014 to 2017. Solid line is the line of perfect agreement.

Changes in bed elevation, including incision and deposition, were simulated in CONCEPTS from 2009 to 2014 and were compared to surveyed bed elevation changes for the Main, SE, and SW tributaries. CONCEPTS was able to simulate the general pattern of incision and deposition during this time period. The RMSE between observed and simulated bed elevation changes was 0.74 m. For the Main channel (Figure 5a), the largest observed change in bed elevation (-1.37 m observed, -0.09 m simulated) occurred at Main9, a cross section downstream of a concrete-lined channel at the SE-Main confluence. At Main8,

CONCEPTS simulated 1.7 m of deposition, although there were only slight differences in the cross-sectional locations between surveys and no observed signs of deposition in that reach. Simulated deposition was due to the narrow culvert geometry upstream of Main8 (<1 m width) draining into the wider geometry (>10 m width) at Main8, which allowed the flow to spread across the channel and for deposition to occur. For the SE channel (Figure 5b), CONCEPTS simulated the major hotspot of incision downstream of a concrete-lined reach at SEC107. Observed incision at SEC107 was 2.36 m compared to simulated incision of 2.39 m.

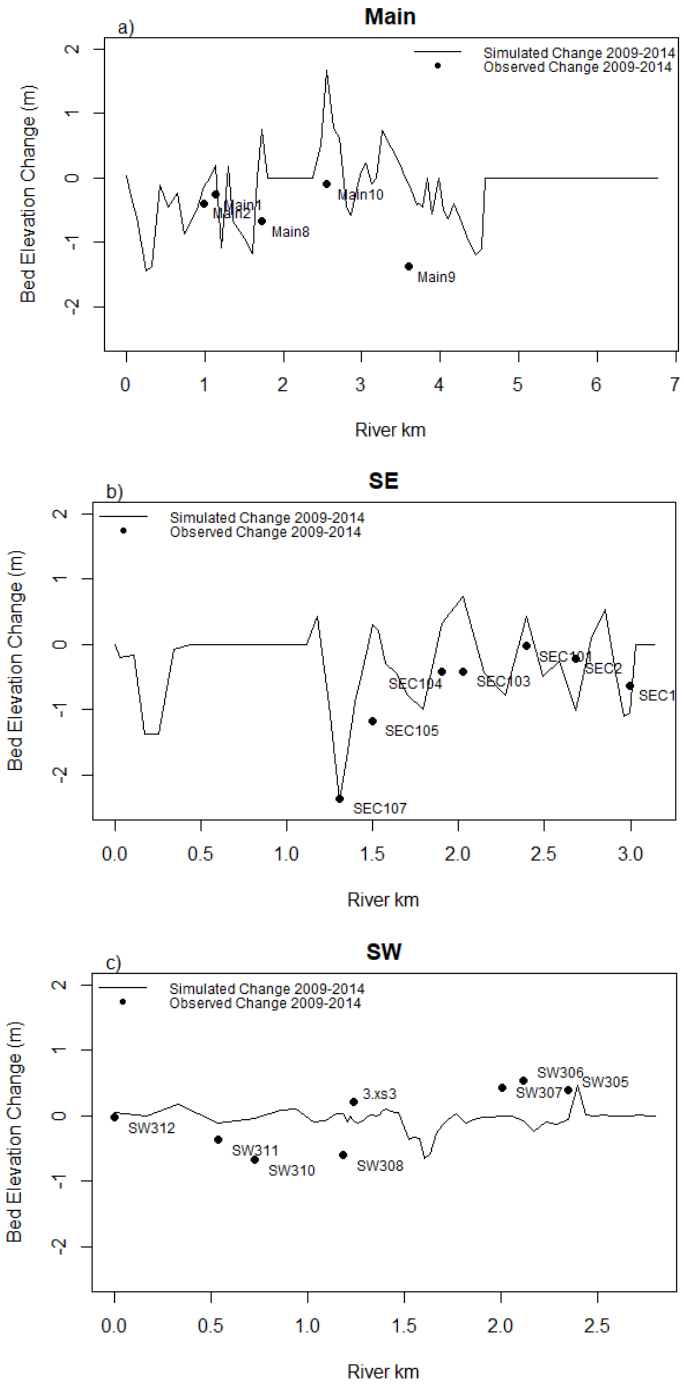

Figure 5. Observed versus simulated bed elevation changes from 2009 to 2014 for the a) Main, b) SE, and c) SW tributaries.

For the SW channel, bed elevation change from two time periods was compared to simulated changes: a) 2001 to 2009 (Figure 6) and b) 2009 to 2014 (Figure 5c). From 2001 to 2009, two major hotspots of incision were observed downstream of a metal culvert (3.xs3)

and downstream of a concrete flume (SW306). At 3.xs3, there was 2.2 m of observed incision and 1.5 m of simulated incision. At SW306, simulated incision (1.7 m) matched observed incision (1.6 m). Upstream of the concrete flume and metal culvert, less than 1 m of deposition and less than 1 m of incision was observed, respectively, but both locations showed less than 1 m of deposition during the simulation period. During the period of 2009 to 2014, observed and simulated bed elevation change indicate that there is less than 1 m of deposition and/or incision throughout the stream network. Simulated results indicate that three upstream cross sections (SW311 SW 310, and SW308) incise, while the three downstream cross sections (SW307, SW306, SW305) aggrade. The majority of simulated bed incision occurred during the period of 2001-2009, with smaller magnitudes of incision or deposition occurring in 2009 to 2014. This indicates that the majority of channel changes occurred during the first eight years following the start of urban development in 2001.

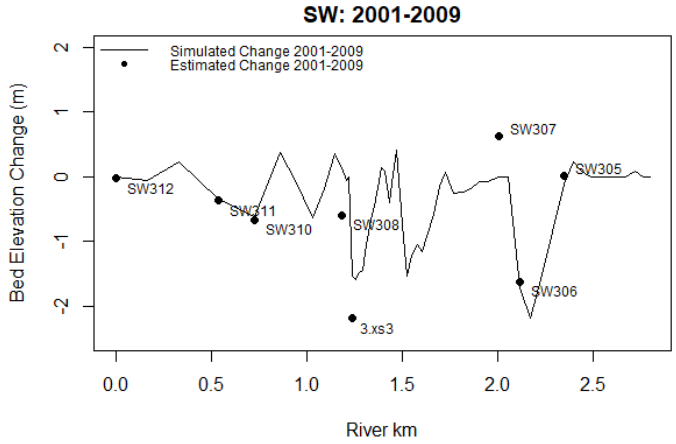

Figure 6. Estimated versus simulated bed elevation changes for the SW tributary from 2001 to 2009.

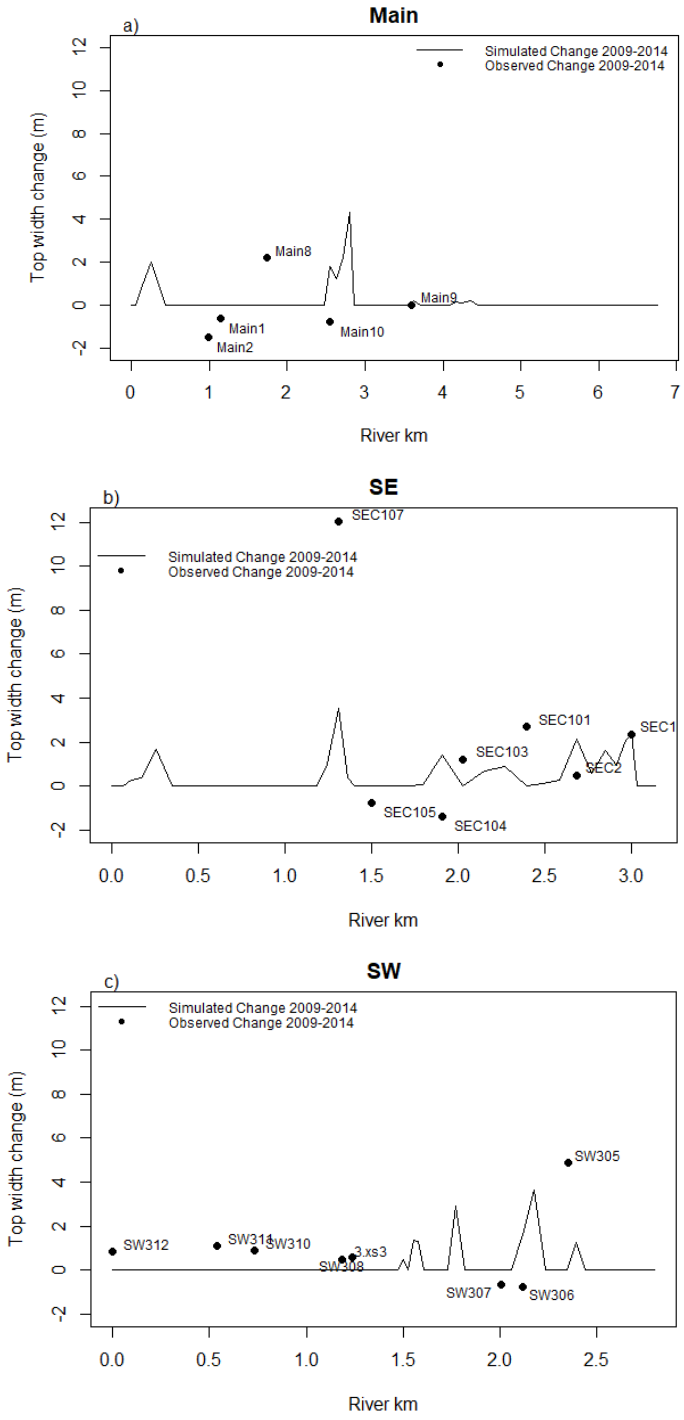

Figure 7. Observed versus simulated changes in top width from 2009 to 2014 for the a) Main, b) SE, and c) SW tributaries.

Simulated changes in width from 2009 to 2014 (Figure 7) were less accurate compared to simulated changes in depth. The RMSE from observed and simulated changes in width was 2.6 m. At Main8, channel widening was observed, but was not simulated in

CONCEPTS due to deposition and local stabilization of the channel, as discussed previously. At SEC107, CONCEPTS simulated bank failure and channel widening of 3.5 m, but widening was underestimated compared to the observed change (12 m).

4.3 Sediment Budget and Channel Sources and Sinks

Simulated sediment load at the outlet of LLCW was compared to sediment excavated from the sediment traps at the Tijuana Estuary and corrected for trapping efficiency from an extended model simulation time period of WY 2006 to 2012 (Figure 8, Table 2) and from the model simulation starting at WY 2010 (grey dots, Figure 8). The extended model simulation (WY 2006 to 2010) showed a relatively small reduction in sediment yield (reduction ranging from 1% to 5%) compared to the 3-year simulation. Overall, simulated sediment load tended to be overestimated during the wetter years and underestimated during lower rainfall years. Simulated sediment load was greater than trapped sediments by >2.5-fold for excavation years 2010 and 2011. Trapping efficiency was calculated for each size class and was used to estimate the amount of fine sediment that does not deposit in the trap, but the trapping efficiency may decrease as the sediment trap fills, resulting in underestimation of the observed sediment load. The excavation period from 2010 and 2011 experienced higher precipitation (302 and 326 mm) compared to 2012 (235 mm), and therefore the sediment traps may have filled. The apparent overestimation from the simulation model suggests that the AnnAGNPS model may be overestimating sediment load to the channel during higher rainfall years, requiring joint calibration of the combined AnnAGNPS-CONCEPTS model. The simulated channel contribution from the excavation periods ranged from 58-66% of the sediment budget.

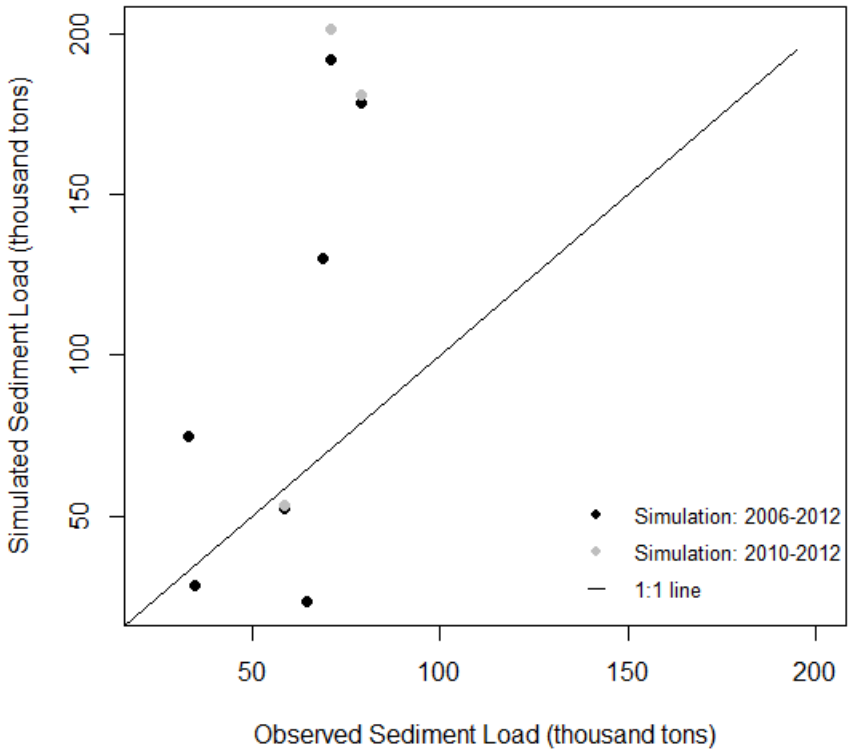

Figure 8. Comparison of observed sediment excavated from the sediment traps at the Tijuana Estuary and simulated sediment load to the outlet of LLCW between excavation dates. Two model simulations are compared: three water years of simulation (2010-2012) and an extended simulation with seven water years of simulation (2006-2012) to include additional excavation data.

Table 2. Observed sediment excavated from sediment traps at the Tijuana Estuary (corrected for trapping efficiency), simulated sediment load between excavation dates, and simulated channel and hillslope contribution on the sediment budget on the extended simulation time period of WY 2006 to 2012.

Year Excavated	Rainfall (mm)	Observed (tons)	Simulated (tons)	Channel Contribution (tons)	Hillslope Contribution (tons)
2006	208	34,642	28,290	18,563	9,727
2007	139	33,079	74,630	53,932	20,698
2008	155	64,580	23,300	13,463	9,837
2009	219	68,949	130,000	84,603	45,397
2010	303	78,935	178,400	118,114	60,286
2011	326	70,965	192,000	122,814	69,186
2012	235	58,513	52,400	30,390	22,010

For the long-term mean annual sediment contribution from water years 2010 to 2017, channel erosion contributes 59%, or 6,482 tons km^{-2} yr^{-1}, and the hillslope contributes 41%, or 3,758 tons km^{-2} yr^{-1} (Table 3). Total mean annual sediment contribution, normalized by drainage area, is 10, 240 tons km^{-2} yr^{-1} for LLCW. Mean annual sediment excavated from traps and corrected for trapping efficiency from 2006 to 2012 is 5,719 tons km^{-2} yr^{-1}, which may be lower than the 2010 to 2017 period because of a drought occurring from 2007 to 2009. Additionally, the simulation period includes 3 relatively wet water years (2010, 2011, and 2017).

The model scenario without cobble in the banks indicates that long-term mean annual sediment contribution from channel erosion is 60%, which is only a 1% increase from the scenario with bank cobble present (observed conditions). Similarly, the scenario coarsening the bed in all cross sections to predominantly coarse gravel shows no change in channel contribution (59%) compared to the scenario of observed conditions. This indicates that the proportion of channel-derived sediment is insensitive to coarsening the bed and bank materials (channel boundary conditions), despite a reduction in channel-derived sediment load by coarsening the bed in the SW watershed (Chapter 3). The steep channel slopes and high discharge from urban areas, create a large enough transport capacity to erode and transport coarse particles from the stream and to the outlet of the watershed.

Table 3. Simulated total sediment yield at the outlet of LLCW and hillslope and channel contribution by water year with model simulation period of WY 2010 to 2017.

Water Year	Total Rainfall	Total Sediment Yield	Channel Contribution		Hillslope Contribution	
	mm	tons	tons	%	tons	%
2010	302	180,771	120,485	67	60,286	33
2011	322	200,900	131,715	66	69,185	34
2012	232	53,400	31,390	59	22,010	41
2013	182	101,100	66,216	65	34,884	35
2014	94	3,800	1,539	41	2,261	60
2015	214	102,200	65,393	64	36,807	36
2016	198	42,900	24,199	56	18,701	44
2017	317	153,100	89,663	59	63,437	41
Mean Annual:						
(tons yr^{-1})		104,771	65,325	59	38,446	41
(tons km^{-2} yr^{-1})		10,240	6,482	-	3,758	-

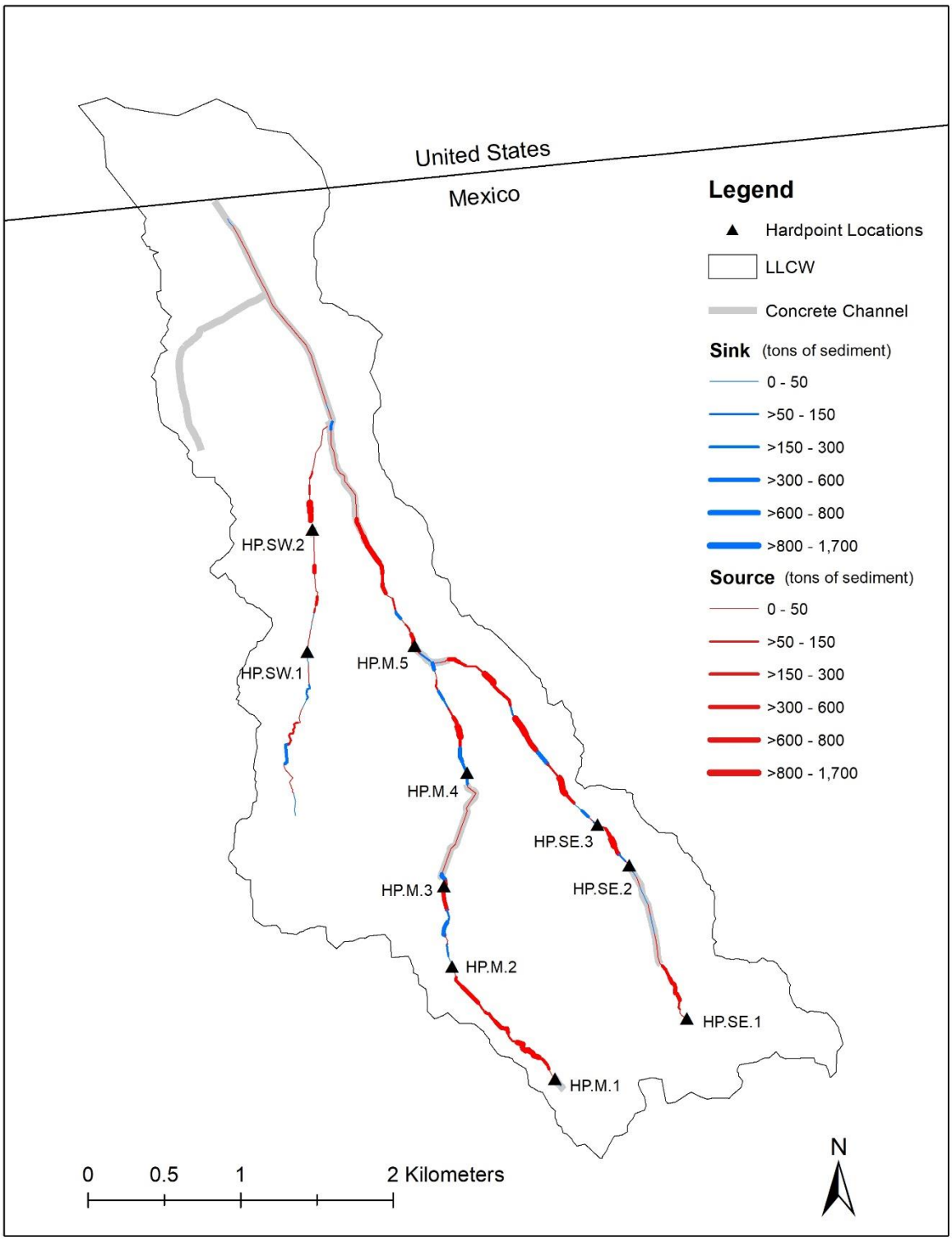

Figure 9. Channel sources and sinks of sediment based on the model simulation from 2009 to 2014. Triangles indicate locations of hardpoints that drain into erodible reaches downstream.

Channel sources and sinks in tons of sediment were calculated and mapped along the river reaches based on simulated channel changes from 2009 to 2014 (Figure 9). All of the reaches that experienced relatively low net channel changes, classified as -50 tons to +50 tons, were concrete-lined except the upstream reach of the SW channel (thin lines, Figure 8). The upstream headwaters of the SW channel is the only undeveloped region of the watershed. Although significant channel changes occurred downstream of HP.SW.1 and HP.SW.2 during 2001 to 2009, the channel at HP.SW.1 at the start of 2009 was already enlarged and appears to be stabilizing during 2009 to 2014. Although incision downstream of HP.SW.2 has ceased during the period of 2009 to 2014, CONCEPTS simulated channel widening during this time period.

The largest magnitude of channel changes for the simulation period were in the Main and SE tributaries. A major source of sediment includes the Salva Tierra stream reach, downstream of HP.M.1, where urban development occurred, including complete vegetation removal, grading of the land surface, and filling in of the channel with loose sediment. Stream reaches in the upper watershed of Main should be stabilized to prevent future instabilities, especially as urbanization continues.

Stream reaches mapped as channel sinks are primarily located where large AnnAGNPS tributaries drain into the CONCEPTS channel. These reaches also correspond to some of the high frequency bed forms observed in Figure 5. Because CONCEPTS is a one-dimensional model, when tributaries drain into a specified cross section, the model spreads the flow and sediment evenly across the bed. In reality, the sediment supplied at confluences oftentimes forms bars that can narrow the channel width and create more concentrated flows that could focus flow against channel banks and intensify erosion locally. Bars at major tributaries were observed in the field at some locations. Additionally, at the confluences there may be backwater effects that may lead to upstream deposition. Deposition occurs at HP.M.3 because the channel geometry changes along-stream from a relatively narrow culvert to a wide cross section at Main8, causing the flow to spread out across the broad channel bed and deposit sediment in the reach downstream. Similar depositional processes occur at the sinks downstream of HP.SE.2 and HP.SE.3. Deposition was observed at the concrete reach downstream of the Main-SW confluence near the outlet of the watershed. Culverts at the outlet of LLCW that convey flow from the Main channel to the

Tijuana Estuary and may cause backwater effects and increased upstream deposition along this reach. These culverts are not simulated in CONCEPTS, and may be the reason why we are not simulating deposition in this reach.

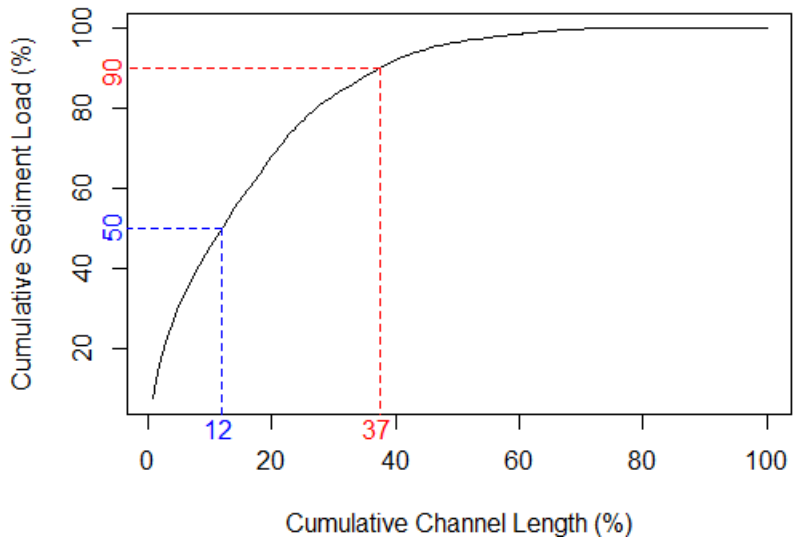

Figure 10. Cumulative channel-derived sediment load versus cumulative earthen channel length. Only 12% of the channel length contributes 50% of the sediment load and 37% of the channel length contributes 90% of the sediment load.

Although channel contribution on the sediment budget is large, only a small proportion of the river network generates the majority of the channel-derived sediment (Figure 10). Fifty percent of the channel-derived sediment load is generated from only 12% of the entire channel network. Additionally, only 37% of the entire earthen channel network contributes 90% of the channel-derived sediment load. This indicates that effective channel stabilization could be implemented on a third of the earthen river network length to provide a 90% reduction in channel-derived sediment yield, or a 54% reduction on the total sediment yield for the watershed.

5. Discussion

5.1 Channel Processes and the Sediment Budget

Rapid urbanization in Los Laureles Canyon has led to stream channel erosion and high loads of sediment to the Tijuana Estuary. Simulated channel evolution from 2001 to 2017 and observed channel changes from 2009 to 2014 indicate that the majority of channel

incision occurred during the initial period of 2001 to 2009, following urban development which was initiated in 2001 and a relatively large storm event (10-year recurrence interval) in 2004. Although the reach downstream of the metal culvert showed little channel changes from 2009 to 2014, the reach downstream of the concrete flume was actively widening. In the Main channel, portions of the channel are actively evolving, including the newly developed urban area of Salva Tierra near the upper portion of the watershed. As urban development increases in this area, channels should be stabilized prior to excessive channel enlargement and disconnection of the channel from floodplain storage, as seen in the SW watershed (Chapter 3). The SE watershed is composed of cobbly conglomerate soils and coarser bed material compared to the Main and the lower SW watersheds. Although channel incision was relatively low in the SE watershed due to bed armoring, except for the reach immediately downstream of a concrete-lined channel, channel widening was observed. Moreover, model scenarios coarsening the bed showed no change in the relative proportion of channel-derived sediment at the watershed scale, but there was a shift in dominant erosional processes. Coarsening the bed has caused a reduction in overall incision, but an increase in bank erosion. This indicates that coarsening the bed alone will not be sufficient in reducing the long-term channel-derived sediment at the watershed scale. With steep slopes both in the hillslopes and channel, increased hydraulic connectivity of the hillslopes to the stream channel via roads and drainages, and a removal of hillslope and riparian vegetation, discharge should be decreased from urban areas and the stream channel should be protected from erosion.

Over 2009-2017, the stream channel of LLCW contributed about 60% of the total sediment load to the outlet of the watershed. Trimble (1997) found that channel erosion accounted for two-thirds of the sediment yield from the San Diego Creek watershed. Although the proportion of channel contribution in LLCW is slightly smaller compared to San Diego Creek, the long-term channel-derived sediment yield of San Diego Creek from 1968-1998 (368 tons km^{-2} yr^{-1}) was 17 times smaller than LLCW (6,411 tons km^{-2} yr^{-1}). A major difference between urban regions of Tijuana and southern California is that in Tijuana there are large proportions of erodible, unpaved roads and open lots that generate large amounts of sediment and may remain unpaved for over 40 years (Biggs et al., 2010). In developed countries, the construction phase lasts only a few years, before exposed soil is

replaced with impervious, or at least stabilized, surfaces (Wolman, 1967). Although the "construction phase" is associated with channel aggradation, in Tijuana, the process of urbanization includes complete vegetation removal, filling the channel, and converting the stream channel into an unpaved road. A new stream channel forms in highly erodible construction fill and is oftentimes straighter, steeper, and more unstable than its unaltered condition (Chapter 3). With an enlarged and confined channel, floodplain storage is completely removed from the stream channel, which leads to larger flow depths, higher shear stresses, and further channel enlargement.

Taniguchi et al. (2018) estimated that channel erosion accounted for approximately 25 to 40% of the total sediment budget. However, this paper suggests that channel erosion may be the dominant (60%) source of sediment at the watershed scale. The sediment budget from Taniguchi et al. (2018) did not include major sediment producing stream reaches that were included in the CONCEPTS model. At the time of the 2014 survey, some sediment producing reaches, including downstream of HP.M1 and reaches in the SE channel near the confluence of Main were filled in with sediment and therefore not included in the sediment budget calculation by Taniguchi et al. (2018), which could lead to an underestimation of channel contribution on the sediment budget.

Model overestimation in total sediment yield at the outlet of LLCW may be explained by various factors. One factor is that the total amount of sediment excavated from the sediment traps is an underestimation of total sediment delivered to the trap because the amount of fine sediments that make it out of the trap and into the estuary is unknown. This would lead to a lower bound estimate of total annual sediment delivery to the estuary, despite utilizing trap efficiency equations to estimate the fine particles not captured. A second factor is that the AnnAGNPS model was calibrated for total annual sediment yield from 2006 to 2012, under the assumption that channel erosion contributes about 25% of the total sediment budget (Taniguchi et al., 2018). This paper suggests that channel erosion may contribute a larger proportion of sediment load to the outlet of LLCW. Future model calibrations of the AnnAGNPS model should assume that channel erosion contributes at least 50% of the total sediment budget.

In order to gain a full understanding of human impacts on fluvial geomorphology, studies need to go beyond the physical sciences and focus on linkages between social and

environmental processes that interact and shape the landscape (Urban, 2002; Ashmore, 2015). Socio-hydrology (Sivapalan et al., 2012) explores interactions, feedbacks, and co-evolution of human behavior with the hydrologic system, and serves as the basis for socio-geomorphology, which provides a hybrid framework for understanding socio-natural systems of landforms (Ashmore, 2015). Socio-geomorphic processes are not considered in computational models, such as CONCEPTS, due to the highly unpredictable nature of such practices. In LLCW, human intervention at the local scale may play a large part in temporarily stabilizing some of the highly eroded stream reaches in the SW channel (Figure 11). However, these stabilization methods are oftentimes temporary and the types of human action depend on the availability of funds at an individual basis.

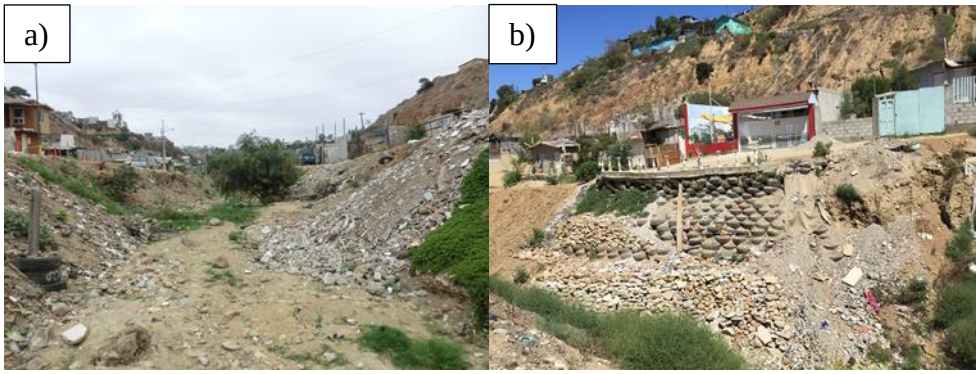

Figure 11. Human intervention at the local-resident scale, including bank stabilization with (a) loose construction fill and (b) more intricate stabilization designs using tires and blocks, which are not incorporated into the CONCEPTS model.

5.2 Model Uncertainties and Limitations

This study is the first to link the AnnAGNPS simulated hillslope sediment to the CONCEPTS channel evolution in a semi-arid region and therefore, model output adjustments need to be implemented. AnnAGNPS was originally developed to simulate the impact of agricultural practices on sediment and pollutant loading in regions in the mid-western United States. Soils on hillslopes in the Midwest typically consist of fine sediments, with minimal proportions of coarse and medium sand. In tectonically active, semi-arid regions in the Western U.S. and along the U.S.-Mexico border, higher proportions of particles coarser than fine sand are found on hillslopes and valley sedimentary fills. AnnAGNPS simulates sediment transport of various sizes of sand particles, but only reports total sand generated for each storm event. In areas with coarser sediment on the hillslopes, such as LLCW, accurate

sediment routing requires partitioning the total sand supply to channels into the various sand size classes (very coarse, coarse-medium, and fine-very fine sand). This study utilizes the hillslope sand particle size distribution to partition out the AnnAGNPS total sand into the three size classes. Scenarios treating all hillslope-derived sand as fine-sand, or washload, indicate that the mean annual channel contribution is 61% of the sediment budget, as opposed to 59%. The magnitude of channel incision and widening was larger when there was no coarser sand supplied from the hillslopes, but the spatial pattern of sources and sinks remained the same compared to the results reported in this paper.

Additionally, no hillslope derived sediments coarser than 2 mm was simulated for this analysis. It is assumed that the majority of coarse sediment delivered to the sediment traps are channel-derived and coarser sediment from the hillslopes are minimal or stored as colluvium. Gravel that has accumulated in the valley fill alluvium is assumed to have been transported from the hillslopes during large, episodic flow events. Although landslides and mass movement may supply coarse material to the channel, hillslope sediment supply of gravel and coarser was not included in this paper for multiple reasons. As previously stated, gravel comes in episodically and gets transported relatively short distances compared to the watershed length and is mixed with the sand load through scour and fill in either the current bed material (i.e. bed and bars) or the older valley fill during high flow events. Our simulation period does not include an extreme wet year when gravel from the hillslopes may have been transported and/or when mass movements are more likely to occur. The exclusion of hillslope-gravel supply may be invalid during large events in our simulation period, but the relatively dry water years being simulated allows for the assumption that relatively few coarse particles are delivered to the channel. Secondly, we have not observed landslides or debris flows that contained coarse materials that were transported to the stream network during our field observations. A landslide did occur in LLCW due to a water main failure but this type of event cannot be simulated in the modeling scheme because it was not caused by rainfall. Lastly, the residents often stabilize the hillslopes in the cobbly portions of the watershed with tires and other features, which would reduce the amount of coarse sediment supplied to the channel.

6. CONCLUSION

This paper demonstrates the utility of linking an empirically-based watershed scale model of hydrology and hillslope processes, AnnAGNPS, with a physically-based channel evolution model, CONCEPTS, in a rapidly developing, semi-arid region. The integrated model was able to realistically simulate the general pattern of incision for three stream reaches in Tijuana, Mexico, and was used to determine the channel sources and sinks of sediment, and the overall sediment budget for the watershed. Channel erosion in LLCW accounts for approximately 60% of the total sediment budget to the Tijuana Estuary. Approximately 37% of the entire earthen channel network contributes 90% of the channel-derived sediment load. This indicates that if effective channel stabilization measures are implemented on a third of the river network length, it could provide up to a 90% reduction in channel-derived sediment yield, or a 54% reduction on the total sediment yield for the watershed. Moreover, model scenarios coarsening the bed did not reduce the long-term mean annual channel-derived sediment yield at the watershed scale. Coarsening the bed caused channel incision to reduce, but increased channel widening. In addition to targeted channel stabilization on the highest sediment producing stream reaches, a reduction in discharge from urban areas will need to be implemented to lead to a substantial reduction of sediment yield to the Tijuana Estuary.

REFERENCES

Ashmore, P. (2015). Towards a sociogeomorphology of rivers. *Geomorphology*, *251*, 149–156. https://doi.org/10.1016/j.geomorph.2015.02.020

Biggs, T. W., Atkinson, E., Powell, R., & Ojeda-Revah, L. (2010). Land cover following rapid urbanization on the US-Mexico border: Implications for conceptual models of urban watershed processes. *Landscape and Urban Planning*, *96*(2), 78–87. https://doi.org/10.1016/j.landurbplan.2010.02.005

Biggs, T. W., Taniguchi, K. T., Gudino-Elizondo, N., Yongping, Y., Bingner, R. L., Langendoen, E. J., & Liden, D. (2018a). *Field measurements to support sediment and hydrological modeling in Los Laureles Canyon* (EPA/600/X-18/0XX). Washington, DC.

Biggs, T. W., Taniguchi, K. T., Gudino-Elizondo, N., Yongping, Y., Bingner, R. L., Langendoen, E. J., & Liden, D. (2018b). *Geology, soil properties and erosion on marine terraces along the US-Mexico Border* (XXXX). Washington, DC.

Bingner, R. L., & Theurer, F. D. (2001). AnnAGNPS: Estimating sediment yield by particle size for sheet and rill erosion. In *paper presented at Seventh Federal Interagency Sedimentation Conference, Subcomm. on Hydrol. and Sediment., Advis. Comm. on Water Inf.* Reno, Nev., 25-29 March.

Bracken, L. J., Turnbull, L., Wainwright, J., & Bogaart, P. (2015). Sediment connectivity: A framework for understanding sediment transfer at multiple scales. *Earth Surface Processes and Landforms*, *40*(2), 177–188. https://doi.org/10.1002/esp.3635

Chow, V. T. (1959). *Open-channel Hydraulics*. New Jersey: Blackburn Press. Retrieved from https://books.google.com/books?id=JG9_PwAACAAJ

Collins, A. L., Pulley, S., Foster, I. D. L., Gellis, A., Porto, P., & Horowitz, A. J. (2017). Sediment source fingerprinting as an aid to catchment management: A review of the current state of knowledge and a methodological decision-tree for end-users. *Journal of Environmental Management*, *194*, 86–108. https://doi.org/10.1016/j.jenvman.2016.09.075

Cunge, J. A., Holly Jr, F. M., & Verwey, A. (1980). *Practical Aspects of Computational River Hydraulics*. *Pitman Publishing Ltd London17 CUN 1980 420*. Retrieved from

http://openlibrary.org/b/OL4421427M/Practical_aspects_of_computational_river_hydraulics

de Vente, J., & Poesen, J. (2005). Predicting soil erosion and sediment yield at the basin scale: Scale issues and semi-quantitative models. *Earth-Science Reviews*, *71*(1–2), 95–125. https://doi.org/10.1016/j.earscirev.2005.02.002

Elshafei, Y., Sivapalan, M., Tonts, M., & Hipsey, M. R. (2014). A prototype framework for models of socio-hydrology: Identification of key feedback loops and parameterisation approach. *Hydrology and Earth System Sciences*, *18*(6), 2141–2166. https://doi.org/10.5194/hess-18-2141-2014

Gudino-Elizondo, N., Biggs, T., Bingner, R., Langendoen, E., Taniguchi, K. T., Kretzschmar, T., … Liden, D. (n.d.). *Contribution of hillslope and gully erosion to total sediment loads in a rapidly urbanizing watershed of the US-Mexico border using the AnnAGNPS model*.

Gudino-Elizondo, N., Biggs, T. W., Bingner, R. L., Yuan, Y., Langendoen, E. J., Taniguchi, K. T., … Liden, D. (2018). Modeling ephemeral gully erosion from unpaved urban roads: Equifinality and implications for scenario analysis. *Geosciences*, *137*(8). https://doi.org/10.3390/geosciences8040137

Hanson, G. J. (1990). SURFACE ERODIBILITY OF EARTHEN CHANNELS AT HIGH STRESSES PART II - DEVELOPING AN IN SITU TESTING DEVICE. *Transactions of the ASAE*, *33*(1), 0132–0137. https://doi.org/10.13031/2013.31306

Harry, H., Barnes, J., & Barnes Jr., H. H. (1987). Roughness Characteristics of Natural Channels. *Technical Report, Geological Survey Water-Supply, United States Government Printing Office, Washington, U.S.A*, 219. https://doi.org/10.1016/0022-1694(69)90113-9

Langendoen, E. J., & Alonso, C. V. (2008). Modeling the Evolution of Incised Streams: I. Model Formulation and Validation of Flow and Streambed Evolution Components. *Journal of Hydraulic Engineering*, *134*(6), 749–762. https://doi.org/10.1061/(ASCE)0733-9429(2008)134:6(749)

Langendoen, E. J., & Simon, A. (2008). Modeling the Evolution of Incised Streams. II: Streambank Erosion. *Journal of Hydraulic Engineering*, *134*(7), 1094–1100. https://doi.org/10.1061/(ASCE)0733-9429(2008)134

Langendoen, E., Thomas, R., & Bingner, R. (2002). Numerical simulation of the morphology of the Upper Yalobusha River, Mississippi between 1968 and 1997. *River Flow*. Retrieved from https://afrsweb.usda.gov/SP2UserFiles/Place/64080510/AGNPS/Concepts/Doc/riverflow2002.pdf

Laursen, E. M. (1958). The total sediment load of streams. *J. Hydr. Div.*, *84*(HY1), 1530–1536. https://doi.org/84, HY, 1: 1530-1536.

Meade, R. H. (1982). Sources, Sinks, and Storage of River Sediment in the Atlantic Drainage of the United States. *The Journal of Geology*, *90*(3), 235–252. https://doi.org/10.1002/job.322

Meyer-Peter, E., & Mueller, R. (1948). Formula for bed-load transport. In *Int. Association for Hydraulic Research, 2nd Meeting*. Stockholm, Sweden.

Morris, G. L., & Fan, J. (1998). *Reservoir Sedimentation Handbook: Design and Management of Dams, Reservoirs and Watersheds for Sustainable Use*. New York: McGraw-Hill Companies, Inc.

NRCS. (1972). SCS National Engineering Handbook. Section 4, Hydrology. In *National Engineering Handbook*.

NRCS. (2018). Natural Resources Conservation Service Soils.

Owens, P. (2005). Conceptual Models and Budgets for Sediment Management at the River Basin Scale. *Journal of Soils and Sediments*, *5*(4), 201–212. https://doi.org/10.1065/jss2005.05.133

Prosser, I. P., Rutherfurd, I. D., Olley, J. M., Young, W. J., Wallbrink, P. J., & Moran, C. J. (2001). Large-scale patterns of erosion and sediment transport in river networks, with examples from Australia. *Marine and Freshwater Research*, *52*(1), 81–99. https://doi.org/10.1071/MF00033

Reid, L. M., & Dunne, T. (1996). *Rapid evaluation of sediment budgets*. https://doi.org/10.1097/00010694-199707000-00010

Shields Jr., D. F., Langendoen, E. J., & Doyle, M. W. (2006). Adapting Existing Models To Examine Effects of Agricultural Conservation Programs on Stream Habitat Quality. *Journal of the American Water Resources Association*, *3220*, 25–33. https://doi.org/10.1111/j.1752-1688.2006.tb03820.x

Singer, M. B., & Dunne, T. (2001). Identifying eroding and depositional reaches of valley by analysis of suspended sediment transport in the Sacramento River, California. *Water Resources Research*, *37*(12), 3371–3381. https://doi.org/10.1029/2001WR000457

Sivapalan, M., Savenije, H. H. G., & Blöschl, G. (2012). Socio-hydrology: A new science of people and water. *Hydrological Processes*, *26*(8), 1270–1276. https://doi.org/10.1002/hyp.8426

Taniguchi, K. T., Biggs, T. W., Langendoen, E. J., Castillo, C., Gudino-Elizondo, N., Yongping, Y., & Liden, D. (2018). Stream channel erosion in a rapidly urbanizing region of the US-Mexico Border: Documenting the importance of channel hardpoints with Structure-from-Motion photogrammetry. *Earth Surface Processes and Landforms (ESPL)*, *43*(7), 1465–1477.

Trimble, S. W. (1997). Contribution of stream channel erosion to sediment yield from an urbanizing watershed. *Science*, *278*(5342), 1442–1444. https://doi.org/10.1126/science.278.5342.1442

Urban, M. A. (2002). Conceptualizing Anthropogenic Change in Fluvial Systems: Drainage Development on the Upper Embarras River, Illinois. *Professional Geographer*, *54*(2), 204–217. https://doi.org/10.1111/0033-0124.00326

Urbonas, B., & Stahre, P. (1993). *Stormwater Best Management Practices and Detention*. Englewood Cliffs, New Jersey: Prentice Hall.

Walling, D. E., & Collins, A. L. (2008). The catchment sediment budget as a management tool. *Environmental Science and Policy*, *11*(2), 136–143. https://doi.org/10.1016/j.envsci.2007.10.004

Wilkinson, S. N., Prosser, I. P., Rustomji, P., & Read, A. M. (2009). Modelling and testing spatially distributed sediment budgets to relate erosion processes to sediment yields. *Environmental Modelling and Software*, *24*(4), 489–501. https://doi.org/10.1016/j.envsoft.2008.09.006

Wolman, M. G. (1967). A Cycle of Sedimentation and Erosion in Urban River Channels. *Geografiska Annaler. Series A, Physical Geography*, *49*(2/4), 385–395. Retrieved from http://www.jstor.org/stable/520904

Yang, C. T. (1973). Incipient motion and sediment transport. *Journal of the Hydraulics Division*, *99*(10), 1679–1704.

CHAPTER 5

CONCLUSION

Few studies have been conducted on the impacts of urban development on stream channel dynamics and sediment transportation in semi-arid, developing countries. This dissertation provides an example of the use of a variety of geomorphic field methods, including traditional topographic survey methods and Structure-from-Motion (SfM) photogrammetry techniques, paired with a comprehensive modelling framework to provide an understanding of the driving mechanisms of channel instability and the overall importance of channel processes on the sediment budget to support local and federal sediment management plans in a rapidly developing, semi-arid region.

Chapter 2 showed that stream channels in Tijuana, Mexico were statistically larger than reference and urban channels in southern California and that major hotspots of channel erosion were located downstream of hardpoints, or non-erodible features. Chapter 3 determined that hardpoints prevented incision in the upstream direction by serving as grade control, and only caused local channel instabilities downstream. Channel erosion is caused mainly by the destruction of the natural channel, including channel burial, straightening, steepening, and removal of riparian vegetation, often performed in the process of turning channels into roads. Reformation of an enlarged river reach that is disconnected from the floodplain, leads to higher flow depths constrained in the channel, larger shear stresses, and accelerated channel incision. Chapter 4 utilized a watershed-scale model to spatially map channel sources and sinks of sediment and determine the role of channel processes on the overall sediment budget. Channel erosion contributes approximately 60% of the total sediment budget and only a third of the entire stream channel network is generating 90% of the channel-derived sediment load. This indicates that channel erosion is a dominant source of sediment in LLCW and targeted stream stabilization measures could potentially reduce a large proportion of sediment load to the Tijuana Estuary. However, coarsening of the bed alone, may not decrease mean annual channel-derived sediment yield, as channel incision is reduced but channel widening is exacerbated.

This dissertation provides a regional comparison of stream morphology of developing and developed semi-arid watersheds and characterization of the sources and sinks of

sediment and mechanisms of stream channel evolution to understand the overall sediment budget of a rapidly developing, semi-arid region. This study provides a greater understanding of channel dynamics and the sediment budget in a rapidly urbanizing semi-arid region for future sediment management plans.

FUTURE RESEARCH

Major uncertainties arise in modeling highly altered and tightly linked socio-geomorphic systems, such a Los Laureles Canyon watershed. This dissertation discusses some of the uncertainties of the physical assumptions used in the integrated AnnAGNPS-CONCEPTS model, such as the uncertainty in the coarse sediment supplied from the hillslopes, but also the limitations of using physically based data and equations alone to predict sediment loadings. Socio-geomorphic processes, such as human intervention, need to be implemented into the modeling scheme to improve the overall understanding of the system. The community sensitivity loop used in socio-hydrology models, which describes how human behavior and management decisions are directly driven by a community's social and environmental values, local action, and lobbying and all reflect on community sensitivity to hydrologic or geomorphic change (Elshafei et al., 2014), can be implemented in the modeling framework used in this dissertation. The community sensitivity state variable, which refers to a community's perceived level of threat to the community's quality of life (Elshafei et al., 2014), can be quantified and used to provide the key linkage between human intervention or action to geomorphic changes expressed in the models. Future research can incorporate the socio-geomorphic processes to help improve the predictability of sediment loadings in such watershed models and the overall understanding of the highly altered systems.

Additionally, future research can utilize the integrated CONCEPTS-AnnAGNPS watershed model to determine the impact of land use changes and best management practices, such as revegetation of the hillslopes and road paving, on stream channel evolution in Tijuana, Mexico and in other semi-arid regions. Both managers and researchers can implement the methods and modeling framework from this dissertation, to improve understanding of geomorphic processes and create more informed sediment management plans.

REFERENCES

Elshafei, Y., Sivapalan, M., Tonts, M., & Hipsey, M. R. (2014). A prototype framework for models of socio-hydrology: Identification of key feedback loops and parameterisation approach. *Hydrology and Earth System Sciences*, *18*(6), 2141–2166. https://doi.org/10.5194/hess-18-2141-2014